UNIVERSITY OF CAPE TOWN
IYUNIVESITHI YASEKAPA • UNIVERSITEIT VAN KAAPSTAD

Investigation of the role of the DNA-modifying enzyme, Activation-Induced cytidine Deaminase (AID), in cancer.

Grant Kenneth Godsmark

BSc, BSc (Med) Honours

GDSGRA001

Dissertation presented for the degree of Master of Science (Medicine) in the Division of Haematology, Department of Clinical and Laboratory Sciences, Faculty of Health Sciences, University of Cape Town, September 2015.

Supervisor: Dr Shaheen Mowla

Plagiarism Declaration

I hereby certify that this dissertation submitted by me for the M.Sc. Med (Haematology) degree at the University of Cape Town is based on my original work and has not been previously submitted for another degree at this or any other university. I waive copyright of the dissertation in favour of the University of Cape Town. I declare that this work is not plagiarised and that each contribution to and quotation in this thesis from the work of others has been cited and referenced.

Signed by candidate

Signature Removed

Grant Kenneth Godsmark

10 September 2015

Date

Acknowledgements

I would like to thank the NRF and the Oppenheimer Memorial Trust for giving me the financial assistance I required to achieve my dreams.

To my Haematology colleagues, Prof Novitsky, Karen, Noni, Gift, Kirsty, Rygana, Jean, Coleen, Valda, Helen, Rashaad, you have all helped me in so many ways, whether it was to listen to me complain, or to help me solve a problem, or to just join me for tea.

To all my friends who helped in your own ways, Rosie and Troy, Kusha, Mal, Jurgens, Brendon, Calvin and both Lukes! Thanks for always listening and giving me valuable advice.

To Ronnie, Susan and Prof Sharon Prince for all your assistance.

To my new family, Mr and Mrs Garson, Carrie, Paul and Scott, thank you for always thinking of me and helping to keep me motivated.

To Mom, Dad, Cherie and Jo, you have all helped me in ways you may never understand, thank you for always being on my team and for your unflinching support. Without you guys I would never have been in the position to continue my education.

To Dr Shaheen Mowla, thank you for always having your door open and making time for me when I needed guidance. You have helped mould me as a scientist and I will always be grateful.

To my darling Christie, without you I would never have begun this journey, and without your unwavering support I would never have completed it. Thank you for all your patience, the many hours/days of listening, for always managing to cheer me up and helping to find a solution. This document is a testament to your faith in me.

Table of Contents

List of Figures

List of Tables

List of Abbreviations

°C	Degrees celcius
AID	Activation induced cytidine deaminase
AM	Affinity maturation
APE	Apyrmidinic endonuclease 1
APOBEC	Apolipoprotein B mRNA editing catalytic subunit
BCA	Bicinchoninic acid assay
BL	Burkitt's lymphoma
bp	Base pairs
BrdU	Bromodeoxyuridine
BSA	Bovine serum albumin
CD	Cluster of differentiation
cDNA	Complementary DNA
CMV	Cytomegalovirus
CO_2	Carbon dioxide
Cp	Crossing point
CRC	Colorectal cancer
CSR	Class switch recombination
DEPC	Diethylpyrocarbonate
dH_2O	Distilled water
DLBCL	Diffuse large B-cell lymphoma
DMEM	Dulbecco's modified eagle medium
DMSO	Dimethyl sulphoxide
DNA	Deoxyribonucleic acid
dNTP	Deoxynucleotide triphosphate
dsDNA	Double stranded DNA
DTT	Dithiothreitol
EBV	Epstein-Barr virus
ECL	Enhanced chemiluminescence
EDTA	Ethylenediaminetetraacetic acid

Et al	*et alia* (and others)
FBS	Fetal bovine serum
FISH	Fluorescent *in situ* hybridisation
g	grams
g	Gravity
GAPDH	Glyceraldehyde-3-phosphate dehydrogenase
GC	Germinal center
GFP	Green fluorescent protein
GIT	Gastrointestinal tract
HAART	Highly active anti-retroviral therapy
HCl	Hydrochloric acid
HCV	Hepatitis C virus
HIGM2	Type 2 hyper-IgM syndrome
HIV	Human immunodeficiency virus
HRP	Horseradish peroxidase
Ig	Immunoglobulin
IL-4	Interleukin 4
IL-6	Interleukin 6
IRAC	International agency for research and cancer
LHS	Left hand side
LPS	Lipopolysaccharide
M	Molar
miRNA	MicroRNA
ml	Millilitres
mm	Millimetres
mM	Millimolar
mRNA	Messenger Ribonucleic acid
ng	Nanogram
NHL	Non-Hodgkin's lymphoma
nM	Nanomolar
nm	Nanometer

PAGE	Polyacrylamide gel electrophoresis
PBS	Phosphate buffered saline
PCR	Polymerase chain reaction
PE	Phycoerythrin
PenStrep	Penicillin-streptomycin
pH	Percent hydrogen
PS	Phospholipid phosphatidylserine
qPCR	Quantitative real-time polymerase chain reaction
RE	Restriction enzyme
RHS	Right hand side
RIPA	Radioimmunoprecipitation assay buffer
RNA	Ribonucleic acid
rpm	Revolutions per minute
RPMI	Roswell Park Memorial Institute
rRNA	Ribosomal ribonucleic acid
SA-β-gal	Senescence-associated β-galactosidase
SDS	Sodium dodecyl sulphate
SEM	Standard error of the mean
SHM	Somatic hypermutation
siRNA	Short interfering ribonucleic acid
TBE	Tris-borate-EDTA
TBS	Tris buffered saline
TLS	Translesion synthesis polymerase
Tris	Tris hydroxymethyl aminomethane
ug	Microgram
uL	Microliter
uM	Micromolar
UNG	Uracil DNA glycosylase
UTR	Untranslated region
UV	Ultra-violet
V	Volts

WHO	World health organisation
β-gal	B-galactosidase

Abstract

The DNA-editing enzyme, Activation-Induced cytidine Deaminase (AID) is essential for antibody diversification and plays an important role in immunity. AID is specifically expressed in activated B-cells and mutates targeted DNA sites, diversifying the antibody repertoire. Due to its mutagenic nature, AID expression is tightly regulated, however, its overexpression has been associated with translocation of the *c-MYC* oncogene, a characteristic of the B-cell derived cancer, Burkitt's lymphoma (BL). Although currently uncharacterised, AID overexpression has also been implicated in non-lymphoid cancers including prostate, liver and colon. The function of AID in the oncogenic process is not well defined and therefore this project is aimed at using cell culture models to study the function of AID in cancer.

AID mRNA and protein expression levels were determined in five cell lines of B-cell origin, and 16 epithelial cell lines (colon, prostate, head and neck and oesophageal). While AID expression was easily detected in the B-cell derived cell lines, no significant expression of both AID mRNA and protein expression was found in all the epithelial derived cell lines. The B lymphoblastoid cell line, L1439A, which is derived from a healthy donor, and harboured relatively low AID expression, was originally selected for ectopic expression of AID. Transfection of this cell line using conventional methods and lipid and polymer based transfection reagents was not successful, and therefore, nucleofection was used, which caused successful uptake of the AID-expressing plasmids as well as corresponding controls. However, this method was too harsh for the L1439A cell line as it did not survive post-nucleofection. Based on this result, the BL cell line Ramos, which expresses relatively low AID compared to the other BL cell lines used in the screen, was selected as an alternative. Plasmids constitutively expressing AID, as well as their corresponding empty vector, were successfully introduced into these cells using an established nucleofection protocol. While cells containing the empty vectors could be selected and expanded in culture, cells overexpressing AID underwent apoptosis approximately three days post-transfection. This is likely due to the highly mutagenic nature of the enzyme. As an alternative approach to studying the function of AID in cancer, a knockdown approach was taken, using siRNA. Four potential siRNAs targeting AID were tested and one was selected for transient AID knockdown in the Ramos cell line. Ramos cells with reduced AID expression were analysed alongside control cells for several features

characteristic of cancer cells. Reduction in AID expression caused a decrease in cell proliferation, as demonstrated by the WST-1 proliferation assays, and confirmed by the incorporation of BrdU and cell cycle profile analysis. The difference in CD10, CD19 and CD20 were unchanged in the knockdown cells. Furthermore, the knockdown of AID sensitized the cells to the chemotherapeutic drug doxorubicin. Interestingly, the expression of phosphorylated γ-H2AX, a biomarker of DNA double strand breaks, was significantly reduced when AID was knocked down, indicating that reducing AID expression leads to a more stable genome. Using the Transwell migration assay, we further demonstrated that cells with reduced AID expression had decreased mobility, indicating that possible downstream effects of AID overexpression enhances cell migration, a key feature of advanced stages of cancer.

This study therefore provided new insight into the cellular effects brought about by AID in cancer and the cellular mechanism by which it may contribute to these. Future studies will focus on validating some of the results observed, as well as elucidating the signalling pathways and specific cellular factors which are affected in cancer cells where AID is overexpressed.

Chapter 1: Introduction

Cancer is the leading cause of mortality worldwide with an estimated 20 million new cancer cases by 2025 (WHO) and according to the GLOBOCAN 2012 statistics, there were 8.2 million cancer deaths and 14.1 million new cancer cases worldwide during 2012 (Ferlay *et al*., 2015). The GLOBOCAN 2012 statistics were produced by the International Agency for Research and Cancer (IRAC) comprised from population-based cancer registries. Cancer, which is defined by a rapid progression of uncontrolled cell growth due to genetic alterations, is increasing in incidence in the developing world. In these regions, cancer makes up 56 % of all worldwide cases and is the second leading cause of death (64% of all cancer deaths worldwide) (Chow, 2010; Jemal *et al*., 2011). This rise in the global burden of cancer, especially in the developing world is due to the increase in cancer causing lifestyles such as smoking, lack of physical activity and the adoption of "westernized" diets (Jemal *et al*., 2011). Cancer is a disease of abnormal gene expression and function, brought about by genetic alterations within the genome. Despite widespread research in the causes and consequences of these genetic alterations, as well as in the development of new therapies, many cancers remain resistant to treatment. Therefore there is a continued need for further research in the field, especially in the identification of potential cancer causing genes which may be targeted by therapy.

1.1 *AICDA*

Sixteen years ago a protein was identified by Muramatsu *et al*. (1999) that has since been described as one of the possible "driver" genes for certain types of cancers. This protein is called Activation-Induced cytidine Deaminase (AID) which is located on the *AICDA* locus on chromosome 12 and is made up of five exons (Figure 1.1). The transcription of the gene has been found to be regulated by four distinct regulatory regions identified within the locus (Maul and Gearhart, 2010). The translated 24 kDa protein is a DNA/RNA-editing enzyme which belongs to the apolipoprotein B mRNA-editing catalytic subunit (APOBEC) family (Fritz and Papavasiliou, 2010; Endo *et al*., 2011). Of the 11 human cytidine deaminases within this family, AID is the only one with DNA-modifying activities under physiological conditions and is fundamental in the process of antibody specificity and diversification (Matsumoto *et al*., 2010; Endo *et al*., 2011; Gu *et al*., 2012). Importantly, AID has been found highly overexpressed in Burkitt's lymphoma (BL), diffuse large B-cell lymphomas (DLBCL), and

follicular lymphoma. Its expression has also been implicated in other human B-cell lymphomas, such as chronic lympholytic leukemia, Hodgkin's lymphoma, mantle cell lymphoma, mucosa-associated lymphoid tissue lymphoma, mediastinal B-cell lymphoma, hairy cell leukemia and acute lymphocytic leukemia (Kotani *et al*., 2007). In humans, complete loss of AID causes type 2 hyper-IgM syndrome (HIGM2), characterized by lack of somatic hypermutation (SHM), class switch recombination (CSR) and lymph node hyperplasia (Revy *et al*., 2000). The current literature on AID's involvement in cancer will be discussed later in more detail, while the next sections will divulge the details of normal AID functions.

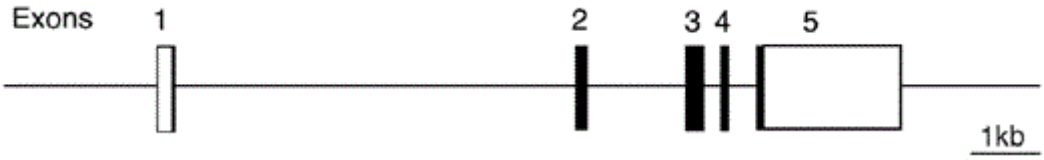

Figure 3.1: Schematic diagram of the *AICDA* gene. Numbers 1 - 5 indicate the position and size of the five exons, while the black boxes denote the coding sequence of the AID protein (taken from Faili *et al.,* 2002).

1.2 Antibody diversification by affinity maturation

Antibody diversification is an important process in generating an effective immune response against a broad range of pathogens. Transient structures called germinal centres (GC) form when introduced to a T cell-dependent antigen. Within these GC cells, antibodies with high affinity are produced and differentiate into memory B cells and plasma cells (De Silva *et al*., 2015). GC B cells proliferate at a rapid rate, much higher than normal mammalian tissues to produce the vast repertoire of antibodies required to mount an effective immune response (De Silva *et al*., 2015). Due to the processes explained below, the body can produce 10^9 antibodies, more than the number of genes that make up the entire human genome (Teng *et al*., 2008). Initially, in the bone marrow, the variable (V) diversity (D) and joining (J) gene segments of the immunoglobulin H (IgH) locus rearrange and link to the constant (C) region of the Cμ chain in a process termed V(D)J recombination (Durandy, 2003). This antigen- and T-cell-independent process produces the primary repertoire of antibodies in the form of naïve B-cells (Durandy, 2003). Once a naïve B-cell has moved to the periphery and encounters a

pathogen, it undergoes a process called affinity maturation (AM), whereby it activates, proliferates and forms a germinal center (GC) in the secondary lymphoid organs (lymph nodes, tonsils, and spleen) (Durandy, 2003; Maul and Gearhart, 2010). AID is expressed in these activated B-cells and is essential for SHM and CSR to occur (Okazaki *et al*., 2007; Endo *et al*., 2011; Gu *et al*., 2012; Mechtcheriakova *et al*., 2012).

1.2.1 Somatic Hypermutation

Somatic hypermutation is defined by the generation of multiple point mutations in the variable region of the immunoglobulin (Ig) exons (Muramatsu *et al*., 1999). This occurs when RNA Polymerase II unwinds the double stranded DNA (dsDNA) allowing AID access to deaminate the cytidine to uracil. As a protective mechanism, AID can only access the cytidines at this point in AM as it can only function on single stranded DNA (ssDNA). The resulting deamination is then processed through one of three pathways (Figure 1.2). Either DNA replication can move over the U-G mismatch and the C:G bases are replaced with T:A bases, or alternatively base excision repair can take place with the help of uracil DNA glycosylase (UNG) which initiates the removal of the uracil base and production of an abasic site. This process may produce a nick in the DNA by the action of apyrimidinic endonuclease 1 (APE). The abasic site is then filled by the error prone translesion synthesis polymerase (TLS) which may cause multiple single point mutations. The final alternative process involves the mismatch repair proteins; these proteins remove the U-G mismatch with the use of exonuclease 1 which is then filled by the TLS therefore giving rise to mutations. Double strand Breaks (DSBs) are created when nicks occur in close proximity to each other, the mechanism by which translocations arise (Gu *et al*., 2012).

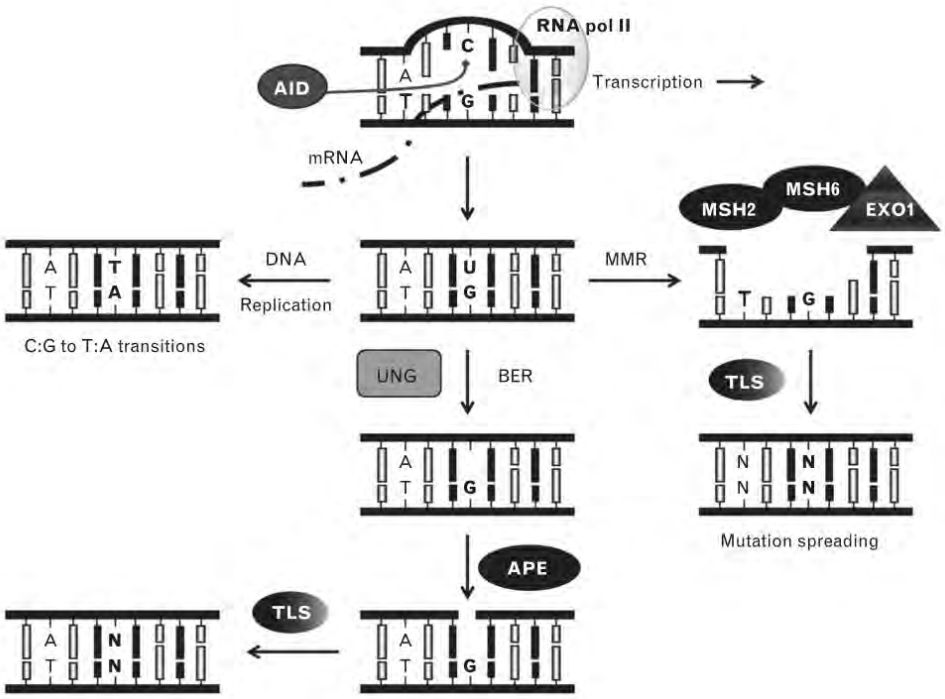

Figure 1.4: Diagram representing the three possible pathways in SHM. They are either a C:G to T:A transition, multiple point mutations by the mismatch repair proteins, or base excision repair, with the help of UNG and APE which creates an abasic site (taken from Gu *et al*., 2012).

1.2.2 Class-switch recombination

CSR is the second AID mediated process that occurs in AM, whereby the exons of the heavy chain constant region (C_H) are replaced by alternative C regions of another Ig isotype (Muramatsu *et al*., 1999; Durandy, 2003). C region replacement is possible by recombination of two different switch regions (S regions) and the removal and deletion of the intervening DNA sequence (Figure 1.3). This allows the replacement of the Cμ with either of Cγ, Cα, or Cε which converts the IgM isotype into IgG, IgA or IgE respectively, and this replacement will not alter the antigen specificity (Durnady, 2003).

In 2004, Ramiro *et al*., showed that AID is essential for antibody diversification, by working with BALB/c mice, which are especially susceptible to IL-6 stimulation. BALB/c $AID^{+/+}$ transgenic mice stimulated with IL-6 induced *c-myc*/IgH translocations. BALB/c $AID^{-/-}$ mice stimulated with IL-6 developed normal B-cells, however, they failed to produce SHM or CSR, the processes which have been shown to be important in antibody diversification (Ramiro *et al*., 2004; Endo *et al*., 2011).

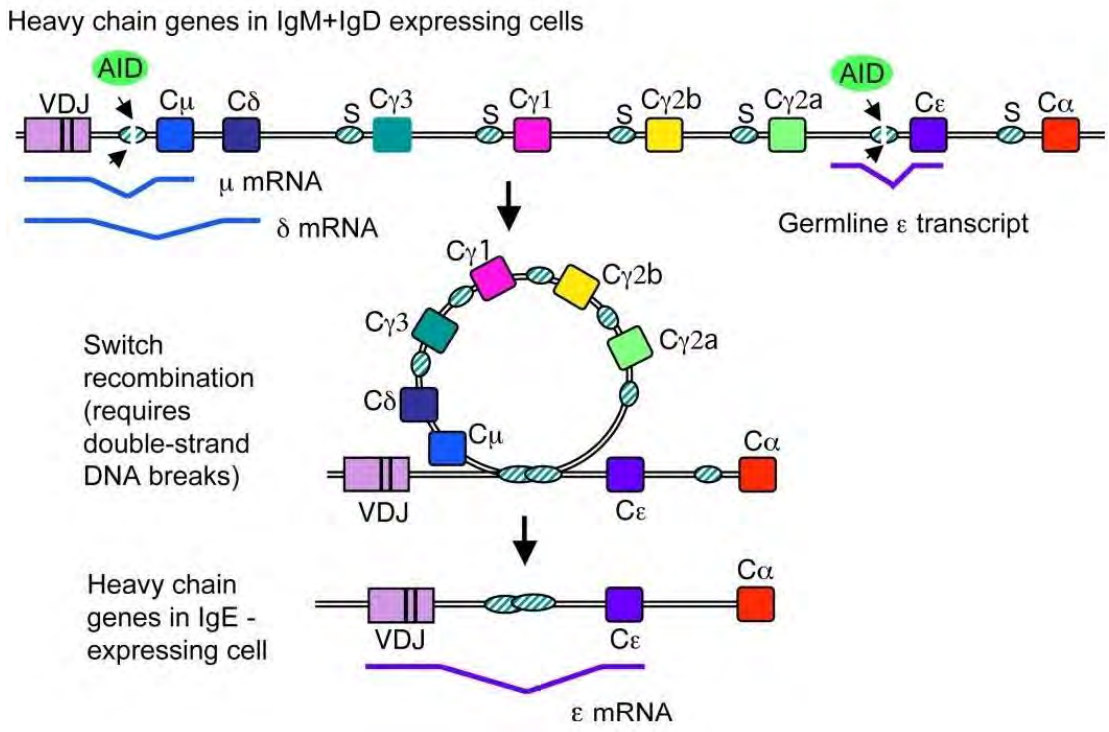

Figure 1.5: Diagram showing CSR. AID causes double strand breaks in the switch regions of the IgH gene and the intersecting piece of DNA is removed. The V(D)J region is joined to a new C_H region forming a different IgH isotype (taken from Stevnezer, 2011).

Over and above AID's role in antibody diversification, it has been shown to mutate non-immunoglobulin loci in B-cells (Fritz *et al*., 2013) and there is mounting evidence suggesting AID is expressed in other normal tissue types (Robbiani and Nussenzweig, 2013). In murine B-cells, AID was shown to act in a broad way on the entire genome, relying on two mechanisms of protection, selective targeting of AID, and high-fidelity repair (Liu *et al*., 2008). Even with these protective mechanisms, 25 % of all the genes expressed in the activated B-cells were found to still be mutated by AID activity (Liu *et al*., 2008). Murine ovaries have 50 - 70 % higher AID expression in comparison to spleen cells (Orthwein and Di Noia, 2012). This indicates that AID has a potentially important physiological role in these cells, however, it is as yet unknown what this role could be. Under oestrogen stimulation, AID levels are increased in breast tissue which increases even further in the ovaries (Orthwein and Di Noia, 2012). Various other organs, including prostate, heart and lungs express AID, however the associated physiological role is not known.

Additionally AID has also been implicated in DNA methylation: it has been proposed that AID can convert 5-methylcytosine (5-mC) in ssDNA to thymine thus allowing one of the T-G mismatch-specific glycoslyases to form an abasic site with the removal of 5-mC (Fritz and Papavasiliou, 2010; Ramiro and Barreto, 2015). This abasic site is then filled with an unmethylated cytidine, thus demethylating the cytidine through a deamination event (Fritz and Papavasiliou, 2010). Although a role during development has been proposed, AID deficient mice develop normally and therefore AID cannot be the only enzyme responsible for epigenetic reprogramming *via* demethylation during development (Fritz *et al*., 2013). Interestingly, Fritz *et al*. (2013) has shown that AID does not regulate DNA methylation in activated B-cells even though there is a high concentration of AID in these cells (Fritz *et al*., 2013). A study independent of the Fritz group, produced at the same time, which was performed by Hogenbirk *et al*. (2013), came to the same conclusions as the Fritz *et al*. (2013) research team. Thus although AID has been shown to demethylate non-lymphoid cells, a possible reason for the lack of this mechanism observed in lymphoid cells may be that there is a co-factor required for AID-dependent demethylation (Ramiro and Baretto, 2015). AID has also been shown to play a role in early development having been conserved in lower vertebrates, this indicates more functions for AID outside of just the immune system (Fritz and Papavasiliou, 2010). Research into the exact link between AID and demethylation is ongoing.

1.3 The many levels of AID regulation

AID has a powerful mutagenic effect on DNA. This effect promotes tumourigenesis, thus AID requires fine regulation to prevent aberrant expression. Extensive studies have been carried out on the various levels of regulation in the context of B-cell activation and these are discussed below.

Transcriptional regulation

Several elements that regulate AICDA transcription have been identified. Comparison of the 50 kb up- and downstream of the human *AICDA* gene to the mouse homolog, identified four conserved non-coding regions (Tran *et al*., 2010) (Figure 1.4).

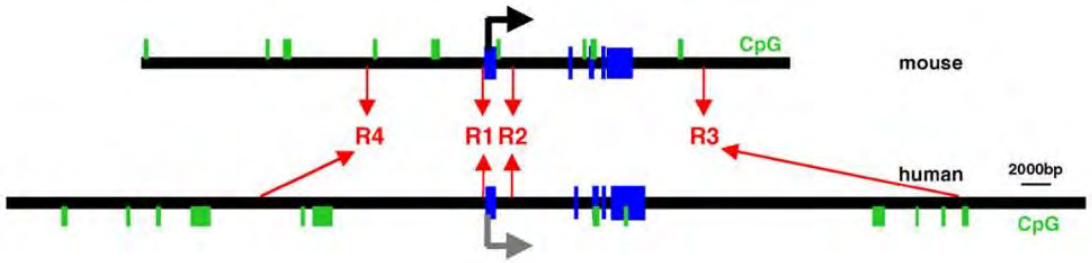

Figure 1.6: Diagram showing the mouse and human *AICDA* loci. Blue boxes are the exons, green boxes are the putative CpG islands, black and grey arrows indicate the transcription start sites for each ortholog, and the four conserved regions are in red (taken from Yadav *et al*., 2006).

Region one (R1) is found immediately upstream of the coding region (Figure 1.4) and luciferase reporter assays indicate that this region is most likely involved in basal transcription (Tran *et al*., 2010). Region two (R2) is located within the first intron of *AICDA* and contains both positive and negative regulatory elements and seems to be involved in expression of AID in activated B-cells (Tran *et al.,* 2010). In disputing studies, Crouch *et al*. (2007) showed that region three (R3), located downstream of the coding region, is essential for AID expression, however, Tran *et al*. (2010) reported no enhancer activity in this region in their luciferase assays (Tran *et al*., 2010). Region four (R4) which is located approximately 8 kb from the transcription start site has been described as a transcriptional enhancer (Tran *et al*., 2010).

Regulation via miRNA

MiRNA molecules have also been identified as regulators of AID expression (Teng *et al*., 2008). MiRNAs are 20 - 23 nucleotides in length and originate from the non-coding sequences in introns and non-translated regions of mRNA transcripts. These miRNA molecules generally bind to 3'-untranslated complementary sequences resulting in either mRNA degradation or inhibition of translation (Bartel, 2004; Stavnezer, 2011). There are four miRNAs that have been identified as AID regulators, miR-155, miR-361, miR-181b and miR-93 (Stavnezer, 2011). MiR-155 has been shown to be expressed concurrently with AID and destabilizes the protein at the 3' UTR (Dorsett *et al*., 2008) with mutational studies of miR-155 causing deregulation of AID expression and disruption of CSR and AM (Teng *et al*., 2008). In addition, miR-361 has been shown to destabilize AID in much the same way as miR-155 (Basso *et al*., 2012). MiR-93 functions in a similar manner to both miR-155 and miR-361, whereby it interacts with the 3' untranslated region (UTR) of AID to block expression (Borchert *et al*., 2011). Interestingly miR-181b expression has been shown to decrease during B-cell activation as opposed to the other

miRNAs described, however, it functions in the same way by downregulating AID thus allowing AID to aid in CSR and SHM (Dorsett *et al*., 2008).

Post-translational regulation

AID is also regulated post-translationally, by both cellular compartmentalization and phosphorylation (Aoufouchi *et al*., 2008). The AID protein is mostly found in the cytoplasm and there are two regions that control localization: a nuclear localization signal in the N-terminus, and a nuclear export signal in the C-terminus (Maeda *et al*., 2010). AID is also unstable in the nucleus with the half-life of the protein being three times shorter when compared to the cytoplasm (Aoufouchi *et al*., 2008). Another level of post-translational modification is dependent on multiple co-factor proteins. For instance, the recruitment of AID to DNA, its transport into the nucleus, and identification of its target sites have been found to be dependent on several proteins, namely RNA Polymerase II, RPA, CTNNBL-1, protein kinase A and GANP (Maeda *et al*., 2010). Phosphorylation of AID, at residues Ser38 and Tyr184, have been found to regulate the protein as the unphosphorylated form is unable to effectively deaminate transcribing dsDNA (Stavnezer, 2011).

1.4 The target of AID

AID specifically targets G-loops formed in DNA. These are characterized by the G-rich non-template strand of the R-loop structure, specifically in the Sγ3 region of the *IgH* gene (Duquette *et al*., 2005; Gómez-González and Aguilera, 2007). Targeting occurs when RNA Polymerase II binds to the transcribed strand of *AICDA*, this causes the non-transcribed strand to form an 11 nucleotide piece of ssDNA, creating a transcription bubble. The transcribed DNA strand is G-rich, which complements the S region of the *IgH* transcript, thus hybridizing to each other forming an R-loop structure. This R-loop structure opens up longer stretches of ssDNA which AID can then target. AID can target both the transcribed and non-transcribed strand with the latter being targeted 1.4 fold more frequently (Stavnezer, 2011). Other studies have shown that AID also targets other regions within DNA, either CpG islands or consensus sequence motifs. The majority of CpG islands targeted by AID are either directly at the CpG island position, or in close proximity (≤ 4 nucleotides) (Greisman *et al*., 2012). Consensus sequences which direct the action of AID in the same way as CpG islands have been identified

(Greisman *et al*., 2012). It has also been shown that *c-MYC* contains regions very similar to the S regions targeted in AID thus upon B-cell activation, *AICDA* and *c-MYC* are both transcribed and AID can target the S regions of AID and the G-rich regions of *c-MYC*. Additionally *IgH* and *c-MYC* are in close proximity to one another in the nucleus during this process, allowing small nicks to form which create DSBs and allow reciprocal translocations to occur (Duquette *et al*., 2005; Wang *et al*., 2009).

1.5 AID overexpression in Burkitt's lymphoma

AID has been implicated in multiple cancers, more notably in BL, a type of non-Hodgkins lymphoma (NHL). This disease is defined by translocations between the *c-MYC* oncogene, and the IgH locus in B lymphocytes, and in 80 % of cases, a t(8;14) translocation occurs, with the remaining 20 % comprised of t(8;22) or the t(2;8) translocations (Taub *et al*., 1982; Blum *et al*., 2004; Spender and Inman, 2014). In 2012 alone there was an estimated 386 000 cases of NHL, accounting for 2.7 % of all cancers (Ferlay *et al*., 2015). As opposed to most cancers where increased age heightens the risk of development, BL is trimodal, with three distinctly different onset ages, infancy, adulthood and old age (Donadoni *et al*., 2013). Burkitt's lymphoma has been classified into three different subtypes: endemic, sporadic and HIV-related. The endemic form is the most common childhood cancer in equatorial Africa as well as Africa as a whole, and is characterized by rapidly growing neoplasms predominantly affecting the jaw and abdomen which without treatment is fatal within months (Blum *et al*., 2004; Wright *et al*., 2009). These cases have been shown to be predominantly in children, with a total of 70 % new cases and deaths affecting this age group (Jemal *et al*., 2012). Almost all endemic BL have EBV infections (Molyneux *et al*., 2012), although EBV is not BL specific (Robbiani *et al*., 2015). Malaria on the other hand has also been strongly associated with endemic BL development, however, its role has remained elusive (Robbiani *et al*., 2015). Robbiani *et al*. (2015) found that infection with *Plasmodium* does not induce cancer development, but require the addition EBV or other mutational events for BL to develop (Robbiani *et al*., 2015). Sporadic BL has been shown to have no specific geographical distribution and affects the abdomen predominantly. HIV-related BL, which is more relevant to the Southern African region (Blum *et al*., 2004), is discussed in the next section.

1.6 Burkitt's lymphoma in an HIV context

BL is classified as an aggressive AIDS-related lymphoma (HIV-BL). With BL accounting for 30 % of all lymphoproliferative malignancies diagnosed in HIV-positive patients and with South Africa having more people living with HIV than any other country, this cancer is especially relevant locally (Dorrington *et al*., 2001; Lim *et al*., 2005; Donodoni *et al*., 2013; Spender and Inman, 2014). BL is 1 000 times more common in HIV patients than the general population (Beral and Peterman, 1991). In Western countries the manifestation of HIV infection is often the first clinical symptoms of BL (Donadoni *et al*., 2013).

Prior to the introduction of highly active antiretroviral therapy (HAART), the chance of developing NHL was 60 - 200 times higher than in HIV-negative patients (Donadoni *et al*., 2013). HAART which consists of a combination of several antiretroviral drugs, was prescribed worldwide in 1996 and greatly improved the outcome of HIV-positive patients. This treatment improved patients' host immune response, reduced the development of opportunistic infections and decreased the incidence of HIV-related NHL (Donadoni *et al*., 2013). Additionally, it allowed HIV-positive patients with cancer to receive chemotherapy which improved their prognosis. Over the years the treatments have changed with high income countries using more advanced techniques compared to lower income countries (Molyneux *et al*., 2012). Montoto *et al*. (2010), retrospectively looked at HIV-BL patients undergoing intensive CODOX-M/IVAC (cyclophosphamide, doxorubicin, vincristine and methotrexate) treatment while on HAART, and the results showed a 52 % survival rate. The chemotherapeutic treatment CHOP (cyclophosphamide, doxorubicin, vincristine and prednisone), is less intensive and has shown more frequent relapses and lower survival (Dave *et al*., 2006). The use of CHOP correlated to AID expression was determined in patients with diffuse large B-cell lymphoma (DLBCL) which is also classified as an aggressive AIDS-related B-cell lymphoma. With the advent of HAART in HIV-positive patients the survival rate increased significantly (Lim *et al*., 2005; Gopal *et al*., 2013) and found that elevated AID expression resulted in a poorer response to CHOP treatment (Kawamura *et al*., 2015), highlighting a possible reason for such a low response in BL which by definition have high AID expression levels. There has also been an improvement in treatment during the contemporary era (2005 – 2010) with increased infusional and intensive regimens with greater use of rituximab, which

was the first monoclonal antibody approved for therapeutic use in cancer patients as this targets the CD20 marker on the surface of B-cells (Smith *et al*., 2003), in combination with HAART (Barta *et al*., 2015, Schommers *et al*., 2015). Although there are currently multiple treatment options for HIV-BL patients, these treatments are inadequate and further therapies need development. A possible mechanism of action in HIV-BL patients is that high HIV viral loads cause a chronic antigenic stimulus, thus increasing AID expression, and leading to enhanced *c-MYC*-IgH translocations. Additionally when the CD40 ligand was incorporated into an HIV virion, it was shown to be able to activate AID (Epeldegui *et al*., 2010). In that particular study, HIV virions containing the CD40 ligand were combined with circulating B-cells, which resulted in increased gene expression of AID as well as increased AID protein. Contrary to what is expected, it has been observed that the risk of developing HIV-BL increases with the increase in CD4 count (majority ≥ 250 per µl CD4, risk lowers at ≤ 50 per µl CD4, with only 15 % of patients having a CD4 count of < 100 per µl) which is in contrast to other HIV-NHL, indicating that a functional immune system may in fact be either a cause of HIV-BL or facilitating the progression of cancer (Donadoni *et al*., 2013). Despite these reports, there is very little evidence, at the pathological and molecular levels, supporting these claims. It is therefore essential to focus research on elucidating the molecular mechanisms of HIV-BL pathogenesis if better therapy is to be developed.

1.7 Relationship between AID and *c-MYC* translocation

In transgenic AID mice, expression of AID was identified as critical for the translocation T(12;15), which corresponds to the human t(8;14) translocation region characteristic of BL (Kotani *et al*., 2007). In 2006, Ramiro *et al*. retrovirally transduced AID into BALB/c $AID^{-/-}$ mice, upon stimulation with LPS and IL-4, a 10-fold overexpression of AID was induced and *de novo c-myc*-IgH reciprocal translocations were produced. This reiterates that AID is required for both SHM and CSR and aberrant expression of this protein can potentially cause the reciprocal translocations that are found in BL patients (Ramiro *et al*., 2006). Interestingly, in a retrospective study, Epeldegui *et al*. (2007), found elevated AID expression in the peripheral blood mononuclear cells of HIV-positive patients who were later diagnosed with NHL. The levels of AID were elevated as compared to AIDS patients who did not develop NHL and HIV-negative patients. Additionally, AID expression differed depending on the subtype of NHL, with those who developed BL having the highest levels. In an earlier study, Müller *et al*. (1995)

investigated the presence of the t(8;14) translocation in 114 HIV-positive patients compared to 99 HIV-negative individuals and found a fivefold greater incidence of the translocation among the HIV-positive patients (10.5 % in HIV-positive versus 2 % in HIV-negative). In that study, AID expression was not implicated since AID was only subsequently discovered in 1999 (Müller *et al*., 1995; Muramatsu *et al*., 1999). It has been shown that IL-6 levels are increased in HIV positive patients, and as previously mentioned, this specific interleukin has been implicated in AID upregulation (Breen *et al*., 1990; Ramiro *et al*., 2004). These separate studies infer that HIV infection lead to an increase in AID expression, thus increasing the chance of aberrant CSR and SHM occurring and thus development of NHL. The type of NHL is also correlated to the level of AID expression, with higher AID expression seen in patients who developed BL (Epeldegui *et al*., 2007).

1.8 Aberrant expression of AID in other non-lymphoid cancers

Although the function of AID is well defined in B-cells, its overexpression has been linked with cancers of mainly lymphoid origins (Shimizu *et al*., 2012). But more recent literature has also implicated AID overexpression in the development of several cancers of non-lymphoid origin, which are associated with an increased immune response and inflammation. For example aberrant expression of AID has been identified in cancers affecting the gastric epithelial tract due to inflammation caused by the hepatitis C virus (HCV) and *Helicobacter pylori* (Marusawa, 2008; Endo *et al*., 2011; Kim *et al*., 2014; Nagata *et al*., 2014). A key feature of inflammation induced cancer is the immune response regulator NF-κB (Shimizu *et al*., 2012). As NF-κB has been shown to regulate AID expression, which itself is expressed under the stimulation of inflammation, it is not surprising that it has been detected in epithelial cells with chronic inflammation (Chiba and Marusawa, 2009; Shimizu *et al*., 2012). NF-κB has been shown to be activated in epithelial cells under chronic inflammation (Shimizu *et al*., 2012), thus implicating AID as a possible driving force behind oncogenesis. Studies have shown that AID is overexpressed in the gastrointestinal tract (GIT) (Fichtner-Feigl *et al*., 2015), with high AID expression in gastric adenocarcinoma (Batsaikhan *et al*., 2014).

In mice, ectopic expression of *aid* causes tumours to develop in various organs, including the liver (Endo *et al*., 2007). Additionally, the expression of endogenous AID could be induced in

human hepatocytes upon treatment with tumour necrosis factor-α, via NF-κB activation, and this expression was even more enhanced in the presence of HCV (Kou *et al*., 2007). AID is also overexpressed in oral squamous cell carcinoma (Nakanishi *et al*., 2013). The oral cavity is exposed to external elements such as microbes and chemicals which trigger inflammatory responses thus inducing AID expression which may contribute to transformation of those cells (Nakanishi *et al*., 2013). Babbage *et al*. (2006), found that Ig rearrangements normally associated with B-cells were identified in breast cancer cell lines overexpressing AID at a comparable level to a known AID overexpressing cancerous cell line. Muñoz *et al*. (2013) showed that AID is needed for the epithelial-to-mesenchymal transition in mammary epithelial cells which both indicate that AID may play a role in breast cancer development. Furthermore, Shinmura *et al*. (2011), found that AID mRNA transcripts were detected in 29.4 % of lung cancer cell lines and 31.4 % of primary lung cancer patients indicating a possible role in lung cancer. Studies in transgenic mice, where AID was constitutively and ubiquitously expressed, found the development of malignancies in the skin, liver, lung and GIT (Morisawa *et al*., 2008). It also appears that AID causes specific nucleotide changes dependent on the organs where AID is over expressed which were identified by investigating at the genotypic changes in organ specific cancers that developed in these transgenic mice. Double stranded DNA breaks have been shown to be associated with certain epithelial cancers, such as in the prostate, however, an association between AID and epithelial cancer development has not been characterised.

1.9 Conclusion

AID is essential for antibody diversification, however, if not appropriately regulated and overexpressed, AID may erroneously target proto-oncogenes, such as the *c-MYC* gene, leading to cellular transformation and the development of malignancies. Although a link between AID and *c-MYC* translocation has been established, little is known about other cellular consequences as a result of AID overexpression. Therefore more detailed studies on its expression and function in carcinogenesis is needed.

1.10 Aims and objectives of the proposed research

As described earlier, AID is highly overexpressed is BL, which is of high prevalence among HIV-positive individuals. Although there have been significant advances in the treatment of HIV-negative patients suffering from BL, the prognosis of HIV-positive patients with BL remains poor, and this is despite the introduction of HAART. Therefore there is an urgent need for further research in elucidating the molecular mechanism of HIV-BL, and studying the function of AID in BL is one way of achieving this, with the ultimate aim to use the findings to design more effective therapies.

As a means to understand the mechanisms by which AID may be leading to cellular transformation, the proposed project aims to create cellular models which will be used to study cellular and phenotypic changes brought about by AID overexpression, in order to study the molecular mechanisms and pathways responsible for the observed changes.

The specific objectives are as follows:

1. **To screen a panel of Burkitt's lymphoma cell lines, and a panel of epithelial derived cancer cell lines, for AID expression. Based on the result, one cell line from each category will be selected for ectopic AID expression.**
2. **To establish AID overexpressing cell lines and study cellular characteristics associated with cancer, including cell proliferation and viability, migration, genome integrity, B-cell phenotype (CD marker expression) and sensitivity to a chemotherapeutic drug.**
3. **To establish AID knockdown models to study AID functions as outlined in objective 2 above.**

Chapter 2: Materials and Methods

2.1 Cell culture

2.1.1 Cell line culturing and medium

A total of 23 cell lines were utilised in this study. The normal EBV-immortalised lymphoblastoid cell line (L1439A) was created at the University of Cape Town, in the Chemical Pathology Department by Ms Ingrid Baumgarten using an adapted protocol (Freshney, 2010). The Ramos cell line (ATCC® CRL-1596™) was obtained from the American Type Culture Collection (ATCC, US), the remaining three Burkitt's lymphoma (BL) cell lines (BL2, P3HR1 and Seraphina) were kindly donated by Professor Bernheim (French Institute of Health and Medical Research), three of the prostate cell lines (PNT1A, PNT2 and PC-3) were kindly donated by Associate Professor Sharon Prince (University of Cape Town) and two prostate cell lines (LnCaP and Du145) were kindly donated by Dr Luiz Zerbini (University of Cape Town). The colon cancer cell lines (Caco-2, DLD-1, Colo205, Colo206F, HT-29 and LoVo), oesophageal cancer cell lines (KYSE-30, KYSE-520, OE19 and OE33) and head and neck cancer cell line (UMSCC22b) were kindly donated by Professor Stoecklein (Heinrich-Heine University Düsseldorf). The culture conditions for each cell line is detailed in Table I below. Two types of medium were used, Dulbecco's Modified Eagle Medium (DMEM) or Roswell Park Memorial Institute (RPMI) medium supplemented with between 10 % to 20 % foetal bovine serum (FBS) (Table I).

Table I: Information and growth conditions for cell lines used in this study.

Cell Line	Cell Type	Database ID	Suspension or Adhesion	Medium
L1439A	Normal EBV-Immortalised Lymphoblastoid Cell Line	N/A	Suspension	DMEM (20 % FBS)
BL-2	Burkitt's Lymphoma Cell Line	DSMZ: ACC-625	Suspension	RPMI (20 % FBS)
P3HR1		ECACC: 86010701	Suspension	RPMI (10 % FBS)
Ramos		ATCC®: CRL-1596™	Suspension	RPMI (10 % FBS)
Seraphina		NCBI: C102	Suspension	RPMI (10 % FBS)
Du145	Prostate Cancer Cell Line	ATCC®: HTB-81™	Adherent	DMEM (10 % FBS)
LnCaP		ATCC®: CRL-1740™	Adherent	RPMI (10 % FBS)
PC-3		ATCC®: CRL-1435™	Adherent	RPMI (10 % FBS)
PNT1A	Normal Prostate Cell Line	ECACC: 95012614	Adherent	RPMI (10 % FBS)
PNT2		ECACC: 95012613	Adherent	RPMI (10 % FBS)
Caco-2	Colon Cancer Cell Line	ATCC®: CLL-121™	Adherent	DMEM (10 % FBS)
DLD-1		ATCC®: HTB-37™	Adherent	RPMI (10 % FBS)
HT-29		ATCC®: CCL-221™	Adherent	RPMI (10 % FBS)
LoVo		ATCC®: HTB-38™	Adherent	RPMI (10 % FBS)
Colo205		ATCC®: CCL-229™	Adherent	RPMI (10 % FBS)
Colo206F		ATCC®: CCL-222™	Adherent/suspension	RPMI (10 % FBS)
KYSE-30	Oesophageal Cancer Cell Line	ECACC: 93052620	Semi-adherent	RPMI (10 % FBS)
KYSE-520		DSMZ: ACC 371	Adherent	RPMI (10 % FBS)
OE19		ECACC: 94072011	Adherent	RPMI (10 % FBS)
OE33		ECACC: 96071721	Adherent	RPMI (10 % FBS)
UMSCC22b	Head and Neck Cancer Cell Line	ECACC: 96070808	Adherent	RPMI (10 % FBS)
COS-7	African Green Monkey Kidney Cell Line	ATCC®: CRL-1651™	Adherent	DMEM (10 % FBS)
HT-1080	Fibrosarcoma	ATCC®: CCL-121™	Adherent	DMEM (10 % FBS)

2.1.2 Resuscitation of frozen cell lines

Each cell line was removed from liquid nitrogen storage, the cells thawed and placed in 4 ml of culture medium and centrifuged for between 1 000 to 2 000 rpm for three to five minutes, the supernatant was removed and cells were gently resuspended in 1 ml of pre-warmed culture medium, then transferred into appropriate culture dishes containing culture medium. All cells were incubated at 37 °C in a humidified atmosphere with 5 % CO_2.

2.1.3 Sub-culturing

2.1.3.1 Suspension cell lines

Confluency of cells in suspension was determined through visualisation under a light microscope, cell counting, and as observation of colour change of medium (from red to yellow), which contained a phenol red dye as a pH indicator. To maintain healthy cells, a proportion of the cells and culture medium was removed once the culture medium turned yellow and replaced with fresh culture medium, thus preventing the cells from becoming too confluent and entering quiescence.

2.1.3.2 Adherent cell lines

Once cells reached a confluency of approximately 80 % (80 % of the surface area of the dish is covered with cells), the culture medium was removed, the cells were washed using sterile 1X PBS, trypsinised using 1X Trypsin-EDTA (Appendix A) (cells were incubated at 37 °C with 2 ml of 1X Trypsin-EDTA for between one to ten minutes, depending on the cell line, and the reaction stopped by the addition of culture medium). The cells were then resuspended, and an aliquot of the cells transferred into a new culture dish containing fresh medium.

2.1.4 Freezing and storage of the cell lines

Freezing of cells was performed using between 5 % and 10 % of either DMSO or glycerol as a cryopreservative agent, depending on the recommendation of each cell line. Adhesion cells were trypsinised as described above, counted, centrifuged and then the appropriate amount resuspended in freezing medium. For suspension cells: cells were counted, then centrifuged and the appropriate amount resuspended in pre-chilled freezing medium. Cells were counted

using the haemocytometer and in general, cells were frozen in 1 ml aliquots at 1 x 10^6 cells per ml in cryovials. The cryovials were cooled to -80 °C overnight using Mr Frosty (Thermo Scientific™, US) which uses isopropanol to decrease the temperature of the samples by 1 °C per minute. The vials were then stored under liquid nitrogen long term.

2.1.5 Mycoplasma testing

All cell lines were tested for Mycoplasma contamination. Cells were initially plated in Penicillin-Streptomycin (PenStrep) antibiotic free culture medium for a minimum of three days in a 35 mm tissue culture dish, thus allowing any mycoplasma present to proliferate to an easily detectable level. The principle of mycoplasma contamination determination in adhesion and suspension cells are the same, however, the protocols differ as described below.

2.1.5.1 Adherent cell lines

Coverslips were sterilized by soaking in 100 % ethanol and placed in a 35 mm dish and allowed to air-dry. Cells were seeded onto the coverslips in PenStrep-free culture medium and allowed to grow for a minimum of three days. The medium was removed, cells were fixed in fixing solution (Appendix A) for 10 seconds, washed using water, and cells stained using Hoechst 33342 stain (#H1399, Invitrogen, US) for approximately eight minutes. Cells were then washed again in water and mounted on a microscope slide in mounting fluid (Appendix A) and visualised.

2.1.5.2 Suspension cell lines

For suspension cell lines, 1 x 10^5 cells were grown in PenStrep-free medium for a minimum of three days and 3 µl was placed directly onto a clean microscope slide and air-dried, fixed for two minutes by adding just enough fixative (Appendix A) to cover the cells, washed with water, then stained with Hoechst 33342 stain (#H1399, Invitrogen, US) (Appendix A) for eight minutes. The stain was removed with water and the cells air-dried. A clean coverslip with a drop of mounting fluid (Appendix A) was placed onto the cells and then visualised.

2.1.5.3 Visualisation

The slides were visualised using a fluorescent microscope (Zeiss Axiovert 200M, Carl Zeiss Microimaging, Germany). Hoechst stain binds to all nuclear material and therefore a positive mycoplasma result is indicated as fluorescent dots on the cellular membrane and in the cytoplasm of the cells. A negative mycoplasma result will only have the nucleus of the cell staining positive.

2.2 Total RNA Isolation

Prior to RNA extraction, all plastic- and glassware used in the RNA isolation were soaked overnight in 0.1 % diethylpyrocarbonate (DEPC) solution in water, which inhibits RNases. These were then autoclaved to cause hydrolysis of the DEPC due to its toxic nature (Blumberg, 1987). The High Pure RNA Isolation Kit (Roche, Germany) was used for total RNA isolation of all cells, according to the prescribed protocol. For the adhesion cell lines, the cells were washed twice with 200 µl 1X PBS and then scraped in 400 µl of Lysis/Binding Buffer. The adhesion cells were then placed in the High Pure Filter Tube. A similar procedure was performed for the suspension cells; the cells were placed in a 1.5 ml tube and washed with 200 µl 1X PBS. The majority of the PBS was aspirated and 400 µl of lysis/-binding buffer was then added to the cells and vortexed for 15 s. The cells were then placed into the High Pure Filter Tube. The procedure was then the same for both the adhesion and suspension cell lines. These filter tubes were then placed in the Collection Tube provided in the kit and centrifuged for 15 s at 8000 x *g*. The flow-through was discarded and the RNA in the filter was treated with DNase I solution for 15 minutes at approximately 15 to 25 °C. Thereafter, the filter was washed with 500 µl of Wash Buffer I, followed by repeating this step twice, first using 500 µl of Wash Buffer II and then with 200 µl of the same buffer, this time centrifuging for two minutes at 13 000 x *g* to remove all excess wash buffer. The total RNA was then eluted from the filter using 60 to 80 µl of Elution Buffer. The purity and concentration of the samples were assessed using the NanoDrop™ ND-1000 (Thermo Scientific™, US) aliquoted and stored at -80 °C.

2.3 Agarose gel electrophoresis of RNA samples

Agarose gel electrophoresis is a technique whereby nucleic acid is separated according to size by using an electric current to pull the negatively charged molecules through the pores of an agarose gel. A very small amount of nucleic acid intercalating agent Ethidium Bromide (10 mg/ml stock; Sigma Aldrich) is added at a dilution of approximately 1:15 000 for visualisation under ultra-violet light (UV). A 1 % agarose gel was prepared as described in Appendix A. The samples loaded contained 300 ng of RNA made up to a total of 10 µl using 2X RNA loading buffer (Appendix A). The samples were then denatured for five minutes at 55 °C before loading onto the agarose gel and electrophoresed for approximately one hour in 1X TBE running buffer (made up in DEPC treated water) (Appendix A). The gel was visualised over a UV-transilluminator.

2.4 Reverse transcription of mRNA samples

The mRNA found in the total RNA samples isolated from the cell lines were converted to cDNA by reverse transcription using the iScript™ cDNA Synthesis Kit (Bio-Rad, US) and oligo (dT) and random hexamer primers using a modified MMLV-derived reverse transcriptase. A total of 200 ng of RNA was used for each sample and Table II below shows the components of one reverse transcription reaction.

Table II: Composition of reverse transcription reaction.

Components	Volume per reaction (µl)
5x iScript reaction mix	4 µl
iScript reverse transcriptase	1 µl
Nuclease-free water	15 µl - *x*
RNA template (150 ng)	*x* µl
Total	20 µl

The recommended reaction protocol was followed, whereby each sample was incubated at 25 °C for five minutes, followed by 42 °C for 30 minutes and then terminated with a five

minute step at 85 °C using the Multigene™ OptiMax Thermal Cycler (Labnet International, Inc., US). The resulting cDNA samples were then stored at -20 °C.

2.5 Generation of standard curve for absolute quantification using qPCR

A standard curve was produced to quantify the total amount of Activation Induced cytidine Deaminase (AID) in each sample compared to two housekeeping genes, GAPDH and RPL27.

2.5.1 Conventional PCR

L1439A cDNA was used as template for amplifying AID, GAPDH and RPL27 using PCR, to use in the generation of the standard curves. Standard PCR was performed using the MyTaq™ DNA Polymerase (Bioline, UK) and setup as shown in Table III with the primers sets shown in Table IV.

Table III: Composition of the MyTaq™ DNA polymerase chain reaction.

Components	Final Concentration	Per 25 µl Reaction
5X MyTaq Reaction Buffer	1 X	5 µl
Forward Primer (10 µM)	250 nM	1 µl
Reverse Primer (10 µM)	250 nM	1 µl
Template DNA		1 µl
MyTaq Polymerase		1 µl
PCR-grade Water		16 µl
Total		25 µl

Table IV: Primer sequences used in the PCR and qPCR reactions.

Target Gene	Orientation	Primer Sequence (5' - 3')	Product Size
GAPDH	Forward	GAAGGCTGGGGCTCATTT	133 bp
	Reverse	CAGGAGGCATTGCTGATGAT	
RPL27	Forward	ATCGCCAAGAGATCAAAGATAA	123 bp
	Reverse	TCTGAAGACATCCTTATTGACG	
AID	Forward	CCAAACCATCTCTCCAAAGC	108 bp
	Reverse	CATCCCCACCCATAACAATC	

The cycling conditions used are as follows: a pre-incubation step at 95 °C for one minute, followed by 30 cycles comprising a denaturation step at 95 °C for 15 seconds, an annealing step at 50 °C for 15 seconds and an elongation step at 72 °C for ten seconds.

2.5.2 Purification of PCR products

PCR products were purified, using the GeneJET™ PCR Purification Kit (Thermo Scientific, US), whereby all the remnants of the PCR reactions such as primers and dNTPs are removed. The manufacturer's protocol was followed. Briefly, 38 µl of PCR product was mixed with equal volume of Binding Buffer and equal volume of isopropanol, and then transferred into a GeneJET purification column, centrifuged for one minute at 14 000 rpm, the flow-through discarded and the DNA trapped in the glass fibre was washed with 700 µl of Wash Buffer, excess buffer was removed using an additional centrifugation step at 14 000 rpm, and then eluted in 40 µl of Elution Buffer. The eluted PCR products were quantified using the NanoDrop™ ND-1000 (Thermo Scientific™, US) and stored at -20 °C.

2.5.3 Agarose gel electrophoresis of DNA samples

Agarose gel electrophoresis is a technique whereby nucleic acid is separated according to size by using an electric current to pull the negatively charged molecules through the pores of an agarose gel. A very small amount of nucleic acid intercalating agent Ethidium Bromide (10 mg/ml stock; Sigma Aldrich) is added at a dilution of approximately 1:15 000 for visualisation under UV light. A 1 % agarose gel was prepared as described in Appendix A. The samples

loaded contained 3 µl 10X DNA loading buffer (Appendix A). The samples were loading onto the agarose gel and electrophoresed for approximately one hour in 1X TBE running buffer (Appendix A). The gel was visualised over a UV-transilluminator.

2.6 Quantitative real-time PCR (qPCR)

To quantify the total amount of AID, GAPDH and RPL27 mRNA in each sample the KAPA SYBR® FAST qPCR Kit (Kapa Biosystems, SA) optimised for the LightCycler® 480 (Roche, Germany) was used. Table V below shows the components of each qPCR reaction.

Table V: Composition of the KAPA SYBR® FAST qPCR reactions.

Components	Final Concentration	Per 20 µl Reaction
KAPA SYBR® FAST qPCR Master Mix	1 X	10 µl
Forward Primer (20 µM)	200 nM	0.8 µl
Reverse Primer (20 µM)	200 nM	0.8 µl
Template DNA	10% of reaction volume	2 µl
PCR-grade Water		6.4 µl
Total		20 µl

The qPCR reactions were setup according to Table V in a 96-well plate and sealed using clear film. The cycling conditions used were as follows: a pre-incubation step at 95 °C for three minutes, followed by 45 cycles made up of a three second denaturation step at 95 °C, and a combined annealing and elongation step at 60 °C for 30 seconds where the fluorescent profile was acquired at the end point of the elongation step. After the 45 cycles, the samples were then subjected to a melting curve. The samples were incubated at 95 °C for five seconds, the temperature then lowered to 65 °C for one minute. The temperature was then continuously ramped up at a speed of 2.2 °C per second with five fluorescent acquisitions for every °C increase until the samples reached the temperature of 97 °C. The qPCR data was captured and analysed on the LightCycler® 480 Software (Version 1.5.0.39, Roche, Germany).

2.7 Protein extraction and quantification

2.7.1 Protein extraction using RIPA buffer

Radio-Immunoprecipitation Assay (RIPA) buffer was used for protein extraction due to its efficacy as it utilises three non-ionic and ionic detergents which lyse and permeabilise the cells. The RIPA solution was prepared according to Appendix A by combining the RIPA buffer with a 7X cOmplete™, Mini, EDTA-free, Protease Inhibitor (Roche, Germany) which protects the extracted protein samples from degradation by proteases present in the cell lysates. The same principles apply to both suspension and adhesion cell lines, however, the processes differ slightly as described below.

2.7.1.1 Adherent cells

Culture plates containing the cells were placed on ice, the medium removed and cells washed three times with ice cold 1X PBS. In a 10 cm plate, approximately 500 µl of RIPA solution was added and the cells were scraped, transferred into a 1.5 ml tube and stored at -80 °C overnight for optimum lysis. Thereafter cells were thawed on ice, centrifuged at 4 °C (12 000 rpm) for 20 minutes to remove cell debris, and the supernatant aliquoted and stored at -80 °C.

2.7.1.2 Suspension cells

Cell suspension was transferred into 15 ml Falcon tubes, and centrifuged for four minutes at 2000 rpm. The supernatant was removed and the pellet was washed three times by resuspending in ice cold 1X PBS followed by centrifugation. The cells were resuspended in RIPA solution (between 200 µl and 500 µl depending on pellet size), transferred into a 1.5 ml tube and stored at -80 °C overnight for optimum lysis. Thereafter cells were thawed on ice, centrifuged at 4 °C (12 000 rpm) for 20 minutes to remove cell debris, and the supernatant aliquoted and stored at -80 °C.

2.7.2 Protein Quantification

The bicinchoninic acid (BCA) reagent was used to determine the protein concentrations, using the Pierce™ BCA Assay kit (Thermo Scientific™, US). This assay utilises a sensitive and selective colourimetric detection where a unique reagent containing BCA detects the reduction of Cu^{2+}

to Cu^{1+} in an alkaline medium. A standard curve is generated using bovine serum albumin (BSA) at a range of concentrations (2000 µg/ml, 1000 µg/ml, 500 µg/ml, 125 µg/ml and 0 µg/ml). Briefly, Reagent A and Reagent B are combined in a ratio of 50:1 respectively to produce the working reagent. In a 96-well plate, 10 µl of protein sample diluted in RIPA buffer (1:2 or 1:5) or standard is added in duplicate, followed by 100 µl of working reagent. The plate is then incubated at 37 °C for 30 minutes and the colour change is measured using the Glo-Max®-Multi+ multiplate reader (Promega, US) at a wavelength of 560 nm. The experimental sample concentrations are then extrapolated from the standard curve.

2.7.3 Protein extraction using 2X boiling blue buffer

Protein was extracted directly by placing the cells into loading buffer and boiling at 95 °C, this denatures and linearises the proteins which can then be immediately loaded onto a SDS-PAGE. Although the principle was the same, the method differed for adhesion and suspension cells as described below.

2.7.3.1 Adherent cells

Media was removed and the cells washed twice with cold 1X PBS. In a 10 cm plate, approximately 70 µl of boiling 2X blue Buffer (Appendix A) was added, the cells scraped and transferred into a 1.5 ml tube. The solution was boiled at 95 °C for ten minutes, pulse spun and either used directly on the SDS-PAGE or cooled to room temperature and stored at -20 °C.

2.7.3.2 Suspension cells

Cell suspension was transferred into a 1.5 ml tube and centrifuged 1 000 rpm for five minutes. The supernatant was removed and the pellet washed twice by resuspending in cold 1X PBS. The cells were resuspended in 2X boiling blue buffer (between 30 µl and 60 µl depending on pellet size) and boiled for ten minutes at 95 °C, pulse spun and either used directly on the SDS-PAGE or cooled to room temperature and stored at -20 °C.

2.8 SDS-PAGE and western blotting

2.8.1 SDS-PAGE

To visualise proteins, a polyacrylamide gel electrophoresis (PAGE) was performed using an anionic detergent, sodium dodecyl sulphate (SDS), to linearise and negatively charge proteins. Using the Mini-PROTEAN 3 casting apparatus (Bio-Rad, US), as per the manufacturer's instructions, a 1.5 mm 12 % resolving gel (Appendix A) and a 5 % stacking gel (Appendix A) were prepared. Components used in the protein sample preparation were made up according to Table VI. Dithiothreitol (DTT) was used as this is a small redox reagent used to reduce the disulphide bridges of the proteins.

Table VI: Components of the protein sample preparation for SDS-PAGE.

Components	Volume (µl)
Protein Sample (20 µg)	*x* µl
5X SDS Loading Buffer	6 µl
100 mM DTT	1 µl
1X RIPA Buffer	1 µl
Nuclease-free dH_2O	35 - *x* µl

Samples were denatured at 95 °C for ten minutes prior to loading. Five microliters of the PageRuler™ Prestained Protein Ladder (Thermo Scientific™, US) and 30 µl of the samples were loaded onto the gel with the addition of 5X loading dye to all empty lanes to ensure proteins electrophorese vertically. This was then connected to the Bio-Rad power pack and electrophoresed for approximately 200 minutes at 100 V.

2.8.2 Protein transfer

The proteins separated on the gel were then transferred to nitrocellulose (Bio-Rad, US). This was achieved by placing the gel and nitrocellulose membrane in the correct order of the cassette as shown in Figure 2.1. The cassette is then placed into the Mini-PROTEAN 3 casting apparatus (Bio-Rad, US), with cold 1X transfer buffer (Appendix A) and an ice pack. The power pack was then set at 100 V for 75 minutes.

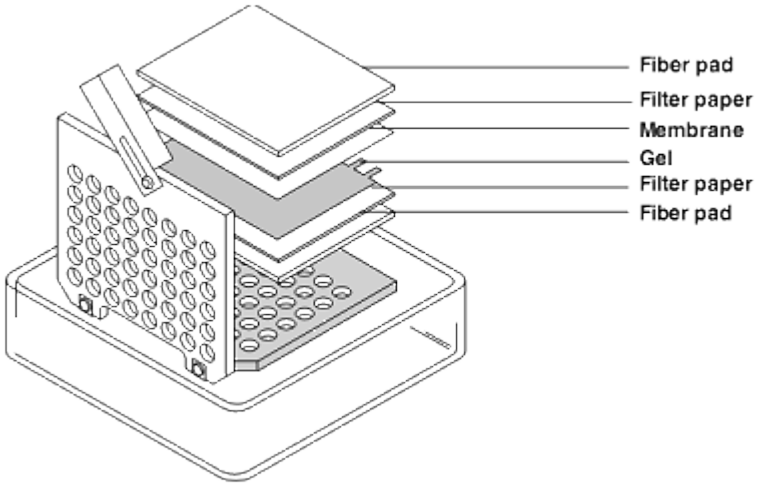

Figure 2.1: Diagram of a western blot cassette setup. Each item was placed in the order shown to ensure the protein was transferred from the gel on the nitrocellulose membrane. This image was adapted from the Mini Trans-Blot® Electrophoretic Transfer Cell manual (Bio-Rad, US).

2.8.3 Antibody incubation and visualisation

Upon completion of the transfer, the nitrocellulose membrane was washed in PBS/Tween and then blocked in PBS/Tween containing 5 % fat-free milk powder for one hour (Appendix A) with gentle shaking at room temperature. After blocking, the membranes were incubated with primary antibody diluted to the desired concentration (Table VII), and incubated overnight at 4 °C in blocking solution with gentle shaking. The membrane was then washed in PBS/Tween (2 x 10 minutes followed by 2 x 5 minute washes) before incubation with the appropriate HRP-conjugated secondary antibody diluted in blocking solution, for one hour at room temperature with gentle shaking (Table VII). The membrane was then washed as before in PBS/Tween and visualised by enhanced chemiluminescence using the Clarity™ Western ECL Substrate (Bio-Rad, USA) as per the manufacturer's instructions. Membranes were exposed to X-ray film and the resulting chemiluminescent signal captured by developing and fixing the film.

Table VII: Primary and secondary antibody concentrations used in this study.

Protein	Primary Antibody Dilution	Secondary Antibody Dilution
AID	1:1000	1:5000 (goat anti-mouse)
p38	1:5000	1:5000 (goat anti-rabbit)
γ-H2AX*	1:1000	1:5000 (goat anti-rabbit)

*For the γ-H2AX protein, TBS (Appendix A) was used in place of PBS for all washes and incubations, with antibody diluted in TBS/Tween containing 5 % BSA (Appendix A).

2.8.4 Membrane stripping

The antibodies were removed from the blot by incubating in 50 °C pre-warmed stripping buffer (Appendix A) at 50 °C for 30 minutes, with brief agitation every ten minutes. The membrane was then washed twice for ten minutes with PBS/Tween. The blot was able to be reused from the blocking stage as described above, in order that the internal loading control protein p38 could be detected. The developed film of the western blots were than scanned and the intensity of the bands quantified and normalised using the Li-Cor Image Studio Lite software (Version 4.0, Germany).

2.9 Plasmid constructs

pEGFP-N3-AID and pEGFP-N3-Empty were kindly donated by Professor Bernhard Lüscher from RWTH Aachen University in Germany. The pcDNA-3.1-AID and pcDNA-3.1-Empty plasmids were kindly donated by Professor Reuben Harris from the University of Minnesota in the United States. The pCMV-β-gal plasmid was kindly donated by Professor Sharon Prince from the University of Cape Town in South Africa.

2.9.1 Restriction enzyme digests of plasmid constructs

Restriction enzyme digests were performed on the pEGFP-N3-AID and pEGFP-N3-Empty plasmids. Two restriction enzymes were selected, *Eco*RI and *Not*I, which both used the buffer system H (Promega, US). The reactions were setup according to Table VIII below.

Table VIII: Reaction components for the restriction digest of the pEGFP-N3 plasmids.

Components	Per 30 µl Reaction
Plasmid Template (500 ng)	*x* µl
*Eco*RI (10u/µl)	1 µl
*Not*I (10u/µl)	1 µl
10X Buffer H	3 µl
Sterile dH_2O	25 - *x* µl
Total	30 µl

The reactions were incubated at 37 °C for two hours and stopped by the addition of 3 µl 1X DNA Loading Dye (Appendix A) and then separated using agarose gel electrophoresis (Section 2.5.3).

2.10 Sequencing

The pEGFP-N3-AID plasmid was sent for sequencing using the forward primer for the cytomegalovirus (CMV) as this region was upstream of the AID and EGFP tag. The pEGFP-N3-AID plasmid was sent to Inqaba Biotec™ (SA) for sequencing. The results were received and analysed using Chromos LITE (Version 2.1.1, Technelysium Pty Ltd).

2.11 Transfection

For successful transfection, cells need to be at optimum confluency (60 – 80 %), upon reaching this level, the cells were counted using a haemocytometer and resuspended in culture medium lacking FBS or antibiotic. In each well of a six-well plate, 2 ml solution of cells and culture medium without FBS or antibiotic were placed and incubated at 37 °C overnight. Each transfection reaction contained 3 µl X-tremeGENE HP DNA Transfection Reagent (Roche, Germany) added dropwise to 97 µl of culture medium without FBS or antibiotic and incubated for five minutes. This solution was then placed into a 1.5 ml tube containing 500 ng of plasmid DNA and incubated for a further 15 minutes. After the incubation, 97 µl of the solution was added to each well of the six-well plate dropwise and gently mixed. The cell with plasmid DNA and transfection reagent were incubated at 37 °C in the CO_2 incubator for 30 hours.

2.12 WST-1 proliferation assay

The WST-1 assay was used to measure cell viability as it contains tetrazolium salts which are cleaved to formazan dye in the presence of cellular enzymes produced by metabolically active cells, thus the more salt cleaved, the greater the colour change which indirectly indicates cell viability.

2.12.1 Standard WST-1 proliferation assay

The standard protocol for the WST-1 proliferation assay was 100 µl of cells plated at approximately 1 x 10^5 cells per well in a 96-well plate, with the addition of 10 µl of the WST-1 proliferation reagent (Roche, Germany), incubated for two hours at 37 °C followed by measurement of colour change using the GloMax®-Multi microplate reader (Promega, US).

2.12.2 Antibiotic kill curve using the WST-1 proliferation assay

To create a stably transfected cell line, cells in which the AID expressing locus has been incorporated into the genome, together with a marker for antibiotic resistance, needed to be selected. Both plasmids used in this study contained the G418 antibiotic resistance gene thus the sensitivity of untransfected cells needed to be established in order to determine the concentration of G418 to use to select stably transfected cells. Cells were plated at 1 x 10^5 cells per well in a 96-well plate, and a range of antibiotic concentrations (0-, 50-, 100-, 200-, 350-, 500-, 750- and 1000 µg/ml) added to each well. For seven days, 100 µl of cells were removed daily, transferred to a new well, and 10 µl of the WST-1 proliferation reagent (Roche, Germany) was added, incubated for two hours at 37 °C followed by measurement of colour change using the GloMax®-Multi microplate reader (Promega, US).

2.13 Nucleofection

The nucleofection process utilises electroporation which causes the cell membrane, comprised of negatively phospholipids, to re-orientate and become porous which allow the entrance of the plasmid (O'Keefe, 2013). Due to the "difficult-to-transfect" nature of B-cells (Maurisse *et al*., 2010), nucleofection using the Nucleofector™ II (Lonza, Germany) system was selected. The Amaxa® Cell Line Nucleofector® Kit V (Lonza, Germany) was used for both

L1439A and Ramos. L1439A cells were plated at 1 x 10^6 and Ramos cells were plated at 2 x 10^6 cells in a 24-well plate. Five programmes were initially selected for L1439A (V-001, X-001, T-020, Y-005 and P-016), with X-001 being selected as the final programme. For Ramos, the programme O-006 was identified from the literature as the optimal programme (Thapa *et al*., 2011). Cells were counted on the haemocytometer, the total cells used for the experiment were centrifuged at 1000 rpm for ten minutes and the supernatant aspirated. This centrifugation step was repeated for two minutes, with any excess supernatant being aspirated. For each sample, 100 µl of Cell Line Nucleofector® Solution V was added and the cells were gently mixed. This solution was then added to 2 µg of plasmid in a 1.5 ml tube. The solution was then placed into the supplied cuvettes and nucleofected, and then 500 µl of pre-warmed medium was added to the cuvette. The supplied plastic pipettes were then used to remove the cells and place them in a 12-well plate which contained 1 ml of pre-warmed medium. The cells were then placed in the CO_2 incubator at 37 °C for 48 hours, after which the cells were viewed under the fluorescent microscope.

2.14 Cell sorting using flow cytometry

To isolate successfully transformed cells, with the assistance from Ronnie Dreyer (Flow Cytometry Core Facility, Institute of Infectious Disease and Molecular Medicine, University of Cape Town) the FACS Aria (BD, UK) flow cytometer was used. This technique uses lasers aimed towards cells and detects forward and side scatter of the light, which determines the cell size and number. If a fluorochrome such as 7-AAD or GFP are bound to a cell, the channel specific for the fluorescence will detect the excited wavelength. The FACS Aria will then use electrostatic deflection, dependent on the type of cell required and sort them into different containers. The cells from these containers can then be placed back into cell culture and expanded.

2.14.1 EGFP tagged cells

Cells successfully transfected with the pEGFP-N3 plasmid express GFP and can therefore be sorted based on fluorescence. These cells were counted, placed in a Falcon flow cytometry tube and diluted in 1X PBS. They were then sorted, and then a portion of the latter cells re-sorted in order to determine the percentage purity.

2.14.2 Live and dead cells using 7-AAD

Cells successfully transfected with the pcDNA-3.1 plasmids (which lacked a fluorescent tag) were sorted based on live/dead selection. Thus 15 minutes before sorting, 5 µl of 7-AAD (BD, UK) dye was added to the cells in the Falcon flow cytometry tubes. This dye binds to DNA, and it is expected that all dead cells have ruptured cell membrane thus allowing the 7-AAD to enter and bind DNA. The cells were then sorted where all cells negative for 7-AAD were selected. After cell sorting, a subset of the sorted population were re-sorted in order to determine the percentage purity.

2.15 Senescence-associated β-galactosidase assay (SA-β-gal)

To detect senescencent cells, the SA-β-gal assay was performed. The cells were centrifuged at 1 000 rpm for five minutes. The medium was aspirated and the pellet resuspended in sterile 1X PBS twice (Appendix A). After a further centrifugation step, the pellet was resuspended in room temperature β-gal fixative (Appendix A) for five minutes. The cells were centrifuged again at 1000 rpm for five minutes and washed twice with sterile 1X PBS as described before. Room temperature X-gal staining solution (Appendix A) was added and the pelleted cells were resuspended and incubated at 37 °C for 24 hours. After the incubation, the cells were counted using the haemocytometer. Cells which are senescent express β-galactosidase, which cleaves X-gal, thus these will develop a blue stain.

2.16 Annexin V detection assay

The Annexin V Apoptosis Kit I (BD, UK) was used which contained the Annexin V protein conjugated to the Phycoerythrin (PE) fluorochrome. When cells undergo apoptosis, one of the earliest features is the translocation of the phospholipid phosphatidylserine (PS) to the outside of the plasma membrane, thus becoming accessible for binding by the Annexin V protein, which has a high affinity for PS to bind.

Cells were washed twice with cold sterile 1X PBS. An amount of 1 x 10^6 cells was resuspended in 1 ml 1X Binding Buffer supplied in the kit. In a 5 ml Falcon flow cytometry tube, 100 µl of cells and Binding Buffer solution were added which equated to 1 x 10^5 cells. Thereafter 5 µl

of PE Annexin V and 5 µl of 7-AAD were added to the cells, the solution was gently mixed and incubated at 15 minutes in the dark at room temperature. After the incubation, 400 µl of 1X binding buffer was added and the cells were analysed on the FACSCaliber flow cytometry instrument (BD, UK). Controls for the experiment were unstained cells to allow for compensation and size determination, cells only stained with PE Annexin V (no 7-AAD) and cells only stained with 7-AAD (no PE Annexin V).

2.17 Cell profiling

To detect alterations to the cell cycle profile, cells underwent flow cytometry with the assistance from Ronnie Dreyer (Flow Cytometry Core Facility, Institute of Infectious Disease and Molecular Medicine, University of Cape Town) using the FACSCaliber (BD, UK). Cells were counted and fixed by adding 8 ml of ice cold 80 % ethanol, drop-wise while simultaneously vortexing to prevent clumps from forming. The cells were placed at -20 °C overnight. The fixed cells were removed and centrifuged at room temperature for five minutes at 1 500 rpm. The ethanol was aspirated leaving behind approximately 1 ml of ethanol. The cells were then resuspended in the remaining ethanol and transferred to a new 1.5 ml tube. The cells were centrifuged at 6000 rpm for one minute and 900 µl of supernatant was aspirated. The cells were washed twice with 1 ml of sterile cold 1X PBS and centrifuged at 6 000 rpm for one minute. After the last wash, all the supernatant was removed leaving approximately 50 µl of 1X PBS with the cell pellet. The cells were then resuspended in RNase A (50 µg/ml) diluted in 1X PBS, dependent on number of cells. The volume of RNase A was twice the first value at 1 x 10^4, therefore 200 x 10^4 cells equalled 400 µl RNase. The cells were incubated for 30 minutes at room temperature and the propidium iodide stain (Appendix A) was added, in a volume nine times the RNase volume, 20 minutes before analysis on the FACSCaliber (BD, UK). The cell solution was then subjected to flow cytometry which dilutes cells in FACS Buffer (BD, UK) and passes them singularly through a capillary. Using the forward and side scatter, the quantity of the cellular DNA content was acquired using the CellQuest Pro software (Version 5.2.1, BD, UK) and plotted using the Modfit software (Version 3.3, Verity Software House).

2.18 AID knockdown using siRNA

To knockdown AID expression, the FlexiTube AID siRNA kit was purchased from Qiagen (Germany) which contains four pre-selected non-validated siRNAs. The efficiency of these siRNAs in targeting AID needed to be determined. The experiments were initially performed using the recommended transfection reagent produced by the same company, HiPerfect (Qiagen, Germany), which proved to be sub-optimal, and subsequently the X-tremeGENE HP transfection reagent (Roche, Germany), was used. A scrambled siRNA (AllStars Negative Control siRNA) (Qiagen, Germany) was purchased to be used as a control.

2.18.1 siRNA knockdown using HiPerfect

Cells were seeded at 2 x 10^5 cells per ml in 10 ml of medium. After 18 hours, the cells were counted using the haemocytometer and 1 x 10^5 cells resuspended in 100 µl of medium and then plated in a 24-well plate. In a separate 1.5 ml tubes, the siRNA was mixed in 100 µl of RPMI (containing 10 % FBS and 1 % PenStrep) after which the HiPerfect transfection reagent was added (Table IX), this was performed for each of the four siRNAs. This mixture was incubated for ten minutes at room temperature before being added dropwise to each well containing the cells, and gently mixed. The cells were then incubated in the CO_2 incubator for six hours before 400 µl of RPMI medium (containing 10 % FBS and 1 % PenStrep) was added. After 42 hours the cells were removed from the CO_2 incubator and protein was extracted using 2X boiling blue buffer as described in Section 2.7.3. This was subjected to western blot analysis to verify knockdown.

Table IX: siRNA concentrations used in the optimisation reaction for each of the four siRNAs.

Components	Tube 1	Tube 2	Tube 3	Tube 4
siRNA Concentration	375 ng	375 ng	750 ng	750 ng
HiPerfect Volume	3 µl	6 µl	3 µl	6 µl

2.18.2 siRNA knockdown using X-tremeGENE HP

Cells were seeded at 2 x 10^5 cells per ml in 10 ml of medium. After 18 hours, the cells were counted using the haemocytometer and 1 x 10^5 cells resuspended in 450 µl of RPMI (containing 10 % FBS and 1 % PenStrep) and were plated in a 24-well plate. In a 1.5 ml tube, 47.5 µl of RPMI medium and 2.5 µl of X-tremeGENE HP were gently mixed. In a separate 1.5 ml tube, 50 µl of RPMI was gently mixed with 1000 ng of siRNA. The RPMI and transfection reagent mix was added dropwise to the RPMI and siRNA mix and gently mixed, taking care not to leave either solution for longer than five minutes before mixing. The solution were incubated for 15 minutes at room temperature before adding dropwise to the 24-well plate containing the cells. The 24-well plate was then placed in the CO_2 incubator for 48 hours. After incubation, the cells were removed and protein was extracted using 2X boiling blue buffer as described in Section 2.7.3. This was subjected to western blot analysis to verify knockdown.

2.19 IC50 of doxorubicin

Doxorubicin was diluted from a stock of 58 mg/ml into a working concentration of 250 µg/ml in dH_2O. Cells were plated at 1 x 10^5 cells per well in a 24-well plate and a range of doxorubicin concentrations (0-, 0.025-, 0.005-, 0.1-, 0.5-, and 1 µg/ml) added to each well. After 48 hours, 100 µl of cells were removed and transferred to a new well, and 10 µl of the WST-1 proliferation reagent (Roche, Germany) was added, incubated for two hours at 37 °C followed by measurement of colour change using the GloMax®-Multi microplate reader (Promega, US).

2.20 BrdU incorporation assay

Bromodeoxyuridine (BrdU) is a thymine analog which is incorporated into replicating DNA in place of thymidine, and can then be detected using a secondary antibody conjugated to a fluorochrome. Coverslips were coated with poly-L-Lysine (Sigma-Aldrich) to enhance the ability of suspension cells to adhere to the surface. Sterile coverslips were placed in 100 % ethanol, dried and placed in a single layer in a petri dish. The slides were then covered by poly-L-lysine (50 µg/ml) and incubated at 37 °C for one hour. The coverslips were removed with sterile forceps and air-dried. Once dry, the coverslips could then be used for the experiment. The slides were placed in 24-well plates into which cells that had been

transfected with siRNA were seeded. The cells were placed in the incubator for 42 hours before 10 µM BrdU was added. After eight hours, the supernatant was removed and replaced by fixative (Appendix A) and incubated at -20 °C for 20 minutes. The fixative was removed and replaced by 2 N hydrochloric acid and incubated for one hour at 37 °C, this was then neutralised by 0.1 M borate buffer (Appendix A). The slides were then washed twice using 1X PBS containing 0.05 % Tween-20 (PBS/0.05 % Tween) and incubated with 5 % human serum for 30 minutes at 37 °C. BrdU incorporation was then detected using an anti-BrdU mouse monoclonal antibody (6 µg/ml) (Roche, Germany) diluted in 0.1 % BSA at 37 °C for 30 minutes. The cells were then washed twice using PBS/0.05 % Tween, and incubated with a donkey anti-mouse secondary antibody (AEC-Amersham) conjugated to Cy3 (1:1000 diluted in 0.1 % BSA). The cells were then washed twice in PBS/0.05 % Tween and incubated with Hoechst 33342 stain (#H1399, Invitrogen, US) for ten minutes. The cells were thereafter washed twice with PBS/0.05 % Tween and placed onto a slide using Moyial which contained anti-fade. The cells were then visualised under a fluorescent microscope (Zeiss Axiovert 200M, Carl Zeiss Microimaging, Germany).

2.21 Transwell migration assay

The Corning® Transwell® assay (Sigma-Aldrich) was performed to determine migratory abilities of cells. In a 24-well plate, 600 µl of RPMI (containing 10 % FBS and 1 % PenStrep) was placed in each well, and using sterile forceps the Transwell insert was placed into each well, ensuring the bottom chamber was submerged taking care that no air bubbles are trapped. A total of 15 Transwell inserts were used, with five inserts for the AID-siRNA3 knockdown cells, five for the scrambled siRNA control cells and five for the untreated Ramos cells. A total of 100 µl of cells (approximately 2.2 x 10^5 cells per ml) were plated into each Transwell insert and placed in the CO_2 incubator for 48 hours. Two of each condition was used as a total control, whereby all the cells were stained to determine total number of cells in each well. The Ramos cells then underwent knockdown as described in Section 2.18.2, with one difference, the cells were resuspended in 1 % FBS and not 10 % FBS. After incubation, each insert was fixed in 100 % methanol for five minutes and then washed in dH_2O. The inserts were then placed in 0.1 % crystal violet stain (Appendix A) for 30 minutes before washing with dH_2O. The upper chambers (three inserts from each group) were swabbed using a cotton wool

tipped applicator in order to remove the cells on the upper side of the insert. The inserts were washed again and swabbed a second time. The inserts were then placed overnight in the fume hood to dry and thereafter the crystal violet stain was dissolved in 150 µl of 50 % acetic acid. The absorbance of 100 µl of each sample was determined at 600 µm using the Glo-Max®-Multi+ multiplate reader (Promega, US).

2.22 Determination of CD expression markers

Cells were subjected to knockdown as described in Section 2.18.2 and placed into the CO_2 incubator. After 48 hours, the cells were removed and placed into 1.5 ml tubes, these cells were centrifuged for five minutes at 2 000 rpm, the supernatant was aspirated and washed with cold 1X PBS. This centrifugation and washing step was repeated twice, and the cells resuspended in 1X PBS. Cells were stained with 5 µl of the conjugated antibodies: CD10-FITC, CD19-APC, CD20-PE (Biolegend, US). The cells were then analysed using the FACSCaliber (BD, UK) and data analysed using the CellQuest software (Version 5.2.1, BD, UK).

2.23 Statistical analysis

2.23.1 SA-β-gal

The results from the SA-β-gal assay were subjected to a one-way ANOVA and significant differences were located using a Tukey post-hoc test (Prism 6, GraphPad, US).

2.23.2 Proliferation

The results from the proliferation assay with Ramos cells treated with Doxorubicin and untreated cells was subjected to a two-way ANOVA and significant differences were located using Sidak's multiple comparison test (Prism 6, GraphPad, USA).

Chapter 3: AID Expression in the Epithelial and B Lymphoblastoid Cell Lines

3.1 Introduction

The DNA mutagenic enzyme Activation Induced cytidine Deaminase (AID) is expressed specifically in activated B-cells and is a key driver in antibody diversification (Shimizu *et al*., 2012). Due to the nature of its function, AID is tightly regulated, however, when it becomes unregulated, there is an overexpression of AID which has been shown to be associated with certain types of cancers (Shimizu *et al*., 2012). For instance, in Burkitt's lymphoma (BL), AID overexpression has been implicated in the *c-Myc/IgH* translocation, leading to upregulation of the *c-Myc* oncogene (Robbiani and Nussenzweig, 2013). AID overexpression has also been implicated in certain non-lymphoid cancers, often of epithelial origin including prostate, colon and liver cancer (Matsumoto *et al*., 2007; Lin *et al*., 2009). In these cancers, AID overexpression is not associated with the translocation of *c-Myc*. Therefore the role of AID in oncogenesis is still poorly understood.

The aim of this study is to investigate the role of AID in the oncogenic process. The initial idea to achieve this aim, was to use AID-overexpressing cell culture models, one of B-cell origin, and a second of epithelial origin. To begin to do this, it was important to identify cell lines, representative of the cancers in which AID has been implicated, which were suitable for ectopic expression of AID. This chapter presents the results obtained when 5 cell lines of B-cell origin, and 16 cell lines of epithelial origin, were screened for AID expression.

Total mRNA and protein was extracted from all the cell lines and subjected to quantitative real-time PCR (qPCR) and western blotting, to determine AID mRNA and protein expression levels respectively. The findings are presented in detail below.

3.2 Results

3.2.1 All cell lines tested negative for mycoplasma infection

Mycoplasma is a small bacteria (0.15 to 0.30 µm) which localises on the cell membrane forming a string circling the cytoplasm (Nikfarjam and Farzaneh, 2012). These bacteria are resistant to most antibiotics, thus the penicillin-streptomycin added to the media is not

enough to prevent infection. To identify mycoplasma infections, Hoechst stain which binds to all nuclear material is added as described in Section 2.1.5. Infections by mycoplasma has been shown to change cell physiology and can potentially alter results (Drexler and Uphoff, 2002), thus regular mycoplasma tests of all cell lines used in this study (Table I) were conducted. All cell lines tested were found to be negative for mycoplasma contamination as only the nucleus of each cell could be visualised under fluorescent microscopy using the Hoechst 33342 stain (#H1399, Invitrogen, US). Figure 3.1 below is representative of a negative mycoplasma result in the EBV-immortalised lymphoblastoid cell line L1439A (A-C) and the Burkitt's lymphoma cell line Ramos (D-F).

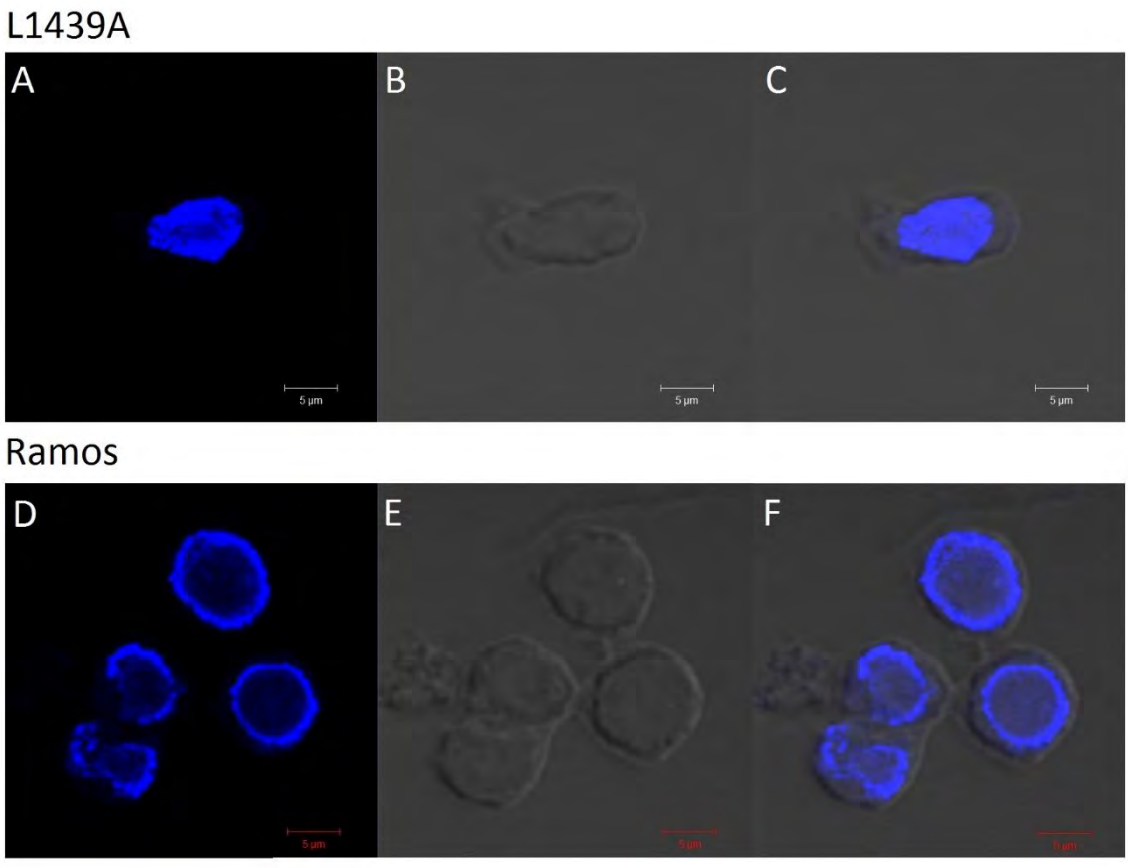

Figure 3.1: Representative mycoplasma result for L1439A and Ramos. Mycoplasma staining using Hoechst Stain in L1439A (A-C) and Ramos (D-F). A & D are fluorescent images, B & E are corresponding phase contrast images and C & F are the overlaid images visualised using the confocal microscope. Both of these results are negative for mycoplasma infection.

3.2.2 Extracted RNA of all but one sample is of good quality and suitable for cDNA conversion

To accurately determine AID mRNA levels in each cell line, total RNA needed to be extracted and quantified. The purity and concentration of the total RNA extracted were determined as shown in Table X. The 260/280 ratio is a measure of RNA purity, a ratio of approximately 2.0 is generally accepted as ideal. A value significantly lower would indicate the presence of either protein, phenol or another contaminant that absorbs strongly at 280 nm. The 260/230 ratio is a secondary measure of purity with the ideal ratio between 2.0 to 2.2. A lower reading would be an indication of contaminants that absorb light within the 230 nm spectrum. The RNA extracted from all cell lines fell within the acceptable parameters with the exception of the BL cell line, P3HR1, which had low 260/280 and 260/230 ratios. RNA extraction was repeated in the P3HR1 cell line, however the result remained the same, although the cell line seemed to grow well in culture. This low yield of RNA obtained could be that these cells appeared much smaller than the other B-cell lines in culture. Despite numerous attempts, including the use of a specialised kit for RNA clean-up with a concentration step (RNA Clean & Concentrator™-5, Zymo Research, USA) the quality of the RNA could not be improved upon (data not shown).

Table X: The purity and concentration of RNA for each of the 21 cell lines used in this study. The lowest concentration obtained, which became the limiting factor in cDNA synthesis, was for the Burkitt's lymphoma cell line, P3HR1, as highlighted in red within the table.

Cell Line	Cell Type	260/280 Ratio	260/230 Ratio	Concentration (ng/µl)
L1439A	Normal EBV-Immortalised Lymphoblastoid Cell Line	2.08	2.10	304.60
BL-2	Burkitt's Lymphoma Cell Line	2.04	2.19	59.50
P3HR1		1.98	1.89	15.30
Ramos		2.03	2.27	33.10
Seraphina		2.09	2.27	1041.30
Du145	Prostate Cancer Cell Line	2.10	2.30	1230.20
LnCaP		2.13	2.36	234.40
PC-3		2.08	2.24	1136.70
PNT1A	Normal Prostate Cell Line	2.04	2.22	252.10
PNT2		2.08	2.28	354.00
Caco-2	Colon Cancer Cell Line	2.07	2.28	536.10
DLD-1		2.08	2.17	1574.40
HT-29		2.10	2.24	490.20
LoVo		2.07	2.24	278.70
Colo205		2.08	2.24	1161.90
Colo206F		2.09	2.26	1285.10
KYSE-30	Oesophageal Cancer Cell Line	2.13	2.41	489.60
KYSE-520		2.13	2.40	155.30
OE19		2.08	2.18	144.50
OE33		2.15	2.39	157.60
UMSCC22b	Head and Neck Cancer Cell Line	2.06	2.36	173.70

The quality of RNA was further determined using gel electrophoresis (Figure 3.2 and Appendix B, Figures B1, B2, and B3). RNA of good quality and integrity displays two distinct bands namely the 28S and 18S ribosomal subunits, with no or minimal smearing. In addition, any bands that appear above the 28S rRNA is indicative of genomic DNA contamination. Figure

3.2, showing the RNA extracted from the colon cancer cell lines, is a representative result of the RNA integrity observed for all the samples and shows characteristics of RNA of good integrity that is suitable for use in cDNA conversion and qPCR.

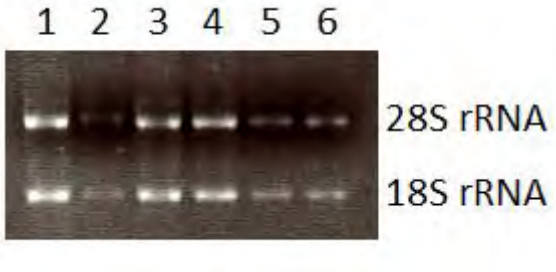

Figure 3.2: Gel electrophoresis of total RNA extracted from the colon cancer cell lines. The two sharp bands representing the 28S and 18S ribosomal subunits were observed in a 1 % agarose gel. (Lanes 1 – 6: Caco-2, DLD-1, HT-29, LoVo, Colo205 and Colo206F).

3.2.3 AID mRNA expression was determined by qPCR

To determine the absolute amount of AID mRNA being produced within these cell lines, total RNA was subjected to qPCR. To accurately quantify and compare AID expression between cell lines, two housekeeping genes (GAPDH and RPL27) were selected which have stable expression levels (De Jonge *et al*, 2007). To be able to quantify the copy number for each sample, standard curves for all three genes were produced.

3.2.3.1 Generation of standard curves

Initially total RNA was isolated from L1439A and cDNA reverse transcription performed as described in Section 2.4. This cDNA was then used to generate three standard curves, one for each of the three genes (AID, GAPDH and RPL27). Initially a standard PCR was performed using the qPCR primer sets, amplifying each gene using the cDNA generated from L1439A as a template (Section 2.5). The successfully amplified products then underwent a PCR purification step (Section 2.5.2). The resulting products (Table XI) were then quantified and the copy number calculated according to the following equation:

$$\frac{Concentration\ (ng/\mu l\ ) \times 10^{-9}\ (g/L)}{Length\ (bp) \times 660} \times (6.022 \times 10^{23})$$

Table XI: Copy number calculation for the genes of interest.

Gene	Length (bp)	Concentration (ng/µl)	Copy Number (molecules of DNA/µl)
AID	108	31.6	2.7×10^{11}
GAPDH	133	35.1	2.4×10^{11}
RPL27	123	58.3	4.3×10^{11}

Two serial dilutions were produced, a 1:10 serial dilution for AID and a 1:100 serial dilution for both GAPDH and RPL27. Figure 3.3 below is a representative qPCR amplification profile for the AID serial dilution in duplicate, with Figure 3.4 representing the standard curves produced from each gene.

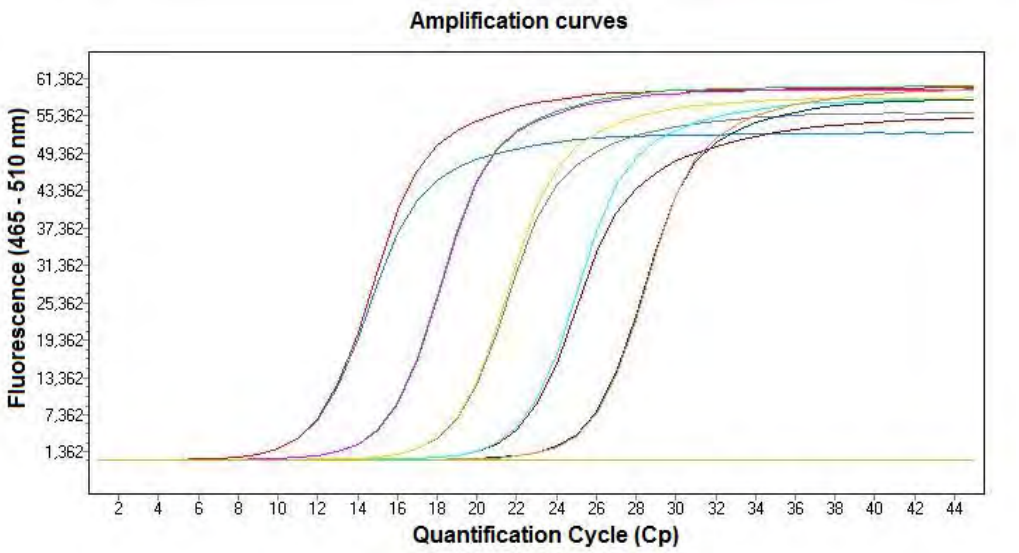

Figure 3.3: qPCR amplification profile of AID. Amplification curves of AID utilising a 1:10 serial dilution from 1×10^6 copies to 1×10^2 copies of the amplified PCR products. Each sample was run in duplicate.

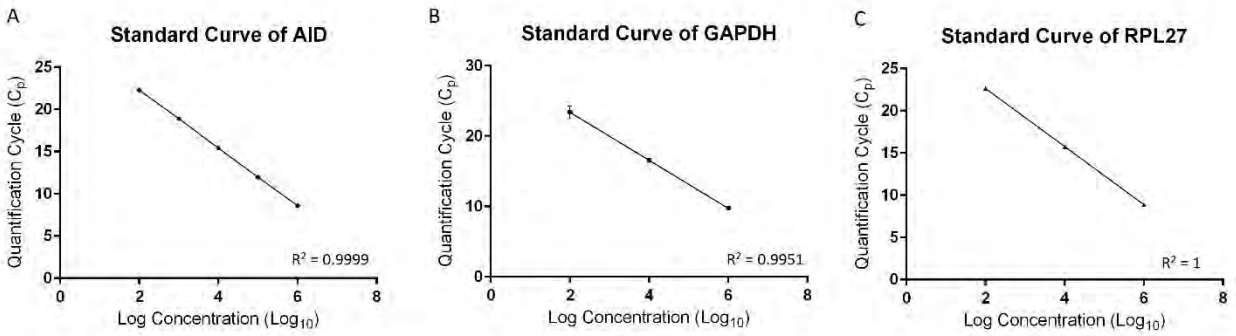

Figure 3.4: Graphically plotted standard curves for AID, GAPDH and RLP27. Standard deviation is shown by the error bars and the R^2 values for each standard curve is on each graph.

Total RNA from each cell line was then extracted, quantified and quality checked as described in Section 2.2 and 2.3. The cDNA generated were then used in the qPCR reaction (Section 2.6) with the same volume of product in each reaction allowing us to quantitatively compare expression levels between each sample.

3.2.3.2 AID mRNA expression in the B-cell derived cell lines

A qPCR reaction was setup for the four BL cell lines (BL2, P3HR1, Ramos and Seraphina) and the EBV-immortalised human B lymphoblast cell line (L1439A). These samples were run in triplicate with all three primer sets (AID, GAPDH and RPL27) as well as each respective standard in duplicate. Copy number for each sample was extrapolated from the standard curves. AID was then normalised against GAPDH and RPL27 where the percent AID expression was determined (Figure 3.5).

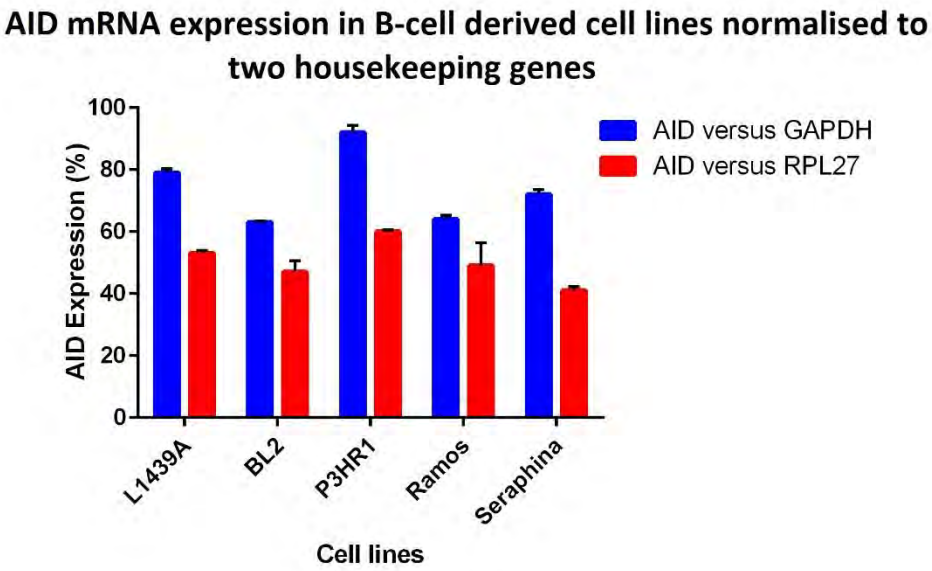

Figure 3.5: AID mRNA expression in the B-cell derived cell lines. AID mRNA expression was normalised to either the housekeeping gene GAPDH (blue bars), or to RPL27 (red bars). Error bars represent the standard deviation.

A single amplified qPCR product was confirmed by performing a melt curve (Figure B7) and by agarose gel electrophoresis (Figure 3.6). The latter also confirmed that fragments of the appropriate sizes were amplified and that no primer dimers were present.

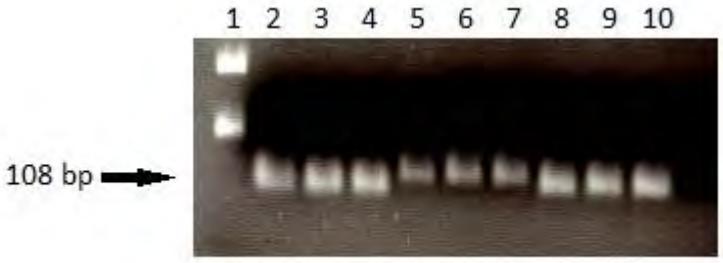

Figure 3.6: Verification of qPCR products by agarose gel electrophoresis. Lane 1, 1kb molecular weight marker, lanes 2-4; AID qPCR product from the 1 x 10^6 standard sample, L1439A, and Ramos respectively, lanes 5-7; GAPDH qPCR product for the 1 x 10^6 standard sample, L1439A, and Ramos respectively, lanes 8-10; RPL27 qPCR product for the 1 x 10^6 standard sample, L1439A, and Ramos respectively. These samples were electrophoresed on a 1% agarose gel.

3.2.3.3 AID mRNA expression in epithelial derived cancer cell lines

The literature indicated that AID overexpression is a feature of some types of epithelial cancers, especially those associated with inflammation, such as cancers of the gastrointestinal tract (GIT), but also prostate cancer (Lin *et al*., 2009; Shimuzu *et al*., 2012).The mRNA from 16

epithelial cell lines, including colon, oesophageal, prostate and head and neck (Table X) were subjected to qPCR to determine the levels of AID which is expressed. Our results in Figure 3.7 below show that AID mRNA was not present in the majority of these cell lines, except for two oesophageal cell lines (OE19 and KYSE-30) which had low levels of AID mRNA.

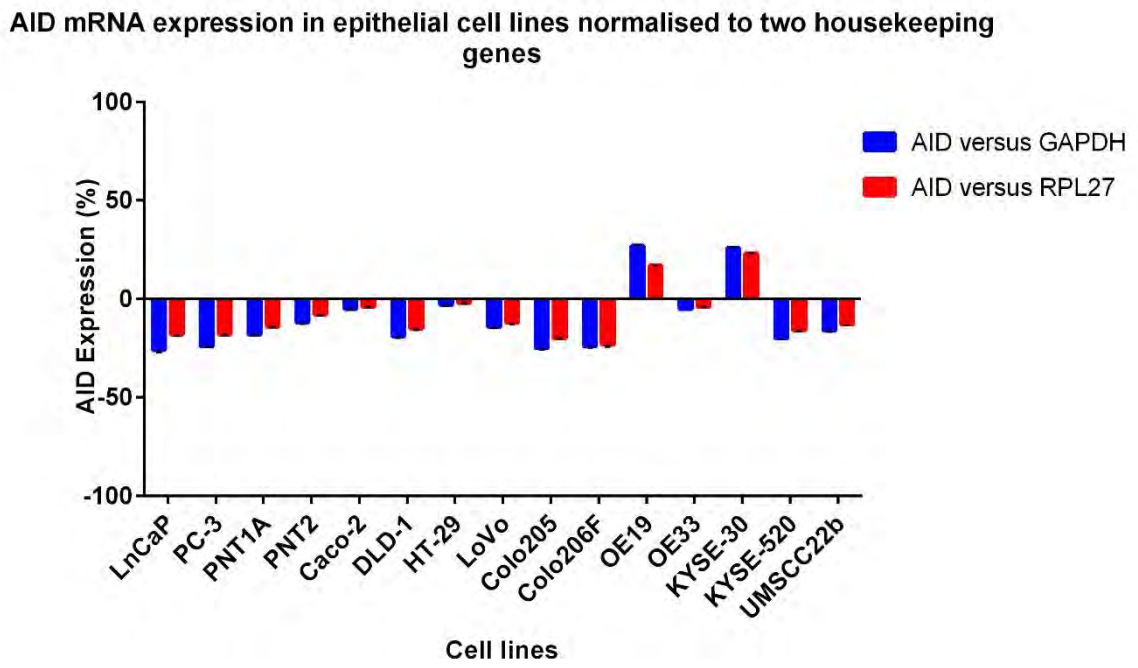

Figure 3.7: AID mRNA expression determined by qPCR for all the epithelial cell lines used in this study. AID expression was normalised to each of the housekeeping genes (GAPDH in blue and RPL27 in red).

The results for Du145 are missing from Figure 3.7 as all three genes failed to amplify in this prostate cancer cell line. The qPCR of this sample was repeated with a new aliquot of reverse transcribed cDNA, however, the experiment repeatedly failed. The 260/280 and 260/230 ratios for Du145 were within the acceptable region (2.10 and 2.30, respectively), and the RNA gel showed good quality and integrity (Appendix B, Figure B1). When conventional PCR was performed, products could be amplified for two of the three sets of primers (Figure 3.8) and therefore indicated that only the qPCR reaction was being inhibited. It is of note that the AID PCR primer set produced a positive band for AID, thus indicating that AID mRNA may be present in this cell line. All the cell lines, including the two oesophageal cell lines which showed AID mRNA expression, had total protein extracted to determine whether the functional unit of this mRNA was produced.

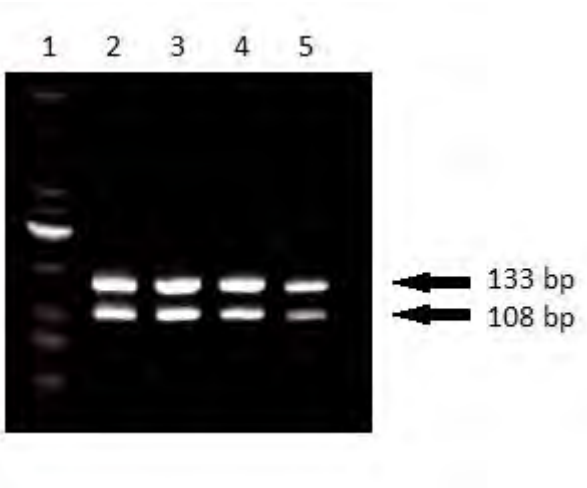

Figure 3.8: Agarose gel electrophoresis of products from conventional PCR using Du145 mRNA. A duplex PCR was performed using primers for GAPDH (133 bp) and AID (108 bp). cDNA derived from the Du145 total mRNA extraction was used at varying volumes. Lane 1; 100 bp molecular weight marker, lane 2; L1439A, lane 3; Du145 (2 µl), lane 4; Du145 (1 µl), lane 5; Du145 (0.5 µl). These samples were electrophoresed on a 1 % agarose gel.

3.2.4 AID protein expression in B-cell derived and epithelial derived cell lines

In order to determine whether the AID mRNA was being translated into protein, and that the mRNA result correlates with the protein result (the functional unit), protein from each cell line was extracted, separated by SDS-PAGE and analysed by western blotting. The results are presented below.

3.2.4.1 Total protein extraction and quantification

Total protein was extracted from each cell line using RIPA buffer (Section 2.7.1) and quantified using the BCA Assay (Section 2.7.2). Table XII show the protein concentrations obtained, which varied between cell lines, with the highest at 9.20 µg/µl for the Colo206F (colon cancer) cell line, and the lowest at 0.96 µg/µl for the prostate cancer cell line, LnCaP.

Table XII: Total protein concentration of each cell line used in this study.

Cell Line	Cell Type	Concentration (µg/µl)

L1439A	Normal EBV-Immortalised Lymphoblastoid Cell Line	2.40
BL-2	Burkitt's Lymphoma Cell Line	1.49
P3HR1		1.77
Ramos		4.39
Seraphina		3.09
Du145	Prostate Cancer Cell Line	1.90
LnCaP		0.96
PC-3		2.02
PNT1A	Normal Prostate Cell Line	1.18
PNT2		1.72
Caco-2	Colon Cancer Cell Line	3.50
DLD-1		2.73
HT-29		5.20
LoVo		7.12
Colo205		8.04
Colo206F		9.20
KYSE-30	Oesophageal Cancer Cell Line	2.24
KYSE-520		1.67
OE19		5.29
OE33		5.28
UMSCC22b	Head and Neck Cancer Cell Line	1.86

3.2.4.2 SDS-PAGE and western blotting to determine AID protein expression in the B-cell derived cell lines

Equal concentrations of total protein extracted from the B-cell derived cell lines were separated in a 12 % SDS-PAGE (Section 2.8.1) and then transferred onto nitrocellulose membranes for western blotting (Section2.8.2). The result is shown below in Figure 3.9 and the intensity of the AID bands, relative to the internal control p38 were analysed using the Li-Cor Image Studio Lite software and displayed as densitographs. AID protein was easily

detected from all the samples, but interestingly did not correlate exactly with the qPCR results.

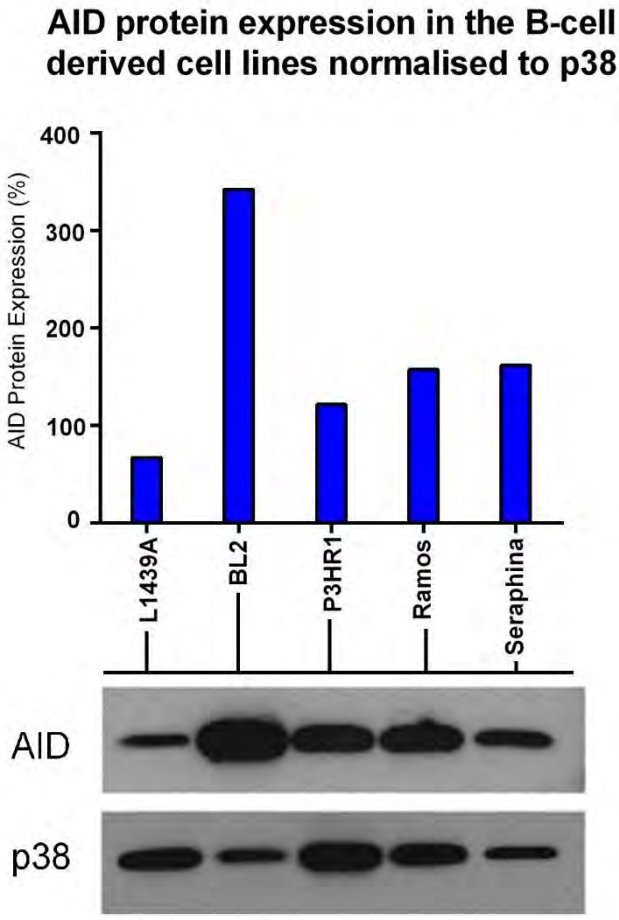

Figure 3.9: AID protein expression in L1439A and the Burkitt's lymphoma cell lines. Western blot analysis displaying the AID protein expression levels in the EBV-immortalised B lymphoblastoid cell line and the four Burkitt's lymphoma cell lines. 6 µl of 5X loading dye and 1 µl of DTT was added to 30 µl of protein (20 µg) in RIPA buffer and boiled at 95 °C for five minutes before being loaded and separated on a 12 % SDS-PAGE gel at 100 V for 200 minutes in 1X running buffer. The protein was then transferred onto a nitrocellulose membrane (Bio-Rad) for 75 minutes at 100 V in 1X transfer buffer. This was then detected using the Clarity™ Western ECL Blotting Substrate (Bio-Rad). To detect AID, mouse anti-AID (Invitrogen) was used, with a HRP bound goat anti-mouse secondary antibody (Bio-Rad). The p38 protein was used as a loading control and detected using the rabbit anti-p38 antibody (Sigma-Aldrich) and the HRP bound goat anti-rabbit secondary antibody. The signal intensity of the bands were analysed using the Li-Cor Image Studio software (Germany), and normalised to p38. This densitometric analysis representing AID protein expression is displayed above the western blot.

3.2.4.3 SDS-PAGE and western blotting to investigate AID protein expression in the epithelial cell lines

In the same way as described above for the B-cell derived cell lines, total protein from the epithelial cell lines was extracted, separated by SDS-PAGE and processed for western blotting

to detect AID protein expression. The result is shown below in Figures 3.10, 3.11 and 3.12, and mostly correlates with the result obtained for the mRNA expression using qPCR. A positive control sample was included in each western blot. This consisted of either Seraphina or the COS-7 cells transfected with the pcDNA-3.1-AID mammalian expression plasmid leading to constitutive expression of AID in these cells as described later in Section 4.2.1.

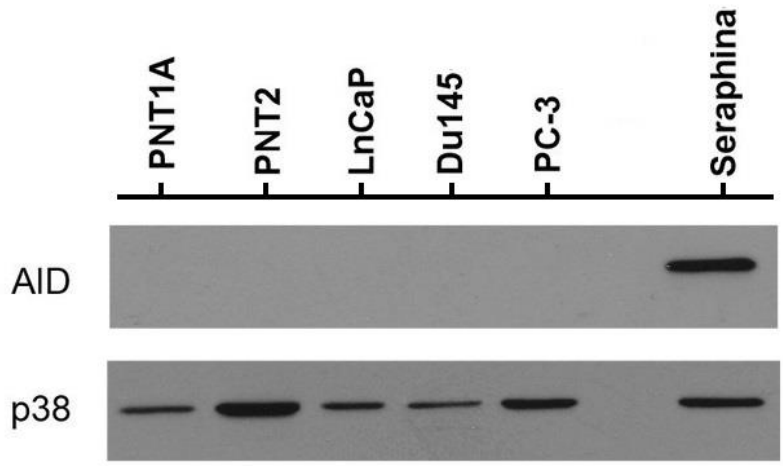

Figure 3.10: AID protein expression in the five prostate cell lines. Western blot analysis displaying the AID protein expression levels in the five prostate cell lines (PNT1A and PNT2 are normal prostate cell lines, while, LnCaP, Du145 and PC-3 are prostate cancer cell lines) with Seraphina (BL cell line) being used as a positive control for AID expression. 6 µl of 5X loading dye and 1 µl of DTT was added to 30 µl of protein (20 µg) in RIPA buffer and boiled at 95 °C for five minutes before being loaded and separated on a 12 % SDS-PAGE gel at 100 V for 200 minutes in 1X running buffer. The protein was then transferred onto a nitrocellulose membrane (Bio-Rad) for 75 minutes at 100 V in 1X transfer buffer. This was then detected using the Clarity™ Western ECL Blotting Substrate (Bio-Rad). To detect AID, mouse anti-AID (Invitrogen) was used, with a HRP bound goat anti-mouse secondary antibody (Bio-Rad). The p38 protein was used as a loading control and detected using the rabbit anti-p38 antibody (Sigma-Aldrich) and the HRP bound goat anti-rabbit secondary antibody.

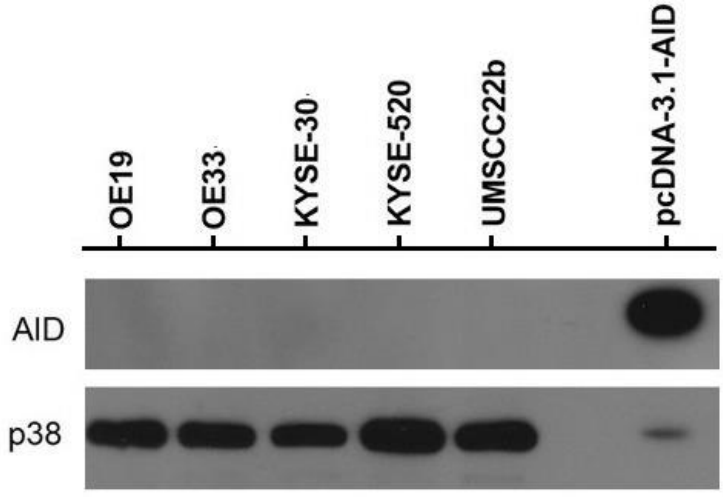

Figure 3.11: AID protein expression in four oesophageal cancer cell lines and one head and neck cancer cell line. Western blot analysis displaying the AID protein expression levels in the four

oesophageal and the head and neck cancer cell lines with pcDNA-3.1-AID as a positive control for AID expression. 6 µl of 5X loading dye and 1 µl of DTT was added to 30 µl of protein (20 µg) in RIPA buffer and boiled at 95 °C for five minutes before being loaded and separated on a 12 % SDS-PAGE gel at 100 V for 200 minutes in 1X running buffer. The protein was then transferred onto a nitrocellulose membrane (Bio-Rad) for 75 minutes at 100 V in 1X transfer buffer. This was then detected using the Clarity™ Western ECL Blotting Substrate (Bio-Rad). To detect AID, mouse anti-AID (Invitrogen) was used, with a HRP bound goat anti-mouse secondary antibody (Bio-Rad). The p38 protein was used as a loading control and detected using the rabbit anti-p38 antibody (Sigma-Aldrich) and the HRP bound goat anti-rabbit secondary antibody.

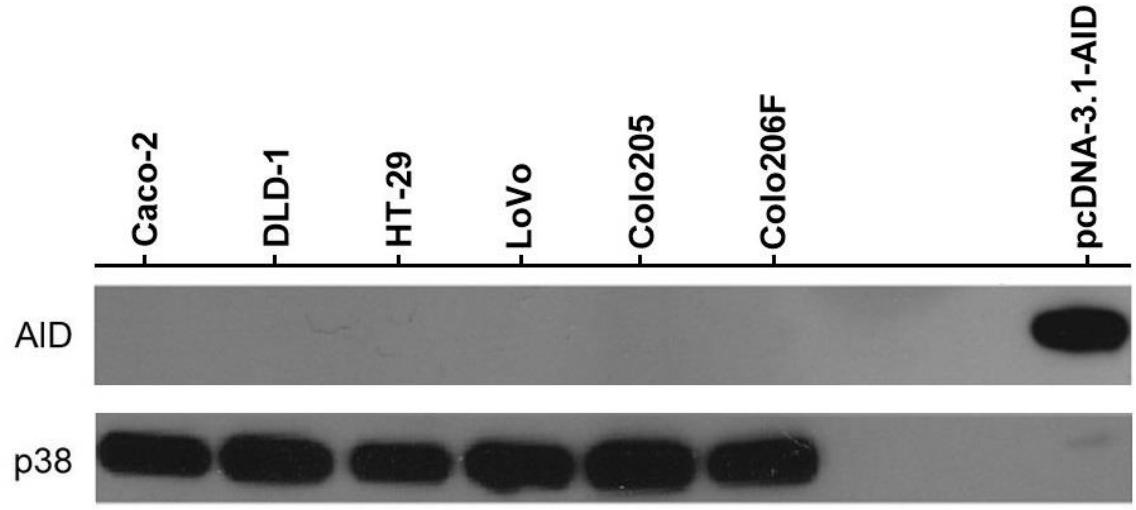

Figure 3.12: AID protein expression in the six colon cancer cell lines. Western blot analysis displaying the AID protein expression levels in the six colon cancer cell lines with pcDNA-3.1-AID as a positive control for AID expression. 6 µl of 5X loading dye and 1 µl of DTT was added to 30 µl of protein (20 µg) in RIPA buffer and boiled at 95 °C for five minutes before being loaded and separated on a 12 % SDS-PAGE gel at 100 V for 200 minutes in 1X running buffer. The protein was then transferred onto a nitrocellulose membrane (Bio-Rad) for 75 minutes at 100 V in 1X transfer buffer. This was then detected using the Clarity™ Western ECL Blotting Substrate (Bio-Rad). To detect AID, mouse anti-AID (Invitrogen) was used, with a HRP bound goat anti-mouse secondary antibody (Bio-Rad). The p38 protein was used as a loading control and detected using the rabbit anti-p38 antibody (Sigma-Aldrich) and the HRP bound goat anti-rabbit secondary antibody.

3.3 Discussion and conclusion

The expression of the B-cell specific enzyme AID has been associated with the onset of cancer due to its mutagenic nature (Shimizu *et al*., 2012). However, the exact function of AID in the oncogenic process has not been well studied. The aim of this part of the study was to identify two cell lines, one of B-cell origin, and another of epithelial origin, which can be used to ectopically express AID, with the aim to use these models to better define the oncogenic role of AID in these two cell types.

A total of 21 cell lines were used in this study, and all were found to be free of mycoplasma infection, which indicates that the qPCR and western blotting results, relating to the expression of AID, are likely to be accurate, and not a result of cells growing under conditions of stress, as they could if they had been infected with an agent like mycoplasma (Nikfarjam and Farzaneh, 2012).

The panel of B lymphoblastoid cell lines were made up of four Burkitt's lymphoma cell lines and one EBV-immortalised B lymphoblastoid cell line derived from a healthy donor. Total mRNA was extracted and qPCR analyses performed using primer sets for AID, GAPDH and RPL27. All the mRNA extracted was of good quality and integrity, except P3HR1, of which low yields and absorbance readings lower than the preferred values were obtained. Re-extraction of RNA from the P3HR1 cell line produced no yield changes, which did not improve after being subjected to an RNA clean-up kit. As this sample's integrity was on the border of acceptance, it was subjected to RNA integrity gel electrophoresis (Appendix B, Figure B1) which showed the sample could be used for further experimentation. A possible reason for this low RNA yield could be due to the small size of the cell, and an appropriate number of cells to get a higher yield of RNA could not be obtained. The RNA integrity of all the remaining cell lines, including P3HR1 were deemed acceptable for qPCR analysis (Figure 3.2 and Appendix B, Figures B1, B2 and B3). The qPCR analysis showed that there was AID mRNA expression in all five B lymphoblastoid cell lines. To control for sample variation, the same concentration of each mRNA sample was subjected to cDNA synthesis and the same volume used in each qPCR reaction. This AID mRNA expression was then normalised against the two housekeeping genes GAPDH and RPL27 (Figure 3.5). As Vandesompele *et al*. (2002) stated, there are no ideal housekeeping genes as there will always be some variation so for this reason we selected two housekeeping genes to control for any experimental variations between samples. Although most studies are moving away from using GAPDH as a housekeeping gene, we used both GAPDH and RPL27 to normalise AID expression. Ribosomal proteins, such as RPL27 (a gene which codes for a component of the ribosomal subunit 60S) are being successfully used as housekeeping genes (Rebouças *et al*., 2013). These two housekeeping genes were selected as there was no differentiating between different disease states within a single cell type, but rather comparing mRNA expression of AID across different cell types. There were only slight and negligible variations between AID expression normalised to GAPDH and RPL27, thus we

can accept both these results as accurate. The qPCR result of AID mRNA expression in the four Burkitt's lymphoma cell lines are in agreement with the published literature concerning AID overexpression in this cancer (Robianni *et al*., 2008). Surprisingly, the amount of AID mRNA in the EBV-immortalised B lymphoblastoid (L1439A) is comparable to that obtained in the Burkitt's lymphoma cell lines (Figure 3.5). The L1439A cell line is the closest representation of a normal B-cell line available for this study. It is interesting that L1439A has such a high AID mRNA expression as it would be expected that AID mRNA expression in a normal cell line would be less than a cancerous cell line known to overexpress this gene. The reason for this high expression could be due to the EBV immortalisation of this cell line. EBV is the only virus known to immortalise B lymphocytes, thus one cannot do without this step, as otherwise the cells will not be able to propagate in culture (Tosato and Cohen, 2007). This EBV immortalisation step was a caveat, as introducing EBV into these cells may affect other downstream processes which could in turn alter AID expression. Studies have shown that two small non-polyadenylated RNAs are expressed with EBV infection, namely EBER1 and EBER2 (Young and Rickinson, 2004). The expression of these EBERs, have been shown to increase tumourigenicity, IL-10 expression and improve cell survival (Wu *et al*., 2007; Brady *et al*., 2008). This improvement in cell survival is one of the key features which allowed for the transformation of the normal L1439A cells to allow them to propagate in culture. Specifically EBER1 has been shown to activate Toll-Like Receptor 3 (TLR3) signalling, which results in an induction of type I Interferon (IFN) and proinflammatory cytokines (Iwakiri *et al*., 2009). Thus with AID expression correlated to an increased immune response, the use of EBV in this cell line may artificially increase AID expression.

The western blot results confirmed that the AID mRNA in L1439A and BL cells was translated into the functional subunit (protein) (Figure 3.9). Though L1439A had high AID mRNA expression, it had the lowest AID protein expression when compared to the Burkitt's lymphoma cell lines. Conversely, the Burkitt's lymphoma cell line BL2 had the highest protein expression, but the lowest AID mRNA expression level. It is interesting that AID mRNA expression levels and AID protein expression differed within each cell line. AID does undergo several post-transcriptional and post-translational regulatory mechanisms which could account for this discrepancy. For example four microRNAs (miRNA), miR155, miR361, miR181b and miR93, have been described to bind to the 3'-untranslated region of the AID

mRNA, causing either mRNA degradation or inhibition of translation (Stavnezer, 2011). The AID protein is also subject to post-translational regulation through cellular compartmentalisation and phosphorylation (Aoufouchi *et al*, 2008). The aim with regards to the cells of B-cell origin was achieved, in that the L1439A cell line was found to express low AID protein levels compared to the BL cell lines, and was therefore a good candidate for the ectopic expression of AID. The results of this overexpression are described in the next chapter.

Similarly, the epithelial cell lines representative of various cancers in which AID overexpression has been implicated were also analysed for AID expression at both the mRNA and protein levels (Figures 3.7, 3.10, 3.11 and 3.12). It would have been ideal to have a "normal" cell line for each type of cancer which was screened, as was the case of the samples of prostate origin, however, these could not be sourced for this study. Since AID expression was undetectable in any of these samples using our methods and in our hands, we suggest that AID does not play a significant role in these cancers, contrary to the few reports in the literature (Fichtner-Feigl *et al*., 2015). It therefore became unimportant for the normal counterparts of these cell lines to be sourced. The mRNA samples for all the epithelial cell lines were found to be of good quality after isolation and could be analysed by qPCR, however, Du145 could not be amplified in the qPCR reaction. Despite several attempts with various modifications, including re-isolation of RNA, qPCR continued to fail for the Du145 sample, while conventional PCR was successful when using GAPDH and AID primer sets (Figure 3.8). This result points towards some AID expression within this prostate cancer cell line, however, due to the properties of conventional PCR, it was not possible to identify the copy number of AID mRNA present in the sample. This cell line, with the other epithelial cell lines, were analysed for AID protein expression levels. Possible reasons for this failure are the presence of an inhibitor that affects only the qPCR reaction but not the conventional PCR. The qPCR and conventional PCR were performed using kits from different companies (Kapa Biosystems, SA *versus* Bioline, UK, respectively). The buffer systems in each of the kit would differ, however, the method of mRNA extraction was exactly the same for each of the cell lines, thus the only other variable is the cell line itself. This cell line possibly produces an inhibitor of the polymerase in the qPCR reaction, but the buffer system and enzyme for the conventional PCR polymerase, which are usually more robust than qPCR reagents, was not affected in the same way. Moreover, conventional PCR is carried out for many cycles, which allows for amplification of even a very

small amount of template, while this is not the case in qPCR. Due to time and cost constraints no further qPCR tests were performed, however, a possible test for the future would be to decrease the volume of sample added to determine whether the inhibitor could be diluted out of the reaction. The result of the conventional PCR indicates that this cell line possibly express a certain level of AID mRNA, however, no protein could be detected by western blotting.

The rest of the epithelial sample qPCR reactions were successfully analysed and all except two cell lines, OE19 and KYSE-30, were negative for AID mRNA expression (Figure 3.7). The OE19 and KYSE-30 cell lines are oesophageal cancer cell lines, and while AID mRNA was detectable, the levels were significantly lower than what was observed in the B-cell derived cell lines.

However, no AID protein expression could be detected in any of the epithelial derived cell lines. Thus although some papers reported a correlation between AID expression and certain types of epithelial cancers (Tomlins *et al*., 2005; Lin *et al*., 2009; Fichtner-Feigl *et al*., 2015), our observations point to an unlikely role for AID in these cancers. As our cohort (n = 16) was quite small, a larger study with more samples needs to be performed with the use of tumour biopsies to conclusively reveal whether AID is associated with these cancers.

Mass spectrometry data generated from a large set of colon cancer samples in Professor Blackburn laboratory at the University of Cape Town was analysed for AID expression. The two cohorts were comprised of normal and tumour biopsies in a colorectal cancer (CRC) cohort (n = 18) and from the Jorissen cohort (n = 155) (Jorissen *et al*., 2008). These cohorts were classified according to two distinct sub-types, the one being immune suppressive and the other inflammatory in nature. The analysis found that AID was weakly downregulated in the inflammatory sub-type of the CRC cohort (fold change of -1.6 and a false discovery rate of 0.00067), with no differential expression observed in the Jorissen cohort or between the tumour *versus* normal biopsy analysed (unpublished data (2015), with thanks to Katie Viljoen and Professor Jonathan Blackburn, University of Cape Town). These results correlate with the mRNA and qPCR results described in this chapter, reiterating that AID overexpression is more pertinent to B-cell derived cancers, such as Burkitt's lymphoma. Therefore, developing an

epithelial derived AID overexpressing model to study the role of AID in cancer was deemed irrelevant.

From the results in this chapter, we were able to confirm that AID is expressed in lymphoblastoid cells, with increased expression in the BL cell lines thus confirming the association of AID with these cancers. Furthermore, the L1439A cell line was identified as a suitable cell line to ectopically overexpress AID and study its role in cancer.

Chapter 4: Ectopic overexpression of AID in the B Lymphoblastoid Cell Lines

4.1 Introduction

AID overexpression has been associated with the development of B-cell lymphomas, especially Burkitt's lymphoma (BL) (Robianni and Nussenzweig, 2013). Additionally, various reports have indicated that it may also contribute to the transformation of cells of non-lymphoid origin, such as epithelial cells of the gastro intestinal tract (GIT) and prostate (Matsumoto *et al*., 2007; Lin *et al*., 2009). However its exact function in the oncogenic process is not well defined. This project aims to use overexpression cell models to better define the oncogenic function of AID. In the previous chapter AID expression was not detected in the sixteen cell lines (14 cancer and 2 normal cell lines) of epithelial origin, while its overexpression was confirmed in BL cells. Thus this chapter focuses on the overexpression of AID in a B-cell line model.

The use of overexpression cell lines as models are useful in studying the role of specific factors in the mechanisms of disease and oncogenic development (Prelich, 2012). Unlike other model organisms where direct genetic manipulation can be performed (eg. transgenic mice models), genetic alterations to humans need to be performed indirectly using cell culture models. With induced overexpression of the gene of interest (AID) in a cell line with relatively low expression levels, comparison of phenotypic and molecular changes between the control and overexpressing models allow for the elucidation of possible mechanistic pathways. Thus with the aim to better define the role of AID in oncogenesis, the development of a cell line of B-cell origin ectopically overexpressing AID was undertaken and the process reported in this chapter. As will become clear in the sections which follow, an AID overexpressing model proved not to be ideal for studying its oncogenic function due to the highly mutagenic nature of this enzyme. The results of this overexpression study are described in detail below.

4.2 Results

4.2.1 Analysis of the mammalian expression plasmids that constitutively express AID

Two plasmids were utilised in this study, the pEGFP-N3 and pcDNA-3.1 backbones which each contained the *AICDA* gene. The identification of pEGFP-N3-AID and pEGFP-N3-Empty

plasmids were verified by restriction digests using *Not*I and *Eco*RI, based on the available plasmid map (Appendix C, Figure C1). Figure 4.1 below shows the three plasmid conformations of the uncut plasmids, namely the supercoiled, linear and nicked circular conformations. While the cut plasmids using the above mentioned enzymes produced two fragments; 4.7 kb and 767 bp fragments for the pEGFP-N3-AID plasmid, and 3.9 kb and 767 bp fragments for the pEGFP-N3-Empty plasmid.

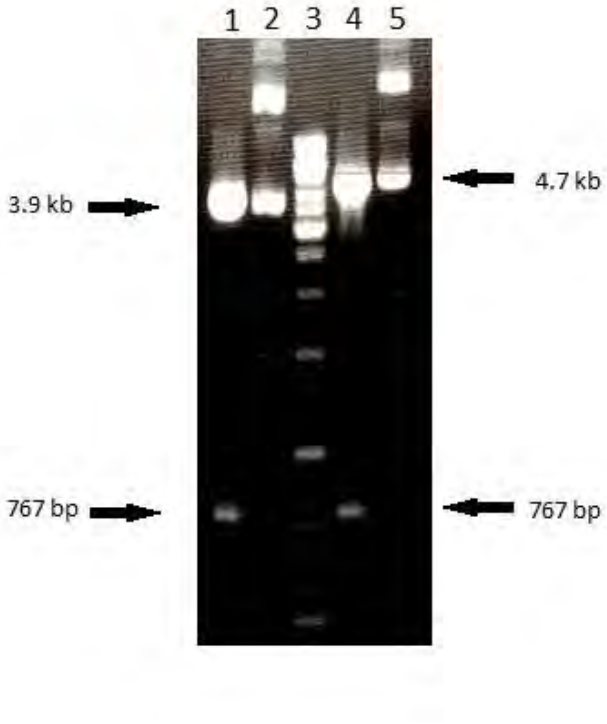

Figure 4.1: Restriction enzyme digestion of the pEGFP-N3-AID and pEGFP-N3-Empty plasmids. Lanes 1 to 5 are as follows: pEGFP-N3-Empty cut with *Not*I and *Eco*RI, pEGFP-N3-Empty uncut, GeneRuler™ 1 kb DNA Ladder (Thermo Scientific™, US), pEGFP-N3-AID cut with *Not*I and *Eco*RI and pEGFP-N3-AID uncut. These samples were electrophoresed on a 1 % agarose gel.

The pEGFP-N3-AID plasmid then underwent Sanger sequencing (Inqaba Biotec, SA) to verify that the *AICDA* gene was cloned in frame with the EGFP tag, which is located downstream of the AID coding region. Figure 4.2 shows the *AICDA* gene was cloned at 65 bp from the primer binding site and after analyses both AID and GFP were shown to be in-frame. Sequencing information and restriction digest information for the pcDNA-3.1-AID plasmid was already available and therefore not repeated.

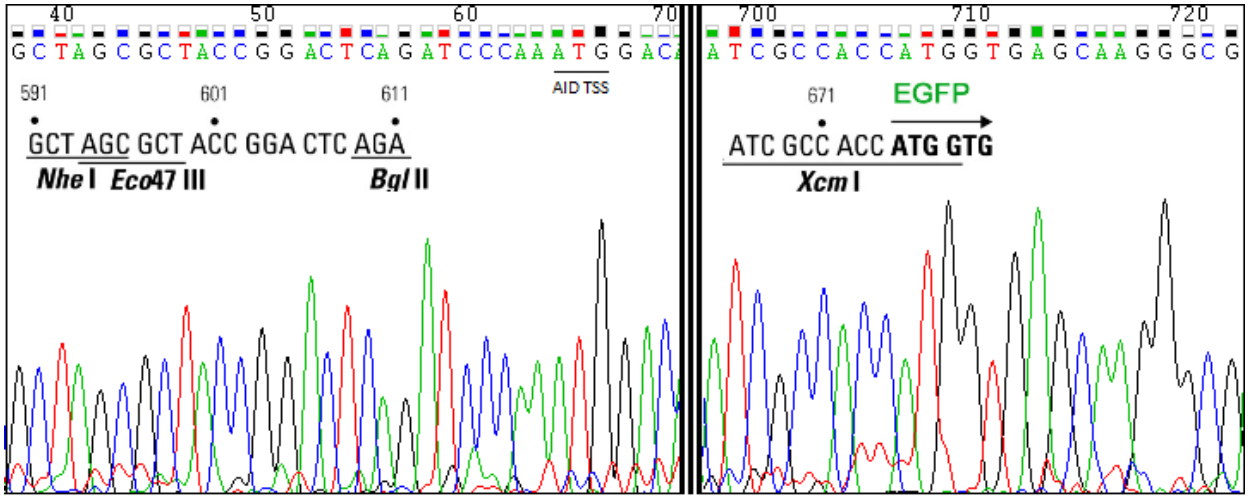

Figure 4.2: DNA electropherogram of pEGFP-N3-AID. The *AICDA* coding region is 597 bp long and shown to be cloned in-frame with the EGFP tag. The GFP selection cassette was also shown to be cloned in-frame. Base pairs are written in black with the restriction enzyme sites from the plasmid map (Appendix C, Figure C1).

To confirm AID protein expression from these plasmids, the COS-7 African green monkey kidney fibroblast cell line, which has relatively high transfection efficiency, was transfected with either pEGFP-N3-AID or pcDNA-3.1-AID, as well as their respective controls (Section 2.11). Table XIII below shows concentrations and purity of the plasmids as determined by the NanoDrop™ ND-1000 (Thermo Scientific™, US), following large scale isolation, performed previously and already available in this laboratory, using the PureYield™ Plasmid Maxiprep System (Promega, US) which ensured the removal of endotoxins (a bacterial contaminant which can interfere with transfection). An amount of 300 ng of each plasmid was transfected and total protein was isolated approximately 30 hours later using the boiling blue method (Section 2.7.3).

Table XIII: Concentrations of the plasmids following isolation.

	Concentration (µg/µl)	260/230 Ratio
pEGFP-N3-AID	308.50	1.88
pEGFP-N3-Empty	379.40	1.87
pcDNA-3.1-AID	419.10	1.88
pcDNA-3.1-Empty	234.00	1.87

Integrity of plasmids was shown to be intact with no degradation as determined by gel electrophoresis (data not shown). A volume of 5 µl of each protein extract was subjected to SDS-PAGE and western blotting using an antibody specific to AID (Invitrogen, US). Figure 4.3 below shows the successful transfection of the COS-7 cells with each plasmid, as well as expression of the protein. Due to the EGFP tag, the band detected for the pEGFP-N3-AID plasmid is larger. As expected, no band was detected when cells were transfected with the empty plasmid.

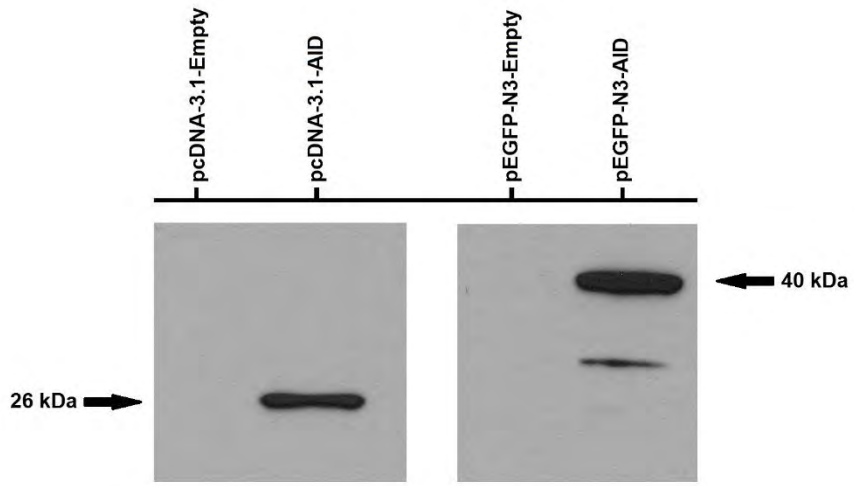

Figure 4.3: Western blot analysis of COS-7 cells transfected with plasmids. COS-7 cells transfected with the empty plasmids (pcDNA-3.1-Empty and pEGFP-N3-Empty) do not express AID, as is expected while cells transfected with the two plasmids which contain the *AICDA* coding sequence (pcDNA-3.1-AID and pEGFP-N3-AID) produce easily detectable levels of AID protein. The band detected in cells transfected with the pEGFP-N3-AID plasmid is larger due to the EGFP tag. 5 µl of protein in 2X boiling blue buffer was boiled at 95 °C for 10 minutes before being loaded and separated on a 12 % SDS-PAGE gel at 100 V for 200 minutes in 1X running buffer. The protein was then transferred onto a nitrocellulose membrane (Bio-Rad) for 75 minutes at 100 V in 1X transfer buffer. This was then detected using the Clarity™ Western ECL Substrate (Bio-Rad). To detect AID, mouse anti-AID (Invitrogen) was used, with a HRP bound goat anti-mouse secondary antibody (Bio-Rad).

4.2.2 The L1439A cell line is recalcitrant to conventional transfection techniques

4.2.2.1 Cell density and optimisation

The L1439A cell line has a relatively long doubling time and requires double the amount of FBS (20 %) for survival, compared to most other cell lines. The optimal growth conditions and cell density to be used for transfection needed to be determined before the experiment was attempted. The characteristics of a healthy L1439A cell population are mostly large, compact, circular shaped clumps, with fewer smaller clumps, and some single cells floating in the

medium (Figure 4.4). Using guidelines from transfection protocols, cells were seeded at various densities (1 x 10^5 cells per well, 2 x 10^5 cells per well, 3 x 10^5 cells per well, 6 x 10^5 cells per well, 8 x 10^5 cells per well and 1 x 10^6 cells per well) in a six-well plate (35 mm) and monitored daily using the light microscope over a period of seven days. Figure 4.4 shows the appearance of the cells seven days post plating and based on this observation, the concentration of 8 x 10^5 cells per well in a six-well plate was chosen as a reasonable density for transfection. This is because for optimal transfection, protocols recommend that cells are between 60 – 80 % confluent.

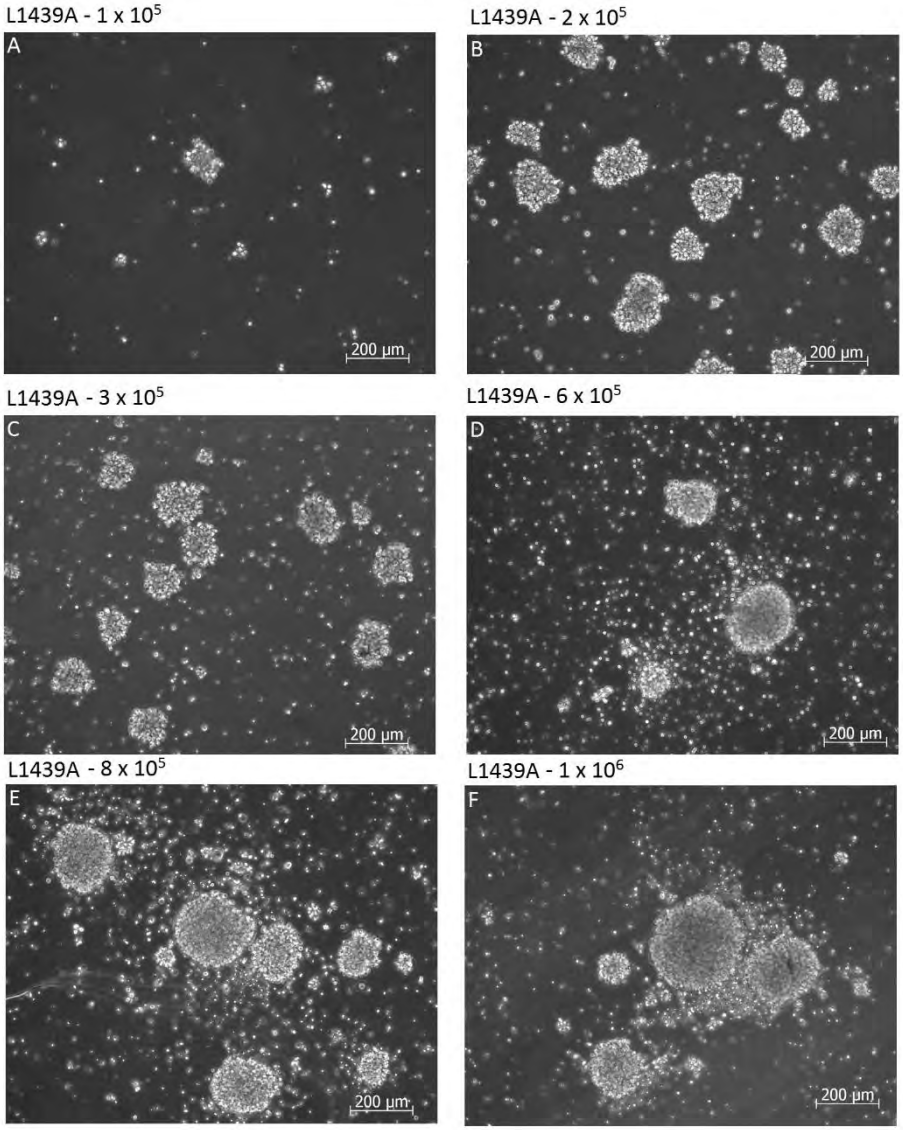

Figure 4.4: Various densities of L1439A cells in culture seven days post plating. L1439A was seeded at 1 x 10^5 (A) 2 x 10^5 (B) 3 x 10^5 (C) 6 x 10^5 (D), 8 x 10^5(E), 1 x 10^6 (F) in a six-well plate (35 mm) and after seven days visualised under the light microscope. Healthy L1439A cells are characterised as compact, circular clumps in combination with scattered single cells. Scale bars are in white.

4.2.2.2 Kill curve for L1439A using G418

Stable transfection requires the integration into the genome of the gene of interest and selection pressure, usually in the form of an antibiotic, for transformed clones which express a gene conferring resistance to the antibiotic. Both of the plasmids used in this study contain the neomycin resistance gene, which confers a resistance to the aminoglycoside antibiotic Geneticin (G418). Most cells, including L1439A are sensitive to G418, thus only successfully transfected cells will be able to survive and proliferate in the presence of this antibiotic. Different cell lines and cell types have different levels of susceptibility to G418, thus with no published data on the susceptibility of L1439A to G418, the concentration of G418 to use to kill all untransformed cells over a period of five to seven days needed to be determined. A range of cell densities were plated (1 x 10^5 cells per well, 2 x 10^5 cells per well, 3 x 10^5 cells per well, 4 x 10^5 cells per well, 5 x 10^5 cells per well and 1 x 10^6 cells per well) in a 96-well plate and observed for seven days to assess the optimal density to use for developing the kill curve. A cell density of 1 x 10^5 cells per well was found to be the most appropriate. The cell density was used to generate the kill curve using the WST-1 assay to measure cell viability over seven days (Section 2.12.2). The result are shown in Figure 4.5 and a concentration of 800 µg/ml of G418 was selected.

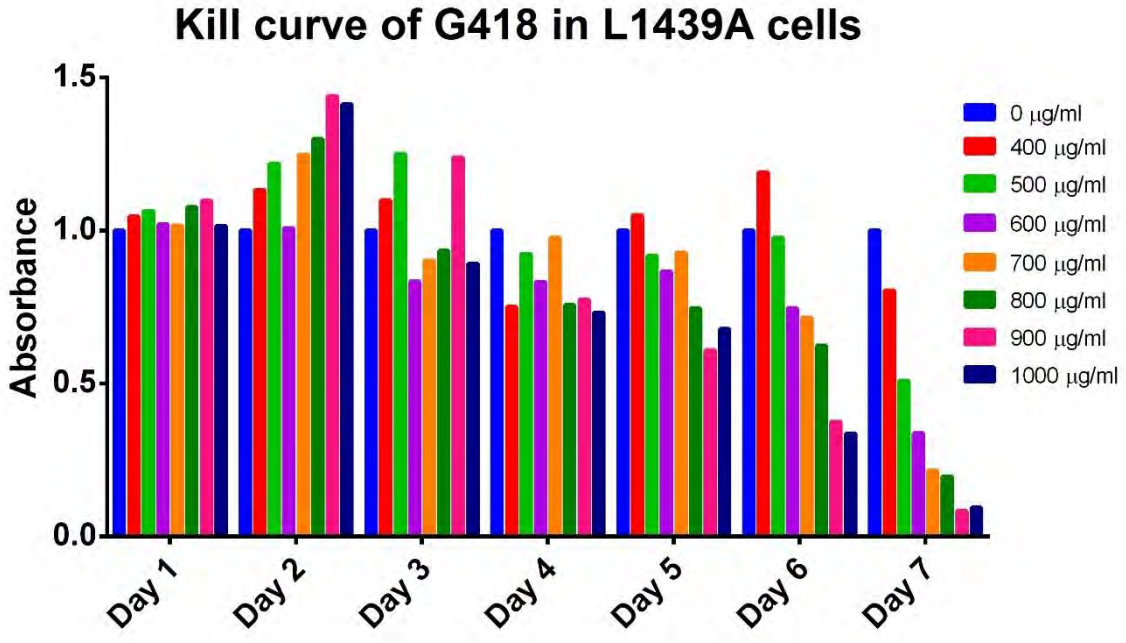

Figure 4.5: Kill curve of L1439A using G418. L1439A cells were seeded at a density of 1 x 10^5 cells per well in a 96-well plate. Varying concentrations of G418 was added to each well, 400-, 500-, 600-, 700-, 800-, 900-, 1000 µg/ml, and cell viability was determined using the WST-1 proliferation assay. Each sample was performed in triplicate. All samples were normalised against the untreated cells (0 µg/ml).

4.2.2.3 Lipid- and polymer-based transfection

B lymphoblast cell lines are known to be notoriously difficult to transfect using conventional techniques (Maurisse *et al*, 2010). Nevertheless, the lipid-based transfection reagent, X-tremeGENE HP (Roche, Germany), which was relatively new on the market, was used in an attempt to transfect L1439A. This lipid-based transfection reagent causes the genetic material, in this case plasmid DNA, to enter the cell by forming a vesicle around the DNA which merges with the cell membrane as both are composed of a phospholipid bilayer. Finding the optimum amount of transfection reagent to use is important, as too much can be toxic to cells and compromise the experiment. The cells were exposed to four different concentrations of the reagent (1 %, 2 %, 3 % and 4 %) and after 30 hours, cell viability in the presence of this reagent was determined using the WST-1 Assay (Section 2.12.1). In addition, the optimal time post-addition of the WST-1 reagent was determined using four different time points (0.5 hours, 1 hour, 2 hours and 4 hours). From the result presented in Figure 4.6 below, 3 % of X-tremeGENE HP was chosen since this volume was the highest that could be used without causing cell death. In addition, the WST-1 incubation time of two hours was selected as the optimal time point in which analyse the results on the GloMax®-Multi microplate reader (Promega, US).

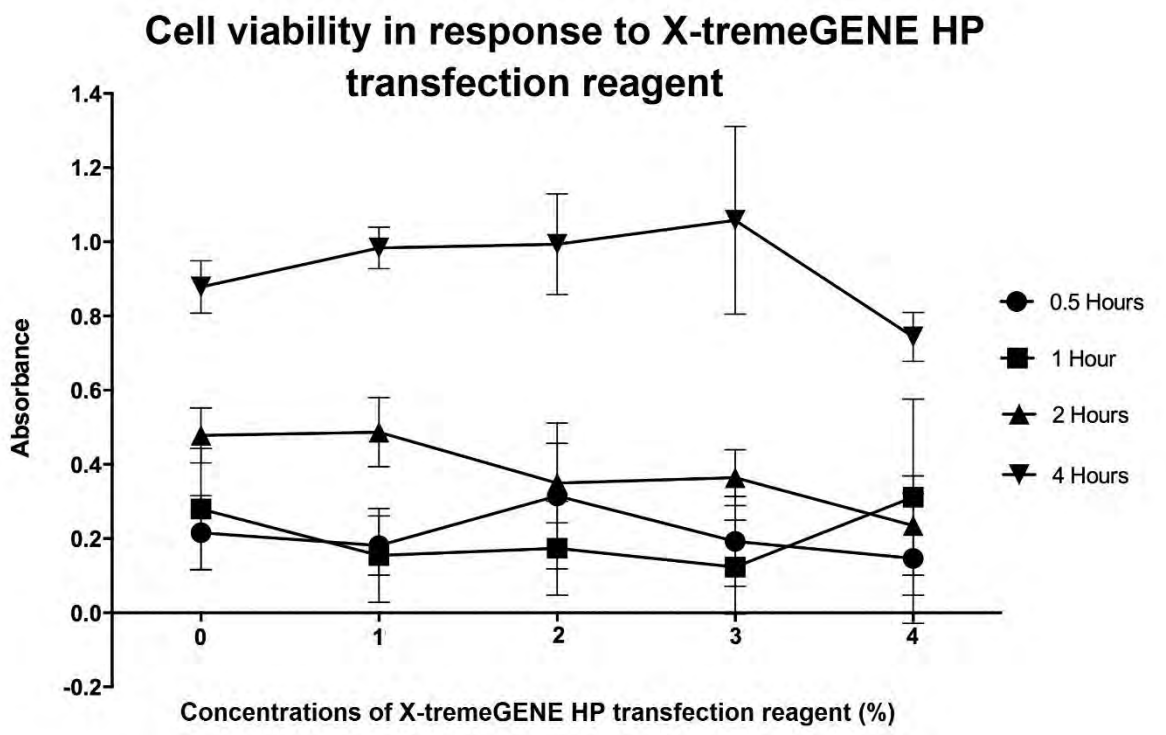

Figure 4.6: Determination of optimal X-tremeGENE HP concentration for transfection of L1439A cells. Four different concentrations of transfection reagent were added to the L1439A cells and incubated for 30 hours, the WST-1 reagent was added and analysed at different time intervals over four hours (0.5 hours, 1 hour, 2 hours and 4 hours). A transfection reagent concentration of 3 % and a WST-1 incubation time of two hours was selected, as this had a low amount of cell death while maintaining a high effective concentration. SEM values are represented by the error bars.

4.2.2.4 Transfection of L1439A

The L1439A cells were therefore transfected with the pEGFP-N3-AID and pEGFP-N3-Empty plasmids using 3 % X-tremeGENE HP (Roche, Germany). This plasmid was used due to the presence of the EGFP tag which allows easy detection of transfected cells using fluorescence microscopy. After an incubation period of 30 hours post-transfection, no successfully transfected cells were detectable (Figure 4.7; A-F). To verify the integrity of the transfection reagent, the human fibrosarcoma cell line HT-1080, which is an established, easily transfectable cell line, was transfected in parallel with the same plasmid. As can be seen in Figure 4.7 below, numerous HT-1080 cells were positive for GFP (Figure 4.7; G-L). This indicated that the transfection of L1439A cells, using this method and this reagent, was unsuccessful.

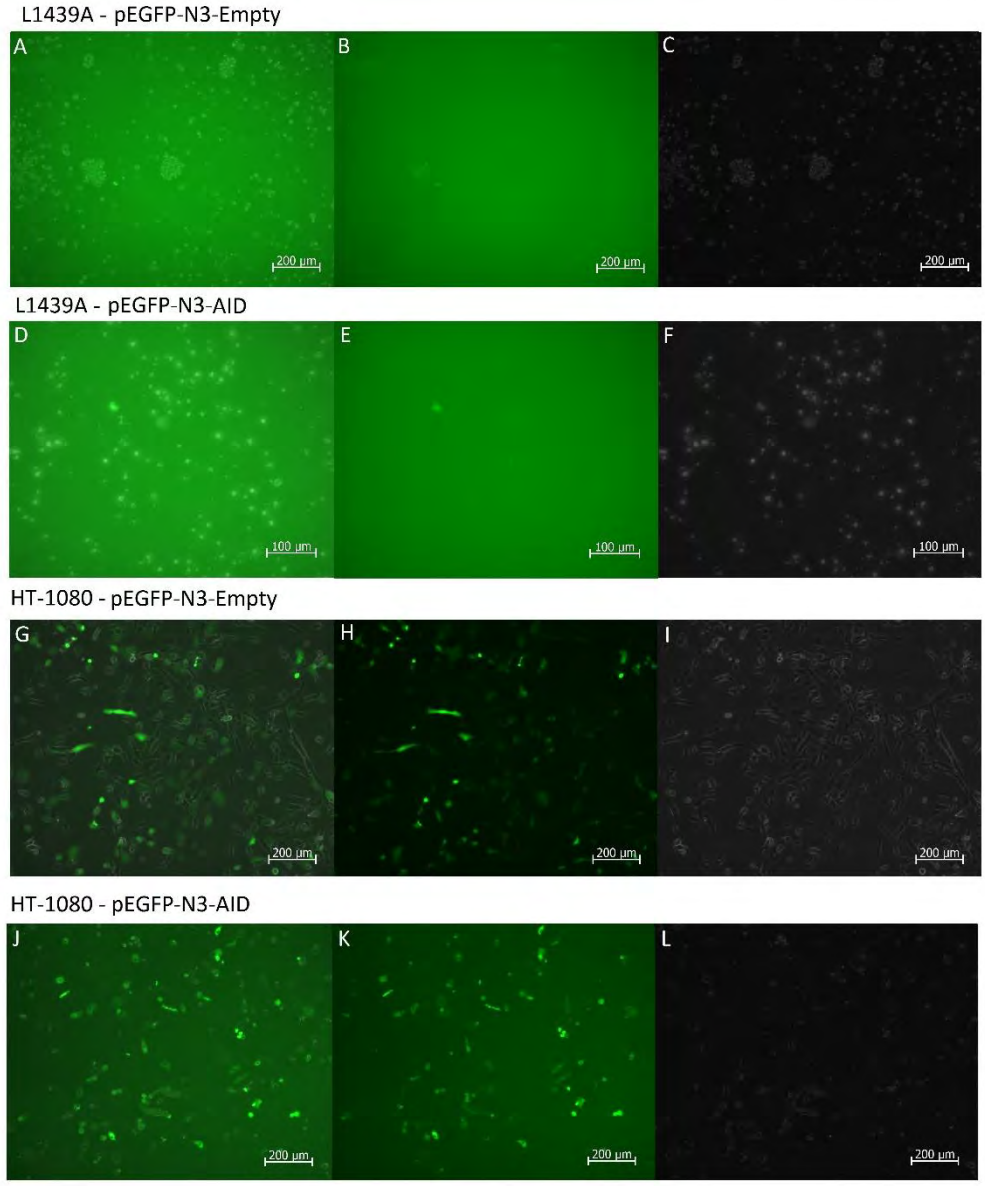

Figure 4.7: Fluorescence microscopy images of L1439A and HT-1080 cells following transfection with pEGFP-N3-Empty and pEGFP-N3-AID using X-tremeGENE HP. Cells were transfected with either the pEGFP-N3-AID or pEGFP-N3-Empty, incubated for 30 hours, and visualised using a fluorescent microscope. A-C is the L1439A cells transfected with pEGFP-N3-Empty and D-F are the L1439A cells transfected with pEGFP-N3-AID. G-I are the HT-1080 cells transfected with pEFGP-N3-Empty and J-L are the HT-1080 cells transfected with the ePGFP-N3-AID plasmid. LHS panels represent the overlaid fluorescent and phase contrast images, the middle panels represent the fluorescent images, while the RHS panels represent the phase contrast images. Scale bars are in white.

As an alternative option, a cationic polymer-based transfection reagent called TurboFect (Thermo Scientific™, US), recommended by the manufacturer for “difficult-to-transfect” cell lines was used. This reagent functions by forming a compact, positively charged complex between the DNA and the polymers, this complex then protects the DNA from degradation

and allows the plasmid to be delivered into the cells. Unfortunately, as with the lipid-based transfection reagent, we were unable to successfully transfect L1439A with this reagent (data not shown). Since chemical transfection was ineffective with L1439A, electroporation was the next recommended course of action in overexpressing AID in these cells.

4.2.4 Nucleofection

Electroporation is a process whereby the cells are subjected to an electric shock. The Amaxa™ Nucleofector II™ (Lonza, Germany) machine was used, with the recommended Amaxa® Cell Line Nucleofector® Kit V (Lonza, Germany). This system produces an electroporatic shock creating pores in the cell membrane, and with the help of the nucleofector solution (a proprietary solution made up of solutes) which protects the cells while carrying the electric charge, allowing the plasmids to enter the cells. This technique is generally quite harmful to cells, and thus a protocol needed to be optimised for the L1439A cell line. Following consultation with the Lonza Technical team in Germany, a list of five nucleofection programmes were recommended, of which we were required to identify one which produced good transfection efficiency without too much cell death. It is important to note that the L1439A cells are extremely sensitive to even small changes to their growth conditions and to stress. They are also highly dependent on growth factors, and grow best in their own conditioned medium.

4.2.4.1 Programme optimisation for the nucleofection of L1439A cells using a control GFP-expressing plasmid

The L1439A cells were subjected to nucleofection with the pmaxGFP™ plasmid provided in the nucleofector kit, using five different programmes recommended by the Lonza Team listed in Section 2.13. Due to the growth requirements of these cells, a mixture of fresh and conditioned media was added post-nucleofection in an attempt to promote cell survival following this harsh treatment. After 48 hours post-nucleofection, the cells were visualised using a fluorescent microscope to identify cells which had taken up the pmaxGFP™ plasmid. Figure 4.8 below shows the results for the three most successful programmes. A control consisted of cells which underwent nucleofection without inclusion of a plasmid. Of the five

programmes used, X-001 was selected as the most effective, as a greater number of GFP positive cells were visible, with the least cell death observed at that time point.

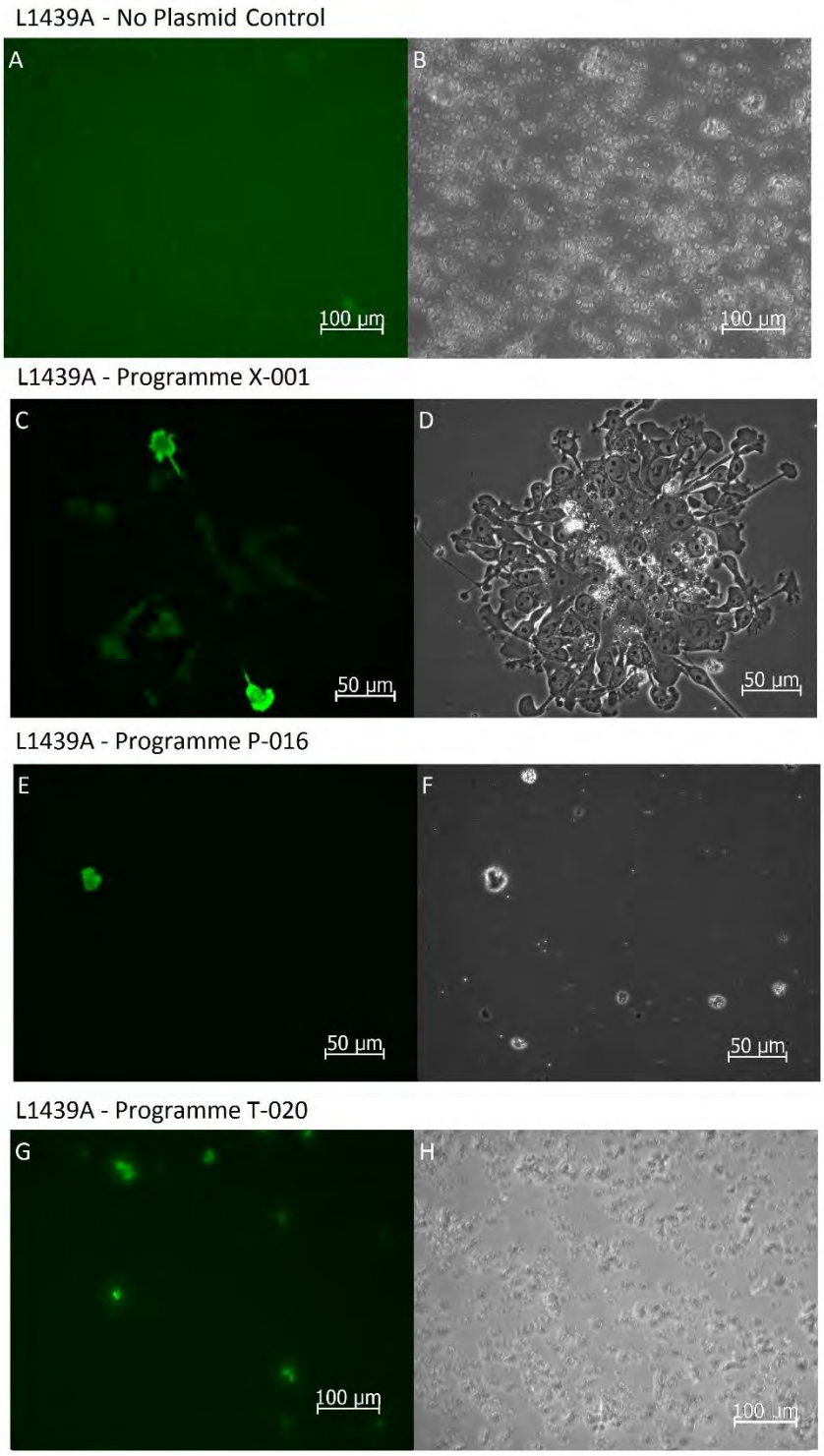

Figure 4.8: Fluorescence microscopy images of nucleofected L1439A cells with the pmaxGFP™ control plasmid. Cells were nucleofected with the GFP-tagged plasmid provided in the nucleofection kit. LHS panel represent the fluorescent images, while the RHS panel are the phase contrast images. A-B are the control cells which did not contain any plasmids, C-D are using programme X-001, E-F are using programme P-016 and G-H are using programme T-020. Scale bars are in white.

4.2.4.2 Nucleofection of the L1439A for AID overexpression

Using the programme X-001, the L1439A cells were subjected to nucleofection using the pEGFP-N3-Empty, pEGFP-N3-AID, pcDNA-3.1-Empty and pcDNA-3.1-AID plasmids. Two sets of plasmids were used as the EGFP tag could interfere with the cellular function of AID, thus using a second plasmid in parallel would confirm the EGFP tagged plasmid results. Forty-eight hours post-nucleofection G418 was added at a concentration of 800 µg/µl to start selecting for positive transformants. Fresh antibiotic (75 % of determined concentration) was added to the medium every 48 hours as G418 is heat labile and is reported to be degraded over time (Adolph, 1996). A gradual decrease in the viability of the cells was observed over the seven days post-nucleofection, with 100 % cell death being achieved at day seven. It was thought that this could be due to either the nucleofection process, or the added stress of the G418 antibiotic selection. Therefore, the nucleofection experiment was repeated with the pEGFP-N3 plasmid and a non-plasmid control without the addition of G418 and observed over seven days. Even without the antibiotic selection, the L1439A cells still did not survive. We therefore concluded that these fragile cells were not suitable for the electroporation process and were therefore not suitable as a cell culture model to study the role of AID.

An alternative cell line was therefore selected for the overexpression of AID. Out of the panel of BL cell lines which were assessed for AID expression by western blot analysis (Figure 3.9 in Chapter 3), the Ramos cell line had relatively low AID expression (approximately 1.5 fold higher AID expression than the L1439A cells) and was therefore selected. Additionally, Ramos is a well characterised cell line which was compatible with the Nucleofector Kit V (Lonza, Germany) and had published nucleofector programmes, thus eliminating the need for time consuming and costly optimisation. The sections below describe the results obtained for the overexpression of AID in Ramos.

4.2.4.3 Nucleofection of Ramos cells

The literature suggests that the nucleofection programme O-006 is suitable for Ramos cells (Thapa *et al*., 2011). Similarly, the concentration of G418 antibiotic to use for the selection of transfected clones was also published at 1 000 µg/ml (Vaughan *et al*., 2014). Nucleofection was performed on the Ramos cells using both the pEGFP-N3 (empty as well as AID expressing)

and pcDNA-3.1 plasmids (empty as well as AID expressing) with G418 added 48 hours post-nucleofection. The G418 was initially added at a concentration of 1 000 µg/ml and every 48 hours, 75 % of the concentration of G418 was replenished due to the unstable nature of the chemical. The cells were expanded in culture for approximately two weeks before undergoing cell sorting to separate viable cells from dead cells. The Ramos cells nucleofected with the pEGFP-N3 plasmid were sorted using a fluorescent channel using the GFP tag as a means to identify viable cells. On the other hand, Ramos cells nucleofected with the pcDNA-3.1 plasmid, which does not express GFP, were sorted through the addition of 7-AAD, a DNA intercalating dye which binds to all exposed DNA and cannot cross the intact viable cell membrane. Thus 7-AAD stains dead or dying cells which usually have punctured cell membranes, allowing entry of the 7-AAD stain which then binds to the DNA. Figure 4.9 illustrates diagrams which depict the cell sorting result. The control cells (A-C) which underwent the nucleofection process but without including any plasmid, are therefore not expected to display any fluorescence, as is the case (RHS panel). The pre-sort analysis of the cells nucleofected with the pEGFP-N3-Empty (D-F) show some GFP positive cells (approximately 2.6 % of the parent population), as can be seen by the cell population in blue in P2 (E) and the peak in P3 (F). After sorting, the cell population was checked for purity (G-I) as can be seen in panel I, the majority of the sorted cells were positive for GFP. However, no GFP positive cells could be detected within the Ramos cell population nucleofected with the pEFGP-N3-AID (J-L). The cell sorting results of Ramos cells nucleofected with pcDNA-3.1 plasmids were similar to what was observed for the pEFGP-N3 plasmids (Figure 4.10). While cells harbouring the pcDNA-3.1-Empty vector (D-I) could be detected and sorted, Ramos pcDNA-3.1-AID cells showed total cell death.

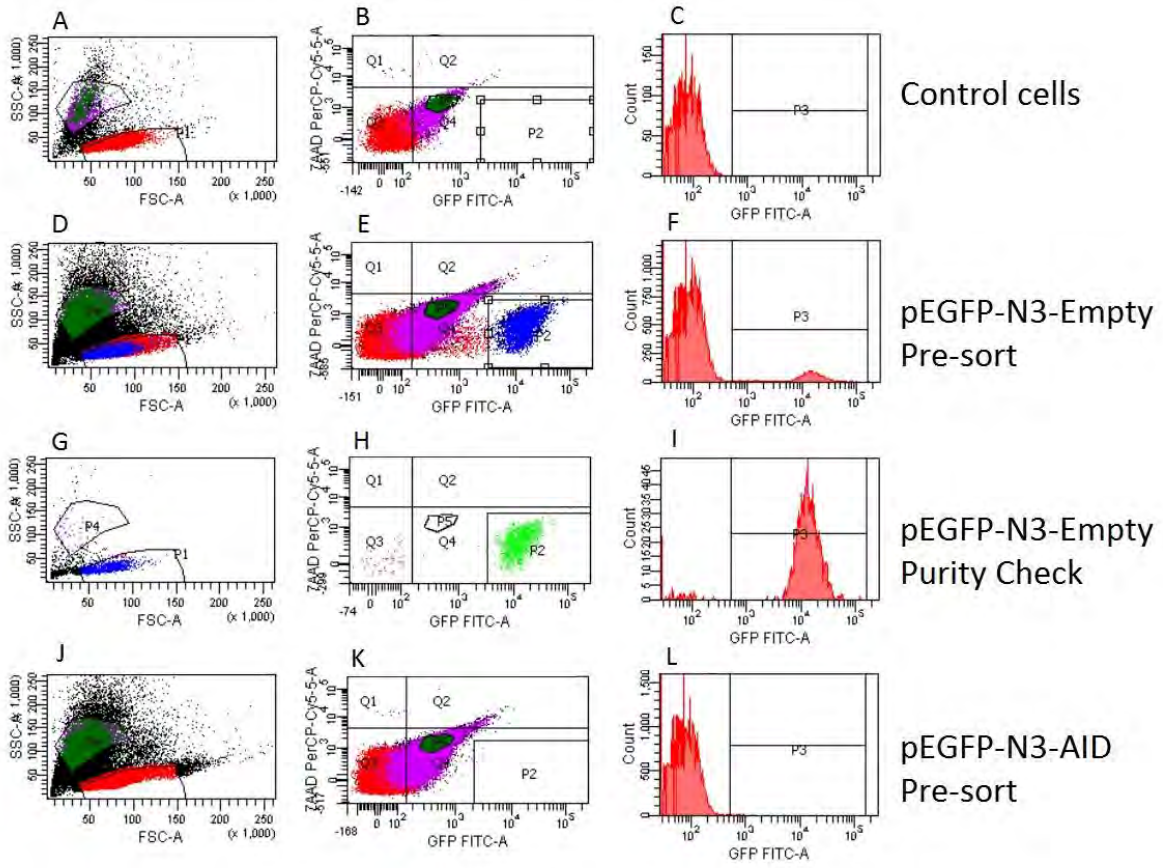

Figure 4.9: Cell sorting analysis of the pEGFP-N3 plasmid transfected Ramos cells. The LHS panel represents the flow cytometric analysis of the forward and side scatter of the cells, the middle panel is the quadrants of expression where P2 represents the live GFP expressing cells, the RHS panel is a histogram analysis of the GFP expression where anything that falls within the P3 quadrant are positive for GFP expression. A-C are the control cells which underwent nucleofection, but contained no plasmid, D-F are the cells nucleofected with pEGFP-N3-Empty before the sorting, G-I are the sorted cells from D-F and a check of the purity of the sort, while J-L are the nucleofected cells with pEGFP-N3-AID.

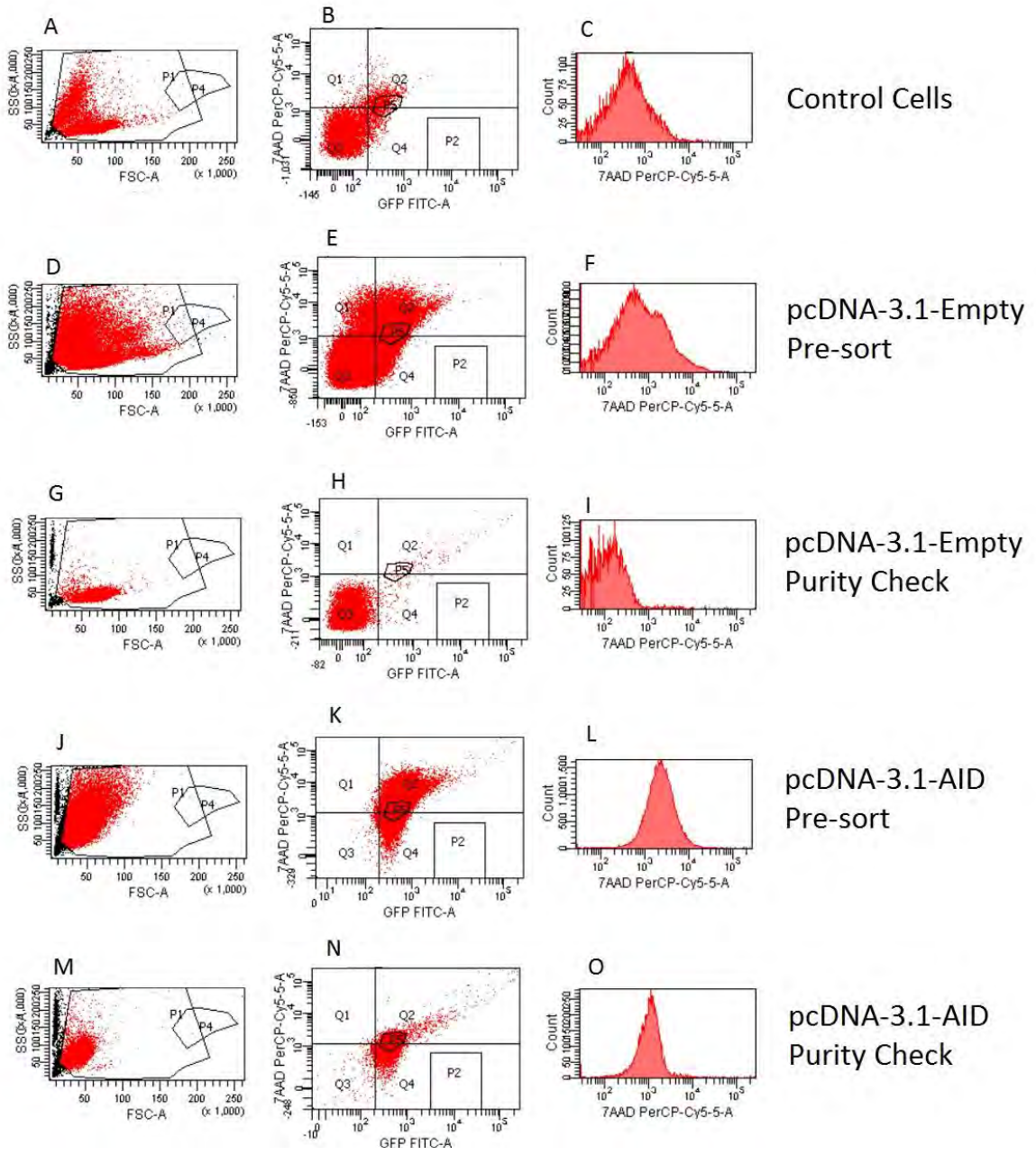

Figure 4.10: Cell sorting analysis of the pcDNA-3.1 plasmid transfected Ramos cells. The LHS panel represents the flow cytometric analysis of the forward and side scatter of the cells, the middle panel is the quadrants of expression where Q3 represents the live cells, the RHS panel is a histogram analysis of the 7-AAD expression. A-C are the control cells which underwent nucleofection, but contained no plasmid, D-F are the cells nucleofected with pcDNA-3.1-Empty before the sorting, G-I are the sorted cells from D-F and a check of the purity of the sort, while J-L are the cells nucleofected with pcDNA-3.1-AID as seen before sorting, M-O are the sorted cells from J-L and a check of the purity of the sorted cells.

From the above results, it would appear that it is the constitutive and relatively abundant expression of AID which is causing cell death. The nucleofection experiment was repeated using the pEGFP-N3 plasmids and GFP expression was monitored by flow cytometry earlier

than in the previous experiment, at day three, to determine how long the AID-expressing cells were able to stay viable before death. This revealed that the majority of cell death occurred three days post-nucleofection, with no further detection of GFP expression within the cell population (Figure B8). Therefore, the deleterious cellular effects of AID overexpression are rapid.

4.2.5 Mechanism of cell death by AID overexpression

In this section, we aimed to ascertain whether the AID-induced cell death observed in the Ramos cells was via senescence or apoptosis. These are the main two possible mechanisms of cell death usually brought about by overexpression of an oncogene. In the case of senescence, cells usually stop dividing, acquire a typically large morphology, and eventually disintegrate. Apoptosis on the other hand is a form of programmed cell death.

4.2.5.1 SA-β-Gal activity

To detect whether AID led to senescence, a senescence-associated β-galactosidase (SA-β-gal) assay was performed (Section 2.15). Cells undergoing senescence produce a biomarker called β-galactosidase (β-gal) at pH 6.0, which is not produced in healthy cells (Lee *et al*., 2006). In the presence of β-gal, a chromogenic substance such as X-gal can be cleaved and used to detect senescence. The AID overexpressing cells were subjected to X-gal and the cells undergoing senescence produced a blue colour which was visualised and counted on the haemocytometer under the microscope. Figure 4.11 is a graphical comparison between the AID expressing and empty pEGFP-N3 vectors compared to a control plasmid which constitutively expresses β-gal (pCMV-β-gal – kindly donated by Associate Professor Prince, Cell Biology, University of Cape Town). The cells transfected with the control pCMV-β-gal plasmid had a positive β-gal expression of approximately 93 %, while both the Ramos cells nucleofected with AID-expressing and empty vectors had a significantly lower, but similar expression of approximately 65 %. This is contrary to the difference in cell death experienced by each nucleofected sample as the AID overexpressing cells had been shown to have a much higher cell death than cells nucleofected with the empty vector. Nevertheless, since no difference in viability could be observed between empty vector and AID-expressing cell, it can

be concluded that a decrease in proliferation and increase in cell death was not attributed to senescence.

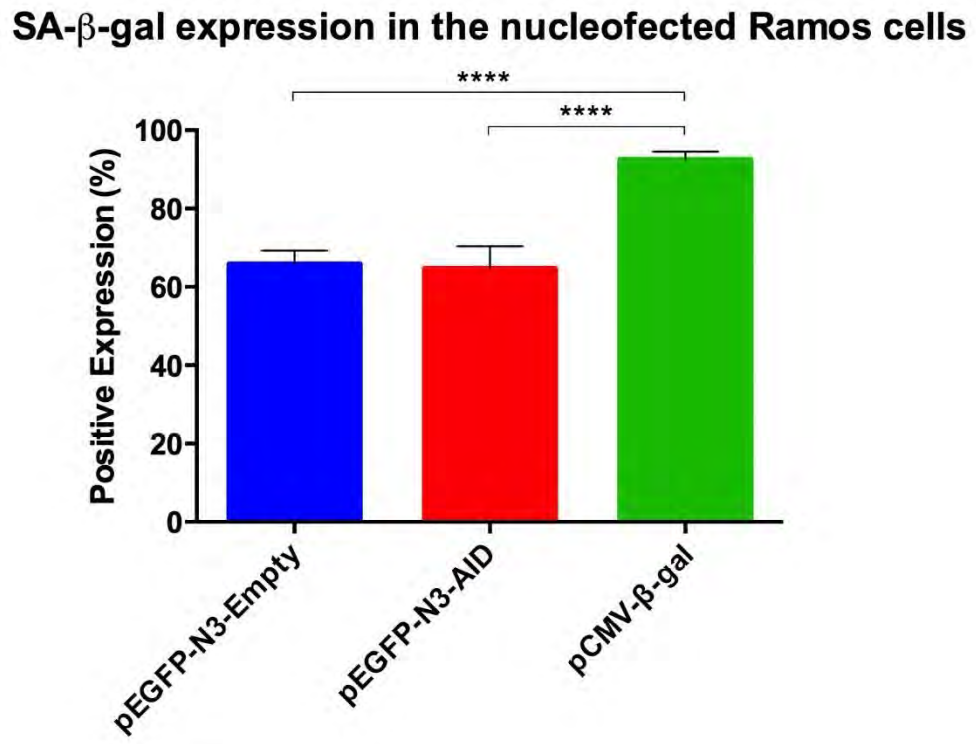

Figure 4.11: Expression of X-gal between different nucleofected plasmids in SA-β-gal assay. Each bar represents the expression of β-gal with the blue and red bar representing cells undergoing senescence. The blue (pEGFP-N3-Empty) and the red (pEGFP-N3-AID) bar are the nucleofected Ramos cells, the green (pCMV-β-gal) bar represents cells nucleofected with a plasmid which constitutively expresses β-gal. **** represents a p value of < 0.0001 (Prism 6, GraphPad, US).

4.2.5.2 Cell cycle profiling

Cells that have sustained an injury, whether mechanical or genomic (as is the case in this study), may undergo a process of programmed cell death to protect the organism. Cell cycle profiling was used as an initial method to determine whether apoptosis is occurring. Cell cycle profiling uses the measure of DNA content to determine the proportion of cells in the various phases of the cell cycle. Cells in the G0/G1 phase will have N amount of DNA, while cells in the G2 phase will have 2N amount of DNA. Cells in the S phase, which are undergoing DNA replication, have DNA content between N and 2N. This method has the ability to also detect cells containing fragmented DNA, in the form of sub-G1 peak, which are usually indicative of apoptotic cells. Figure 4.12 below represents the cell cycle profiling of the Ramos cells

nucleofected with the pEGFP-N3 plasmids. The Ramos cells nucleofected with pEGFP-N3-Empty (A) has 22.69 % apoptotic cells, however, there is a population of healthy looking cells (77.31 %) which display a normal cell cycle profile. The Ramos cells nucleofected with the pEGFP-N3-AID plasmid has a lot more apoptotic cells as depicted by a large sub-G1 peak which is merging with the G1 peak, and no distinct S phase or G2 phase cells can be seen. This shows that the majority of cells in this population have fragmented DNA, indicative of apoptosis.

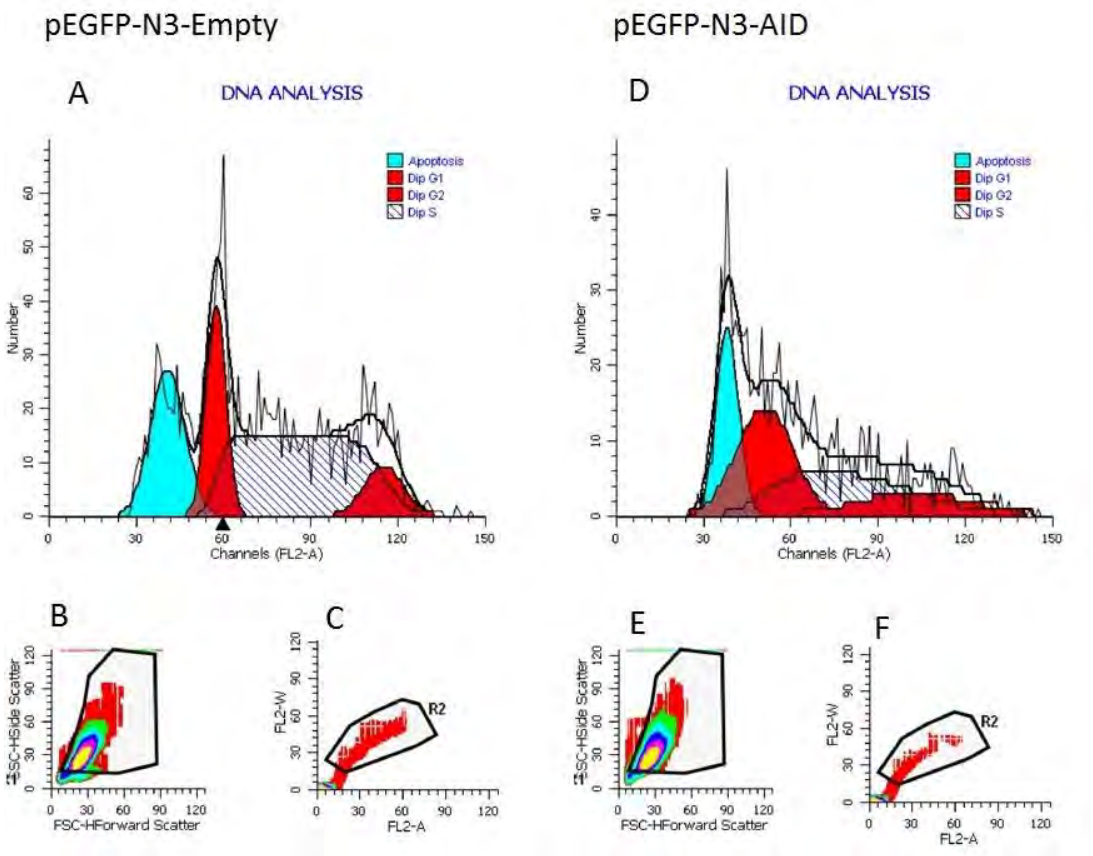

Figure 4.12: Cell cycle profiling of the nucleofected Ramos cells. A is the cell cycle profile of Ramos cells nucleofected with pEGFP-N3-Empty, B and C depict the cells which were selected for the profiling. D is the cell cycle profile of Ramos cells nucleofected with pEGFP-N3-AID, E and F are the cells which were selected for the profiling. The sub-G1 peaks, in blue, represent cells with fragmented DNA, indicative of apoptosis.

4.2.5.3 Apoptosis

To determine whether the cells overexpressing AID were undergoing apoptosis, the Annexin V Kit (BD, UK) (Section 2.16) was used. This kit contained a fluorescently tagged Annexin V antibody that binds to cells undergoing apoptosis. As can be seen in Figure 4.13 below, Ramos

cells nucleofected with the pEGFP-N3-Empty vector had 19.24 % of the cells positive for Annexin V (A), while the pEGFP-N3-AID cells were 51.49 % positive (B), showing that more of the cells overexpressing AID were undergoing apoptosis..

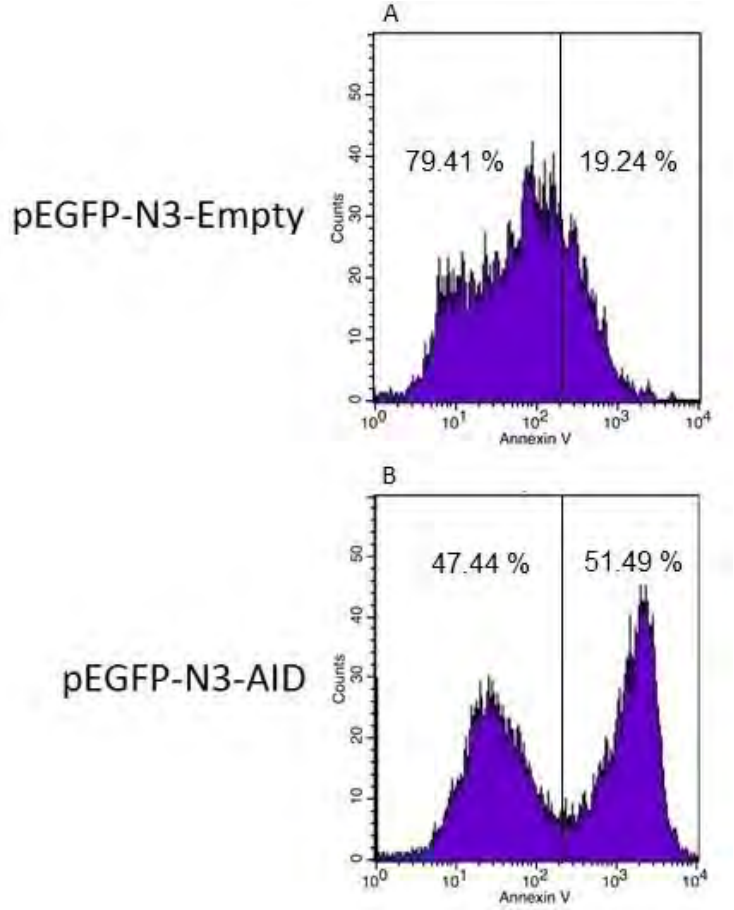

Figure 4.13: Flow cytometric analysis of Annexin V for the nucleofected Ramos cells. (A) is the Annexin V expression profile of pEGFP-N3-Empty and (B) is the Annexin V expression profile of pEGFP-N3-AID. The values in each block represent the percent of cells counted.

4.3 Discussion and conclusion

Results from the previous chapter indicated that the EBV-immortalised B lymphoblastoid cell line, L1439A, would be a potentially good model to use for the ectopic expression of AID to study its oncogenic function. To achieve ectopic expression, mammalian plasmids constitutively expressing AID were obtained and needed to be verified. Two different plasmid sets were available for use in this study, and both were found to express the AID protein when transfected in the COS-7 cell line (Figure 4.3).

The optimal culture conditions and cell line maintenance of L1439A had to be determined prior to introducing AID ectopically (Figure 4.4). This cell line which was created at the University of Cape Town, had not been used by many researchers, and information about the optimal culture conditions were mostly anecdotal. Furthermore, no protocols were available for the introduction of a plasmid into these cells. As these cells were taken from a healthy donor, and then immortalised using EBV, it had a relatively slow growth rate and required high concentrations of growth factors (20 % FBS) to grow efficiently. These cells also prefer conditioned culture medium, since a decrease in cell density led to growth arrest and cell death. In this study, it was established that the optimal cell number for healthy growth was seeding 8 x 10^5 cells per ml in a six-well plate (35 mm), and at this confluency, cells grew well over a period of seven days, during which time experimental procedures could be carried out. Transfection reagents are known to elicit a cytotoxic response in cells, thus a balance needs to be established for efficient transfection with low toxicity. The WST-1 assay was used to determine the efficient transfection concentration to use for the lipid- and polymer-based transfection reagents. This experiment had two objectives, to identify the ideal concentration of transfection reagent, while at the same time determining the best incubation time for the WST-1 reagent (Figure 4.6). Two hours was selected as the optimal WST-1 incubation time as the four hour reading approached the absorbance saturation levels detectable by the Glo-Max®-Multi+ multiplate reader (Promega, US) and thus would have decreased the assay's sensitivity. The concentration of 3 % was selected for the transfection reagent as it maintained the same toxicity levels as the lower concentrations, as toxicity increased with higher transfection reagent concentrations. This value maintained a high enough concentration of transfection reagent for greater transfection efficiency, while maintaining low enough cytotoxicity so as to prevent cell death.

A concentration of 800 µg per ml of the antibiotic G418 was found to be optimal for the selection of positive transfectants as this concentration killed the majority of cells after seven days (Figure 4.5). It can be noted here that generating the kill curve required many attempts, since the control cells that were used for normalisation were not subjected to G418 selection, became over-confluent prior to the endpoint of the experiment. A fine balance exists between too few and too many cells: too few means the cells do not grow; too many means the cells become confluent too soon. Thus several attempts were made, with various cell

densities at the start of the experiment, in order to reach a satisfactory result. The particularly demanding growth requirements of these cells made a seemingly simple process complicated. However, this hurdle was eventually successfully overcome.

The literature indicated that B lymphoblastoid cells are notoriously difficult to transfect (Maurisse *et al*., 2010; Potter and Heller, 2010), however, with several new transfection reagents on the market claiming to transfect "difficult-to-transfect" cell lines, we first attempted conventional transfection using two of these lipid- and polymer-based reagents (Figure 4.7). However, these did not prove successful for the L1439A cells and thus the Amaxa® Nucleofector™ II (Lonza, Germany) machine was selected. The nucleofection process required significant optimisation, which was performed with assistance from the Lonza technicians in Germany, and a low level of nucleofection was achieved using one of the suggested programmes (Figure 4.8).

However, this process proved detrimental to these cells which did not survive post-nucleofection, even when no plasmids were transfected into them. While this system has been used successfully in published reports for EBV-immortalised B lymphocyte cell lines (Choi *et al*., 2011), it did not work in our hands. A possible explanation may be the cell line itself since EBV has the ability to integrate in many different locations in the genome, this results in a high level of heterogeneity among various clones. Future attempts could focus on sourcing a different clone from the same source, or purchasing a cell line in which a nucleofection protocol has been tried and tested successfully. Alternatively, a different nucleofector could be used, for instance, the Neon® system from Thermo Scientific (US), which seems to have been used with some success by other researchers (unpublished report; informal discussion). The Neon® Transfection System (Thermo Scientific, US) requires less cells and has been shown to successfully transfect other lymphoblast cells, such as the BL cell line P3HR1, which has similar growth requirements to L1439A (Cancian *et al*., 2011).

As an alternative to L1439A, the BL cell line Ramos was selected as a model of AID overexpression due to its relatively low AID protein expression compared to the other BL cell lines which were screened in this study. This is a well characterised cell line for which much of the optimal nucleofection conditions and G418 selection information is available in

published reports (Thapa *et al*., 2011; Vaughan *et al*., 2014). Using these conditions, the Ramos cells were successfully nucleofected with both of the AID overexpressing plasmids, as well as their respective empty control plasmids. However, it soon became clear that cells which expressed AID had a definite growth disadvantage. Cells containing the empty vector could be selected by flow cytometry and expanded well in culture, while cells overexpressing AID did not survive (Figures 4.9 and 4.10). This was confirmed when the experiment was repeated, and even with reduced selection and expansion periods, AID overexpressing cells still died. We therefore propose that the highly mutagenic nature of AID lead to significant cellular damage, triggering the cell stress pathway leading to cell death. This was found to occur mostly by apoptosis, as demonstrated by Annexin V incorporation (Figure 4.13). Although Ramos already has high AID expression compared to a normal B-cell line, it is likely that this cancer cell line, has some but not all checkpoints compromised. Even though Ramos can tolerate a certain level of genomic instability, this cell line has a threshold which was breached when AID was overexpressed, triggering DNA damage checkpoints leading to apoptosis.

One of the main drivers of apoptosis is the tumour suppressor transcription factor p53. Since cancers need to evade apoptosis, it is not surprising that approximately 50 % of all human cancers have a mutated form of p53 (Wang *et al*., 2011). The normal function of wild-type p53 is to promote senescence, inhibit cell cycle progression and induce apoptosis (Freed-Pastor and Prives, 2012). However, when this gene is mutated, it not only loses its tumour suppressor function, the mutated p53 forms complexes with proteins which further repressor cellular function (Freed-Pastor and Prives, 2012). In previous studies, Wang *et al*. (2011) were unable to detect functional or even a mutated form of p53 in Ramos and thus classified this cell line as p53 deficient, however, further studies have revealed that Ramos does contain mutant p53 (Farrell *et al*., 1991; O'Connor *et al*., 1993; Nazari *et al*., 2011). Wang *et al*. (2011) showed that the mutant form of p53 in Ramos cells still maintains some function (ability to translocate to the mitochondria), but has no effect on apoptosis. It is therefore likely that the apoptosis observed in this study is independent of p53 (Fulda and Debatin, 2006; Elmore, 2007). The most likely cause of apoptosis in the AID overexpressing cells resulted from AID's ability to cause double strand DNA (dsDNA) breaks, thus accumulating genetic alterations and creating genome instability which then induced apoptosis. An alternative mechanism of cell

death could be the intrinsic apoptotic pathway which has been shown to be independent of p53 (Fulda and Debatin, 2006; Elmore, 2007).

In future studies, the use of a plasmid with an inducible promotor, as opposed to the constitutively active one which was used here, could be more successful. An inducible promotor will allow time for the cells to be nucleofected, selected and expanded as required, before the AID expression is induced. However, it is likely that the outcome would be the same, *i.e.*, that the cells will undergo apoptosis once AID expression reaches a certain level within the cells which cannot be tolerated.

An alternative approach was adopted for studying the function of AID in the oncogenic process; the use of a knockdown model. This was performed in the Ramos cell line and the results are presented and discussed in the chapter which follows.

Chapter 5: Knockdown of AID Expression in the Burkitt's Lymphoma Cell Line Ramos Using siRNA

5.1 Introduction

As demonstrated in the AID-overexpression study (Chapter 4), high expression levels of AID can be deleterious to cells, thus highlighting why this enzyme is under such tight regulation under normal conditions (Zan and Casali, 2013). With the cells unable to propagate post-electroporation, we could not study the downstream effects of AID overexpression as a means to study AID's role in oncogenesis. As an alternative, a knockdown approach was adopted. This was done using siRNAs which specifically target AID mRNA for degradation, thereby reducing the AID protein expression. As a control, a scrambled siRNA was used, which did not target any known sequences in human cells. The cell line Ramos, which is a Burkitt's lymphoma (BL) cell line, was selected for AID knockdown as it had relatively low AID overexpression compared to the other BL cell lines and closer expression levels to the normal EBV-immortalised human B lymphoblastoid cell line, L1439A (Figures 3.5 and 3.9). The Ramos cell line has been extensively researched upon and thus the optimal cell densities and knockdown protocols had been established. This chapter presents the results of the cellular effects observed in cells where AID was knocked down, relative to control cells, and particular effects were measured which relate to carcinogenesis. These include cell proliferation and viability, migration, genome integrity, B-cell phenotype (CD marker expression) and sensitivity to a chemotherapeutic drug.

5.2 Results

5.2.1 Identification of the most effective siRNA and knockdown conditions to be used in this study

Since no validated siRNA for AID were available, a pack of four siRNAs, each targeting a different region of the AID mRNA, which putatively targeted AID was purchased (Qiagen, Germany) and each one was tested for its effectiveness in knocking down AID expression in the Ramos cell line. For this knockdown experiment, as with transfection of AID overexpressing plasmids described in Section 4.2.2.3, optimisation of conditions was required with regards to transfection reagent concentration and cell density. Kusao *et al*. (2012)

previously published their knockdown conditions of the Ramos cell line, which included the optimal cell density and plate format using Qiagen (Germany) siRNA. These guidelines were therefore followed, which entailed plating 1 x 10^5 cells per well in a 24-well plate format.

5.2.1.1 Selection of transfection reagent

The siRNA manufacturers recommended the use of the transfection reagent HiPerfect (Qiagen, Germany). This experiment was performed as outlined in Section 2.18.1 using either 375 ng or 750 ng of each of the four siRNAs. Similarly, various concentrations of the HiPerfect transfection reagent was used, *i.e.* 3 µl or 6 µl per reaction as shown in Table XIV below.

Table XIV: siRNA concentrations used in the optimisation reaction for each of the four siRNA.

Concentration of siRNA	375 ng	375 ng
Volume of HiPerfect Reagent	3 µl	6 µl
Concentration of siRNA	750 ng	750 ng
Volume of HiPerfect Reagent	3 µl	6 µl

Following transfection, total protein was extracted using 2X boiling blue buffer (Section 2.7.3) and AID protein expression determined by SDS-PAGE followed by western blotting (Section 2.8). Using these conditions, no effective knockdown of AID could be observed for any of the siRNAs used (Figure 5.1).

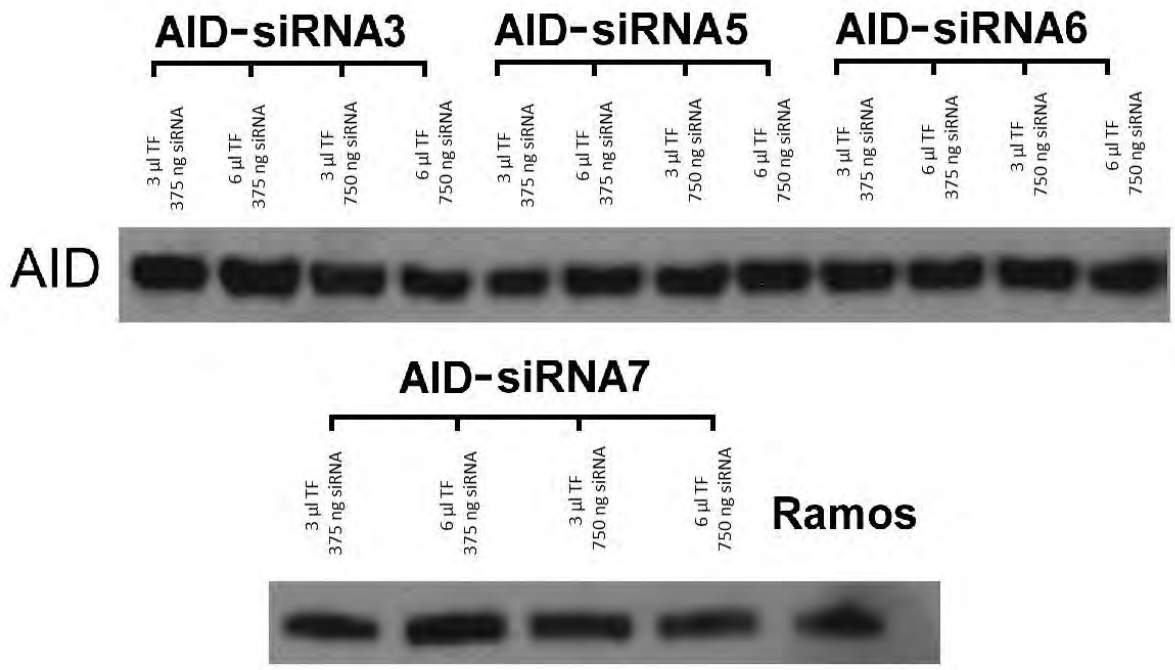

Figure 5.1: AID protein expression in BL cell line Ramos after transfection with AID siRNA using the transfection reagent HiPerfect. Western blot analysis displaying the protein expression levels of AID after these cells had been transfected with 375 ng and 750 ng of each of the four siRNA, using 3 µl or 6 µl of HiPerfect (Qiagen, Germany) transfection reagent. Untreated Ramos cells were used as a comparison. 12 µl of protein in 2X boiling blue buffer was boiled at 95 °C for ten minutes before being loaded and separated on a 12 % SDS-PAGE gel at 100 V for 200 minutes in 1X running buffer. The protein was then transferred onto a nitrocellulose membrane (Bio-Rad) for 75 minutes at 100 V in 1X transfer buffer. This was then detected using the Clarity™ Western ECL Substrate (Bio-Rad). To detect AID, mouse anti-AID (Invitrogen, US) was used, with a HRP bound goat anti-mouse secondary antibody (Bio-Rad).

The knockdown was then attempted using the X-tremeGENE HP (Roche, Germany) transfection reagent that was previously used in Section 4.2.2.4 following the methodology described in Section 2.18.2. In the initial attempt, 500 ng of each siRNA was used and AID-siRNA3 showed significantly more knockdown with an 84 % reduction in AID protein expression compared to Ramos, as is shown in Figure 5.2 below. This siRNA was therefore selected for further experiments.

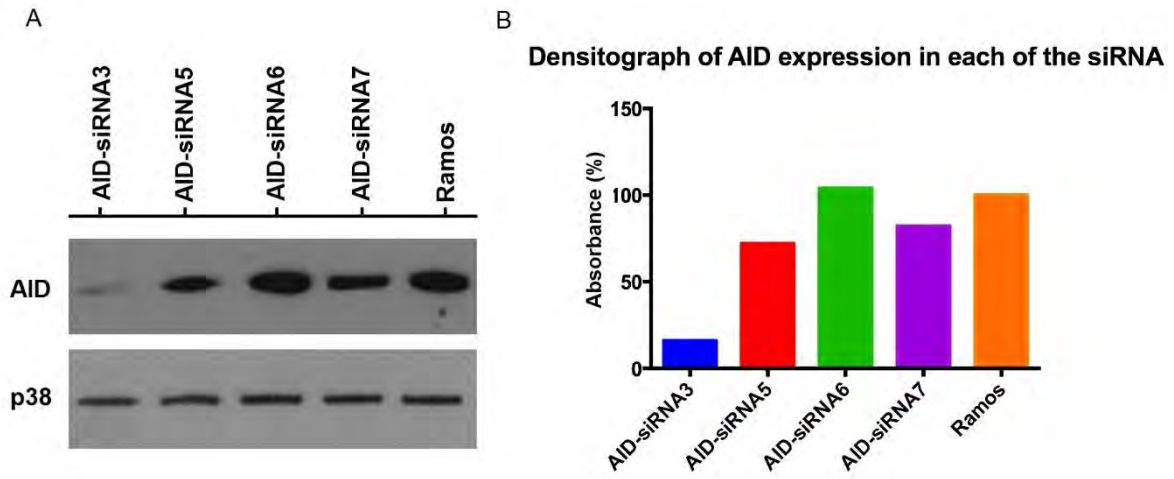

Figure 5.2: AID protein expression in BL cell line Ramos after transfection with AID siRNA using transfection reagent X-tremeGene HP. (A) Western blot analysis displaying the protein expression levels of AID after these cells had been knocked down with 500 ng of each of the four siRNA. Untreated Ramos cells were used as a comparison. 12 µl of protein in 2X boiling blue buffer was boiled at 95 °C for ten minutes before being loaded and separated on a 12 % SDS-PAGE gel at 100 V for 200 minutes in 1X running buffer. The protein was then transferred onto a nitrocellulose membrane (Bio-Rad) for 75 minutes at 100 V in 1X transfer buffer. This was then detected using the Clarity™ Western ECL Substrate (Bio-Rad). To detect AID, mouse anti-AID (Invitrogen) was used, with a HRP bound goat anti-mouse secondary antibody (Bio-Rad). The p38 protein was used as a loading control and was detected using the rabbit anti-p38 antibody (Sigma-Aldrich) and the HRP bound goat anti-rabbit secondary antibody. (B) Densitometric analysis of the signal intensity of the bands analysed using the Li-Cor Image Studio Lite software (Version 4.0, Germany), and normalised to p38 and the Ramos control.

5.2.1.2 Optimisation of AID knockdown using AID-siRNA3

Once an effective siRNA was identified (AID-siRNA3), the most ideal concentration of the siRNA reagent to use for further experiments needed to be determined. A range of siRNA concentrations (500 ng, 750 ng, 1 000 ng and 1 250 ng) was therefore used in knockdown experiments, and a scrambled siRNA, at the same concentrations, was used as a negative control. Figure 5.3 below shows the AID knockdown using AID-siRNA3 *versus* the scrambled siRNA (siRNA Neg), for the two most effective concentrations of 1 000 ng and 1 250 ng. From these results it was determined that 1 000 ng was the ideal concentration.

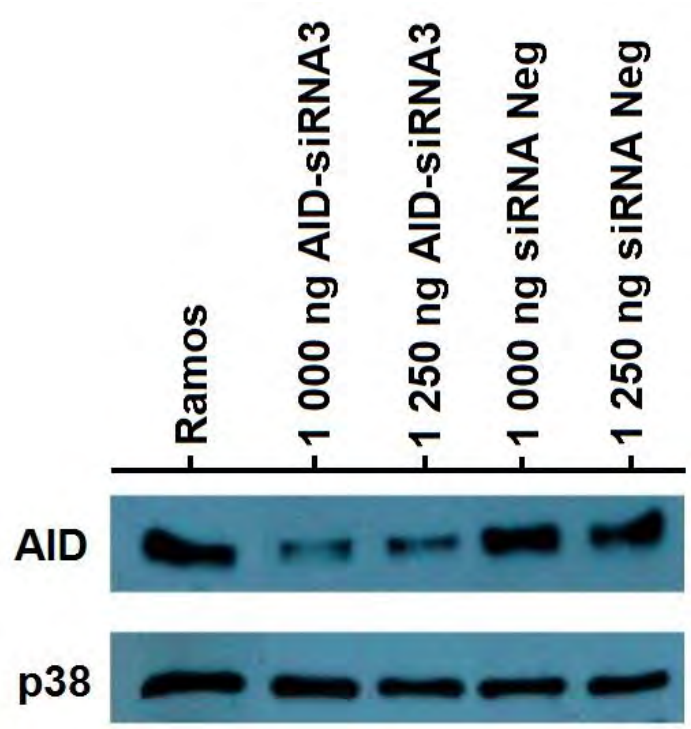

Figure 5.3: Optimisation of AID-siRNA3 concentration for knockdown in the BL cell line Ramos. Western blot analysis displaying the protein expression levels of AID after these cells had been knocked down with 1000 ng and 1250 ng of AID-siRNA3 and scrambled siRNA (negative control). 12 µl of protein in 2X boiling blue buffer was boiled at 95 °C for ten minutes before being loaded and separated on a 12 % SDS-PAGE gel at 100 V for 200 minutes in 1X running buffer. The protein was then transferred onto a nitrocellulose membrane (Bio-Rad) for 75 minutes at 100V in 1X transfer buffer. This was then detected using the Clarity™ Western ECL Substrate (Bio-Rad). To detect AID, mouse anti-AID (Invitrogen, US) was used, with a HRP bound goat anti-mouse secondary antibody (Bio-Rad). The p38 protein used as a loading control and detected using the rabbit anti-p38 antibody (Sigma-Aldrich) and the HRP bound goat anti-rabbit secondary antibody.

5.2.2 Investigation of the effects of reduced AID expression in the Burkitt's lymphoma cell line Ramos, compared to control cells

Once AID could be knocked down reproducibly in Ramos cells, the resulting cellular effects could be measured. In each case, AID knockdown in the cells were confirmed by SDS-PAGE and western blotting (Section 2.8) to ensure that the observed effects were indeed caused by the AID knockdown (Appendix B, Figure B4).

5.2.2.1 Assessment of genome integrity as measured by Phospho-Histone H2A.X (γ-H2AX) expression

As described in Section 1.2.1, AID incorporates mutations in genomic DNA, which leads to dsDNA breaks through the DNA repair pathway (Zan and Casali, 2013). Through this pathway, certain factors are recruited to repair the dsDNA break site, one of these being the Phospho-Histone H2A.X (Ser139) (γ-H2AX) protein (Kuo and Yang, 2008). We anticipated that the higher expression of AID in the Ramos cell line, relative to normal cells (Figures 3.5 and 3.9), maintains a certain level of dsDNA breaks, and hence phosphorylated γ-H2AX expression, and that this will be reduced when the level of AID is knocked down. After 48 hours post-knockdown, total protein was isolated, separated by SDS-PAGE and phosphorylated γ-H2AX expression analysed by western blot analysis (Section 2.8). Figure 5.4 below clearly shows that compared to the Ramos cells transfected with the scrambled siRNA, as well as the untreated cells, no phosphorylated γ-H2AX protein could be detected in the AID knockdown cells. Confirmation of AID knockdown are shown on the right hand side of Figure 5.4.

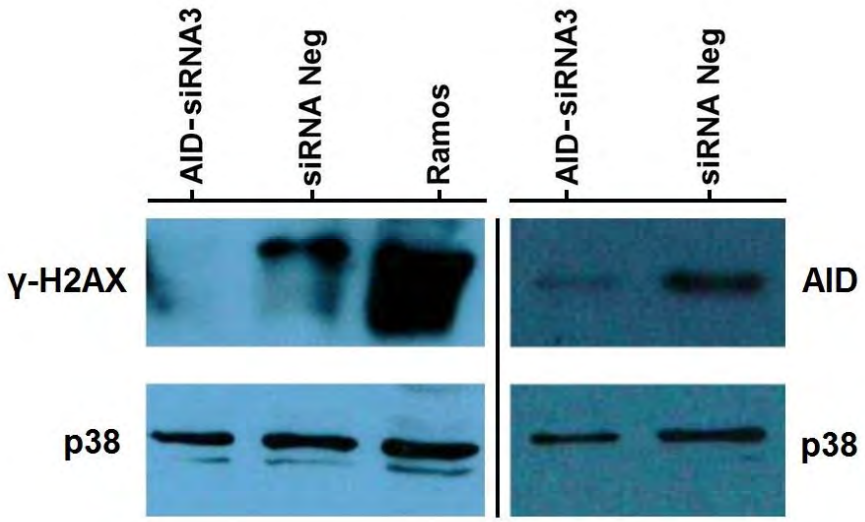

Figure 5.4: Phospho-Histone γ-H2AX protein expression levels in untreated, knockdown, and negative control Ramos cells. Western blot showing the expression levels of phosphorylated γ-H2AX between untreated Ramos cells, siRNA Neg and siRNA-AID3, with the respective knockdown confirmation western blot with the corresponding AID-siRNA3 and siRNA Neg samples on the RHS. 12 µl of protein in 2X boiling blue buffer was boiled at 95 °C for ten minutes before being loaded and separated on a 15 % SDS-PAGE gel at 100 V for 180 minutes in 1X running buffer. The protein was then transferred onto a nitrocellulose membrane (Bio-Rad) for 75 minutes at 100V in 1X transfer buffer. This was then detected using the Clarity™ Western ECL Blotting Substrate (Bio-Rad). To detect phosphorylated γ-H2AX, rabbit anti-Phospho-Histone γ-H2AX (#2577, Cell Signalling, US) was used, with a HRP bound goat anti-rabbit secondary antibody (Bio-Rad). The p38 protein was used as a loading control and detected using the rabbit anti-p38 antibody (Sigma-Aldrich) and the HRP bound goat anti-rabbit secondary antibody.

5.2.2.2 Measure of proliferation of Ramos cells in which AID is knocked down, compared to control cells, with and without treatment with the chemotherapeutic drug doxorubicin

One of the features of cancer cells is the ability to proliferate faster than normal cells (Hanahan and Weinberg, 2011). In this experiment, cell proliferation was determined by measuring cell viability, using WST-1. WST-1 contains tetrazolium salts which are cleaved to formazan dye in the presence of cellular enzymes produced by metabolically active cells, thus the more cleaved salt, the greater the colour change which indirectly indicates cell viability. Cells were plated according to Section 2.12.1, transfected with the respective siRNAs, and 48 hours post-transfection, the WST-1 reagent was added to the medium. The cell viability was measured two hours later using the Glo-Max®-Multi+ multiplate reader (Promega, US). Complete remission of adult BL patients is only achieved in 60 to 70 % of adults, with relapse resulting in early death, thus this experiment was performed to determine whether sensitivity to chemotherapeutic drugs could be achieved with reduced AID expression (Richter-Larrea *et al*., 2010). The chemotherapeutic drug doxorubicin, which is currently part of the regimen used for BL patients, was used to treat the cells (Dunleavy *et al*., 2013). The correct concentration of doxorubicin needed to be determined so as to be a high enough concentration to induce cell death, but low enough to be able to determine whether a change in AID protein expression could alter proliferation. An IC50, which is a process of determining how much drug is required to reduce cell viability by half, was performed with a concentration gradient of 0.025 to 1 µg/ml and proliferation determined using the WST-1 assay (Figure 5.5). This range of concentrations was determined according to the literature published on the Ramos cell line (Lee *at el*., 1999; Nazari *et al*., 2011). From Figure 5.6 a concentration of 0.5 µg/ml was selected as the ideal doxorubicin concentration. As shown in Figure 5.5, in the untreated cells, there was an approximate 8.6 % decrease in proliferation of the AID-siRNA3 *versus* siRNA Neg cells, and an approximate 20.5 % ($p < 0.05$) decrease in AID-siRNA3 *versus* Ramos control cells. In the presence of doxorubicin, the AID-siRNA3 *versus* siRNA Neg cells had an approximate 27.7 % decrease ($p < 0.05$) in proliferation and viability, while the AID-siRNA3 *versus* Ramos control cells had an approximate 26.5 % decrease ($p < 0.05$). There was an approximate 1.1 % change in proliferation between the siRNA Neg and the Ramos control cells in the doxorubicin treated cells. From these results it can clearly be seen that reducing AID produces a change in proliferation and viability, which becomes more pronounced when

the cells are exposed to doxorubicin thus indicting that cells with decreased AID may be more susceptible to chemotherapeutic drugs.

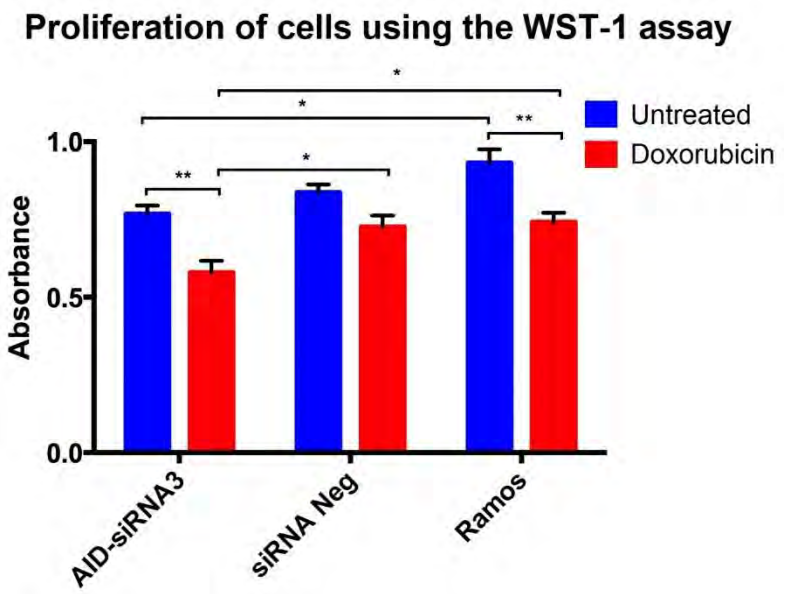

Figure 5.5: Measure of proliferation using the WST-1 assay of normal, AID knock down, and siRNA negative control Ramos cells, in the presence or absence of doxorubicin. Proliferation of normal Ramos cells and knocked down cells either in the presence of doxorubicin (red) or absence (blue). After 48 hours post-knockdown, 4 x 10^4 cells were placed in 100 µl of medium with 10 µl of WST-1 reagent and incubated for two hours, after which the absorbance at 450 nm was normalised against the control absorbance of 750 nm. Error bars represent the standard deviation. ** represents a p value of < 0.01, and * represents a p value of < 0.05 (Prism 6, GraphPad, USA).

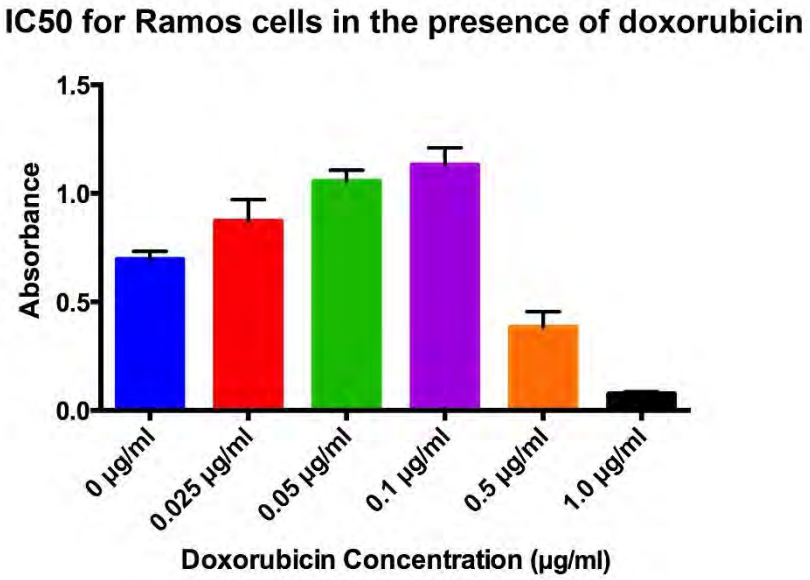

Figure 5.6: IC50 measure for Ramos cells in the presence of the chemotherapeutic drug, doxorubicin. Ramos cells were exposed to a concentration gradient of doxorubicin (0.025 µg/ml to 1 µg/ml) over 48 hours and the cell viability was determined using the WST-1 assay. Error bars represent the standard deviation.

5.2.2.3 Measure of proliferation of Ramos cells in which AID is knocked down, compared to control cells using BrdU incorporation

To confirm the WST-1 results above, the BrdU assay was performed. This assay utilises the pyrimidine analogue, BrdU, which is added to the medium in which cells are growing. It gets incorporated into the replicating DNA of actively dividing cells, replacing the thymidine base in nascent DNA. An antibody specific for BrdU, followed by a fluorescently bound secondary antibody can then be used to detect the incorporation of these nucleotides. The cells are then mounted on slides and visualised under the fluorescent microscope. Figure 5.7 below shows that the BrdU nucleotides were incorporated into both the untreated Ramos cells (approximately 71 %), as well as the siRNA Neg cells (approximately 85 %) with significantly reduced BrdU incorporation into the AID knocked down cells (approximately 11%).

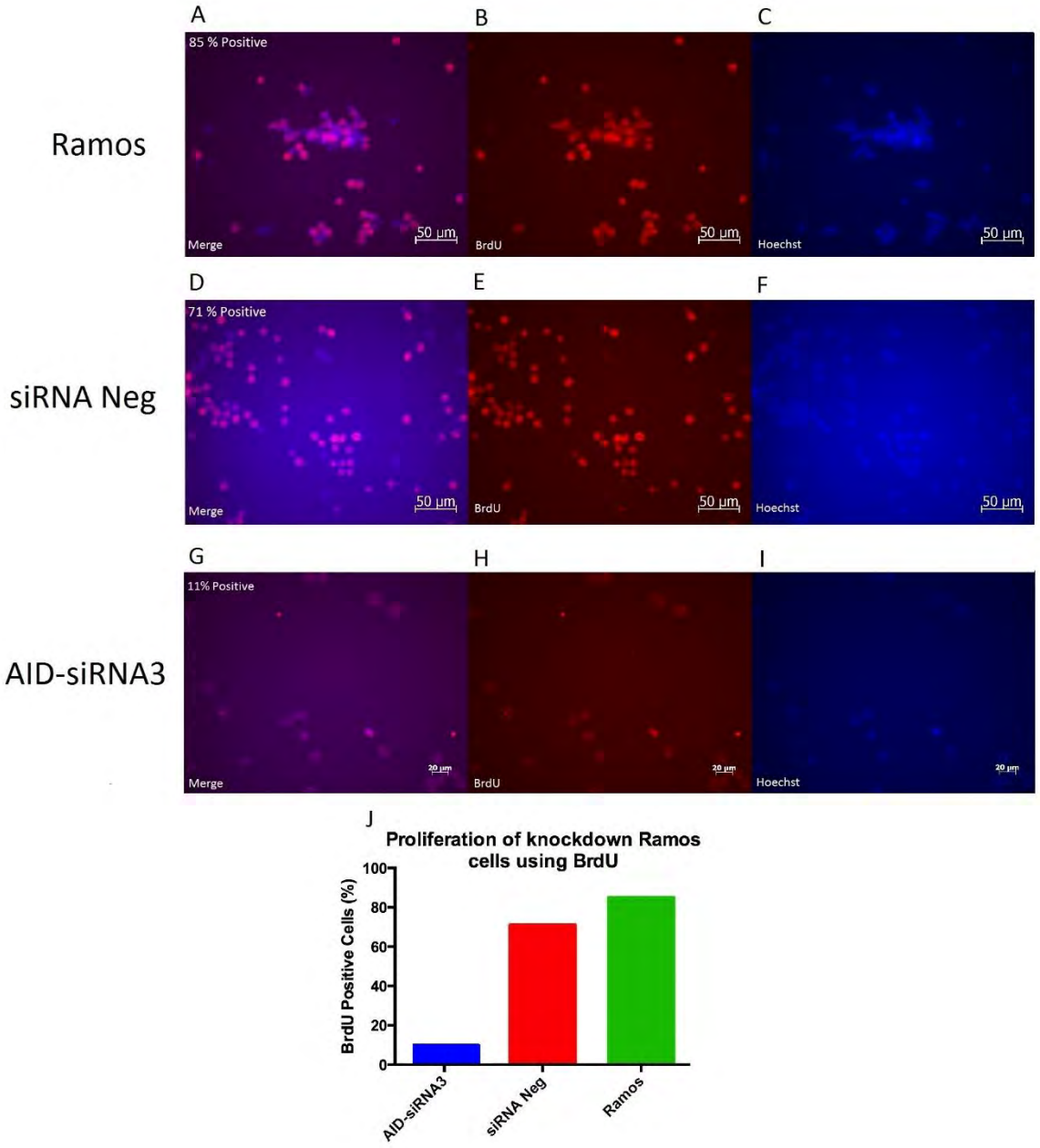

Figure 5.7: BrdU incorporation, as a measure of proliferation in untreated Ramos, siRNA Neg and AID-siRNA3 cells. BrdU staining was performed on untreated Ramos cells (A-C), Ramos cells using the siRNA Neg (D-F) and Ramos cells where AID was knocked down (G-I). Total cells were counted and percent positive cells and the results shown in panel J. BrdU was added to cells 42 hours post-knockdown, or seeding, and mounted onto glass slides. These cells were stained with mouse anti-BrdU (Roche, Germany) followed by the Cy3 donkey anti-mouse secondary antibody (AEC-Amersham, SA). Cells were additionally stained with Hoechst stain to visualise the nucleus. Cells were visualised under the fluorescent microscope. A, D & G are overlaid fluorescent images, B, E & H are the BrdU fluorescent images, and C, F & I are the Hoechst stained images. J is the graph showing the percent positive BrdU cells for the images in A-I.

5.2.2.4 Measure of apoptosis using Annexin V and flow cytometry, with and without treatment with the chemotherapeutic drug doxorubicin

As discussed in Section 4.2.5.3, apoptosis is a process of programmed cell death and cancer cells are normally resistant to apoptosis. In this experiment, we wanted to determine whether knocking down AID would influence the number of Ramos cells which undergo apoptosis, using the Annexin V kit and flow cytometry. Annexin V functions by detecting the phospholipid phosphatidylserine (PS) which translocates to the outside of the plasma membrane in the early stages of apoptosis. The PS is then accessible to the Annexin V protein which has a high affinity for the PS. The Annexin V protein is conjugated to the phycoerythrin (PE) fluorochrome and thus detectible using flow cytometry. A second fluorophore called 7-AAD is used to identify dead/necrotic cells as this protein binds to DNA which is only exposed in cells with a compromised plasma membrane. Both Annexin V and 7-AAD are used in combination to determine the stage of apoptosis. Ramos cells were additionally exposed to the chemotherapeutic drug doxorubicin to determine whether a knockdown in AID expression makes the cells more susceptible to apoptosis. As shown in Figure 5.8 below, no change in the level of apoptosis was detected between the AID-siRNA3 and the siRNA Neg control cells in the untreated cells. In the cells exposed to doxorubicin, there was an increase in Annexin V positive cells from 49.75 % in the siRNA Neg cells compared to 56.08 % in the AID-siRNA3 cells, thus showing an increase in apoptosis when AID-siRNA3 cells are treated with doxorubicin.

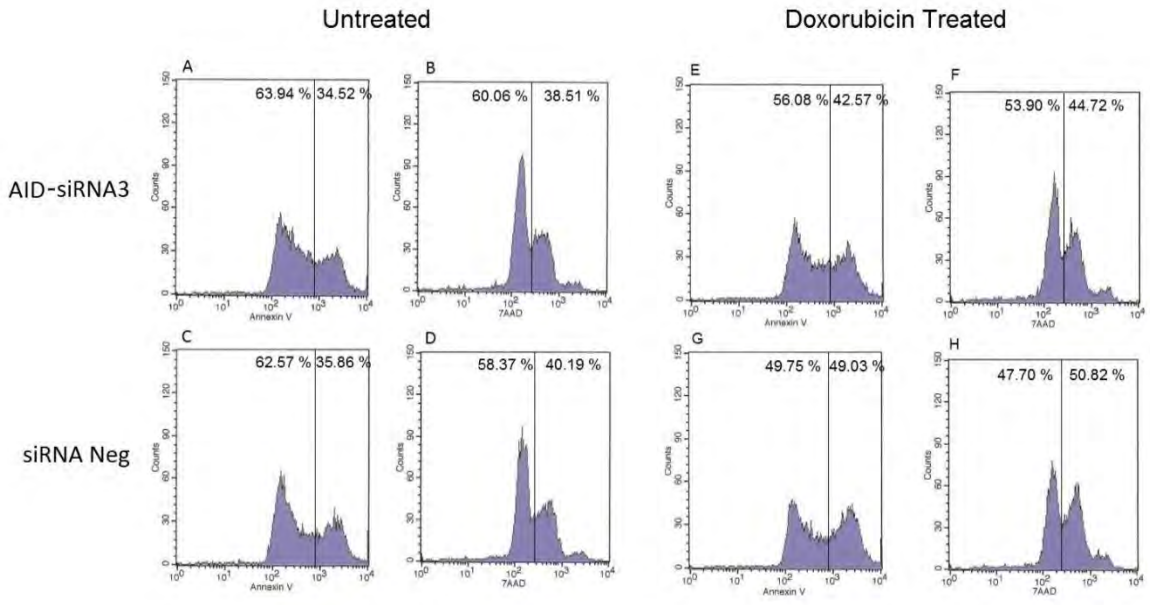

Figure 5.8: Flow cytometric analysis of Annexin V and 7-AAD for the siRNA Neg control and AID-siRNA3 Ramos cells with or without doxorubicin. Panels A-D are the results for the untreated Ramos cells, while panels E-H are the Ramos cells exposed to doxorubicin. A is the expression profile of Annexin V for the AID-siRNA3 Ramos cells, while B is the 7-AAD expression for the same cell population, panel C is the Annexin V profile for the siRNA Neg Ramos cells and panel D is the 7-AAD profile for the same cell population. E is the expression profile of Annexin V for the AID-siRNA3 Ramos cells with doxorubicin, while F is the 7-AAD expression for the same cell population, panel G is the Annexin V profile for the siRNA Neg Ramos cells with doxorubicin and panel H is the 7-AAD profile for the same cell population.

5.2.2.5 Measure of migration ability of Ramos cells in which AID has been knocked down, compared to control cells, using a Transwell assay

Cancerous cells have increased motility, as shown during the epithelial-to-mesenchymal transition, when epithelial cells move down into the mesenchyme, acquire a mesenchymal phenotype, and can progress further by metastasizing to different locations within the body (Rokavec *et al*., 2014). Though B-cells are not of epithelial origin, advanced lymphomas do acquire migratory abilities and metastasizes from the lymph nodes to other sites in the body. Thus we wanted to determine whether a decrease in AID expression would reduce the motility of Ramos cells using a Transwell migration assay as described in Section 2.21. This assay functions by plating cells in an upper chamber low in serum conditions (culture medium containing 1 % FBS only) separated by a membrane with pores which are small enough to prevent the Ramos cells from falling through, but big enough to allow the cells to move through the membrane into the lower chamber which contains culture medium with 10 %

FBS. The nutrient gradient should induce the cells to move from the upper to the lower chamber, where the cells in the lower chamber are stained and quantified based on the amount of stain which is incorporated. The Ramos cells with knocked down AID expression had an approximate 6 % decrease in migratory ability compared to the siRNA Neg Ramos cells (Figure 5.9). Although this result was not significant, the same trend could be observed in all three replicate chambers.

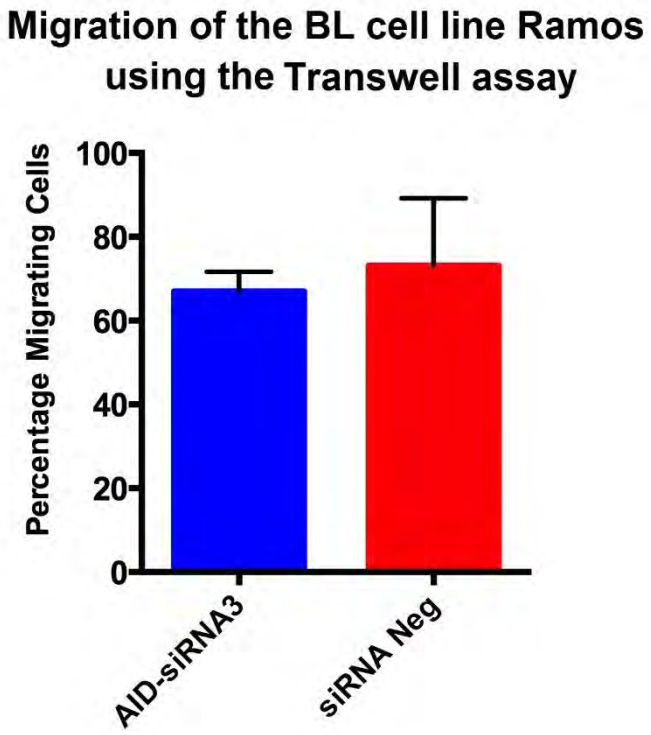

Figure 5.9: Migration using the Transwell migration assay of Ramos cells in which AID is knocked down, compared to untransfected and siRNA Neg control cells. The migratory ability of the Ramos cells were determined by plating the cells in the upper chamber (1 % FBS) of the Transwell plate. The number of cells that pass from the upper chamber into the lower chamber (10 % FBS) through the 5 µm pores were stained with 0.1 % crystal violet. This stain was then solubilised and the intensity, as a measure of the number of cells stained, was detected at a wavelength of 600 nm on the GloMax®-Multi microplate reader (Promega, US). The result was normalised against the total number of cells plated, as determined by counting cells in both the upper and lower chambers. The experiment was performed in triplicate with the AID knockdown Ramos cells (blue) and siRNA Neg cells (red). Error bars represent the standard error of the mean (Prism 6, GraphPad, USA) and no statistical significance was detected.

5.2.2.6 Detection of specific CD markers in Ramos cells with knockdown AID expression, compared to control cells

Cluster of differentiation (CD) markers are leukocyte cell surface markers which can be used to determine the different stages of cell maturity. Three different CD markers were used in

this study, CD19, CD20 and CD10 conjugated to different fluorophores. These three markers were selected by comparing the phenotypic profile of the Ramos cells (taken from the DSMZ database, Appendix B, Figure B6) to a normal B-cell line to determine which markers may be changed with knockdown of AID. The CD19 marker is a highly conserved co-receptor for cell growth with high expression which increases throughout B-cell maturation and differentiation (Ginaldi *et al*., 1998), thus CD19 was used as a B-cell selection marker for a positive B-cell population.

The CD20 marker is a transmembrane phosphoprotein which has a role is in the calcium channel and is important in B-cell activation and differentiation. It also appears later in development with mature B-cells having a greater expression compared to precursors. (Ginaldi *et al*., 1998). This marker is expressed on most B-cell non-Hodgkin's lymphomas but is not found on stem cells, pro-B cells, normal plasma cells or normal tissues, and importantly, it is the target of the chemotherapeutic agent rituximab which is used to treat B-cell non-Hodgkin's lymphomas (Hauptrock and Hess, 2008).

The CD10 marker is also known as enkephalinase which is a human membrane-associated neutral endopeptidase (Dogan *et al*., 2000). CD10 is known to be expressed in activated germinal centre B-cells (Alizadeh *et al*., 2000). It was thought that knocking down AID could alter the CD marker expression back to the CD markers expression for a normal lymphoid cell line. As shown in Figure 5.10 below, no changes in the cell surface expression of any of the markers were found in the AID knockdown cells, compared to the control cells.

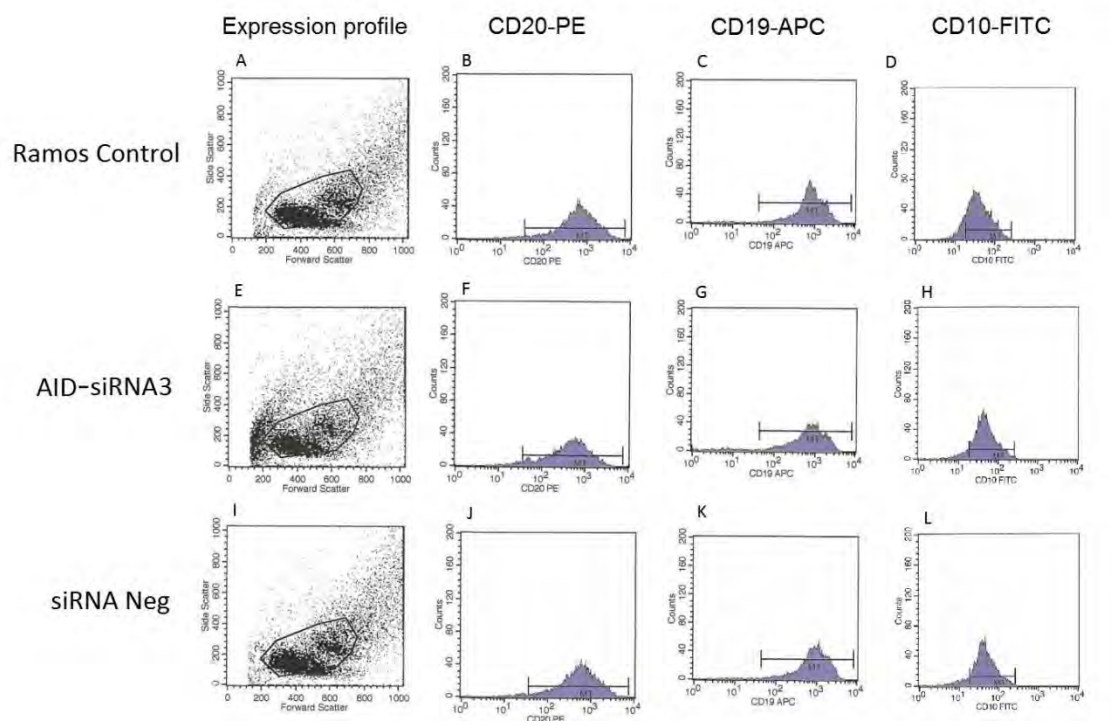

Figure 5.10: Flow cytometric analysis of the CD20, CD19 and CD10 cell surface expression in control Ramos cells, AID-siRNA3 and siRNA Neg cells. Panel A-D are the expression profiles for the control cells, E-H are the AID-siRNA3 cells, and I-L are the siRNA Neg cells. The left panel are the selected cell populations, the second panel are the CD20 markers, the third panel are the CD19 markers and the final panel are the CD10 markers.

5.2.2.7 Cell cycle profiling of Ramos cells in which AID is knocked down, compared to control cells

Cancer cells often have an altered cell cycle profile (Vermeulen *et al*., 2003). This is because in cancer cells, cell cycle checkpoints are often disrupted. We wanted to determine whether knockdown of AID caused alterations in the cell cycle checkpoints with accumulations of cells in a specific phase of the cell cycle. This was determined using flow cytometry which detects the total amount of DNA content within each cell, and separates the cells according to cell cycle phase as described in Section 4.2.5.2. We thus determined the cell cycle profile of control Ramos cells and AID knockdown cells using propidium iodide and flow cytometry (Section 2.17). Figure 5.11 below shows the results for the control Ramos cells (A-C), Ramos cells with reduced AID expression (D-F) and the siRNA Neg control cells (G-I). From these results it was shown that the effect of reduced AID expression did not alter the growth phase of these cells as there was no difference between each cell line.

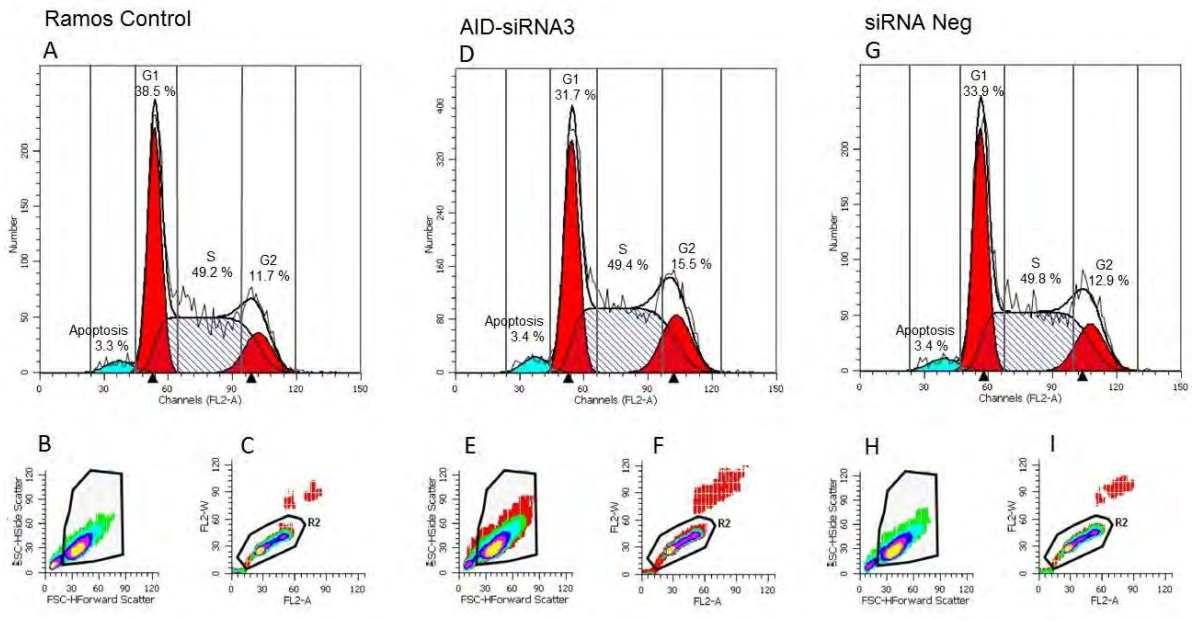

Figure 5.11: Cell cycle profiling of untransfected Ramos cells, cells in which AID is knocked down, and siRNA Neg control cells. A is the cell cycle profile of normal untreated Ramos cells, B and C are the gated cells. D is the cell cycle profile of Ramos cells with reduced AID expression using AID-siRNA3, E and F are the cells that were gated. G is the cell cycle profile of Ramos cells with the control siRNA Neg, H and I are the cells that were gated. The sub G1 blue peak represents the apoptotic cells, the first red peak are the cells in the G1 phase, the second red peak are the cells in the G2 phase, while the shaded black lines represent the S phase cells.

5.3 Discussion and conclusion

In normal cells, AID is tightly regulated due to its function in incorporating mutations in DNA (Zan and Casali, 2013). Overexpression of AID has the potential to have catastrophic consequences for the cells and the body. With AID implicated as the cause for the canonical *c-myc/IgH* translocations, which is a hallmark of BL, we wanted to determine what other oncogenic functions are associated with this enzyme. Given that an overexpression model of AID could not be produced due to the severity of the cellular damage caused by AID (Chapter 4), a knockdown model was instead generated. This was successfully achieved using siRNA in the BL cell line Ramos. To confirm the results observed and ensure these were not from any pleiotropic effects, at least two siRNAs capable of knocking down AID are usually used. AID-siRNA5 was selected as a second candidate, however, AID knockdown could not be improved above the 28 % obtained in Figure 5.2. Being unable to identify a second siRNA from the four tested, only AID-siRNA3 was used. A scrambled siRNA was used in conjunction with the AID-siRNA3 to control for any effects which could be a remnant from the experimental procedure.

Once knockdown of AID was reproducibly achieved, specific cellular features were investigated. These include, as described in Chapter 1, whether AID induces dsDNA breaks, which is linked to the canonical *c-myc/IGH* translocations observed in BL cells. It was expected that a reduction in AID expression would decrease the amount of dsDNA breaks. In the presence of dsDNA breaks, the 139th serine residue is phosphorylated on the H2A molecule, producing the phosphorylated form of the protein, γ-H2AX (Kuo and Yang, 2008). For every dsDNA break, hundreds to thousands of phosphorylated γ-H2AX are recruited which in turn causes a DNA damage repair cascade (Kuo and Yang, 2008). As cancer cells have a higher phosphorylated γ-H2AX expression, it was of interest to determine whether phosphorylated γ-H2AX protein expression was altered with the decrease in AID expression (Kuo and Yang, 2008). This was shown to be the case with the knockdown of AID in the BL cell line Ramos causing a near total reduction in phosphorylated γ-H2AX. The untreated Ramos cells as expected produced large quantities of phosphorylated γ-H2AX, while the siRNA Neg had reduced, while still high, phosphorylated γ-H2AX expression (Figure 5.4). This difference could have been due to loading of the western blot as the Ramos control cells had greater p38 expression. Thus it can be stated that the abolishment of phosphorylated γ-H2AX protein expression is indicative of a decrease in dsDNA breaks. This result highlights that AID is related to the induction of dsDNA breaks which adds credence to the implication that AID overexpression causes the *c-myc/IgH* translocations, and is likely responsible for other genomic abnormalities in these cells (Ramiro *et al*., 2006). Love *et al*. (2012) fully sequenced the genome of BL patient and 59 BL tumour exomes and identified 70 genes which were regularly mutated in these samples, thus showing that BL cells are subjected to increased mutagenesis, as highlighted by the high expression of phosphorylated γ-H2AX protein expression.

One of the hallmarks of cancer cells is their ability to proliferate uncontrollably (Hanahan and Weinberg, 2011). Thus it was of interest to determine whether the knockdown of AID expression caused a decrease in proliferation. The proliferation and viability of the cells was determined using the WST-1 assay, and compared to untreated Ramos cells, AID-siRNA3 had significantly lower ($p < 0.01$) proliferation (Figure 5.5). This, approximately 20 % decrease in proliferation, highlights a potentially important, though indirect, role for AID in maintaining cell viability and proliferation. One of the genes implicated in cellular proliferation is the *c-*

Myc proto-oncogene (Neganova and Lako, 2008), which is especially relevant in Ramos as BL is classified as having deregulated expression of c-Myc due to the canonical translocation between *c-Myc* and *Igh*. AID overexpression has been associated with this translocation (Duquette *et al*., 2005) thus a possible mechanism for the reduction in proliferation may be due to the reduction of AID, thereby reducing the expression of the *c-myc/IgH* mutated protein. This could also be due to the ability for AID to alter other genes which play a role in proliferation. Three such genes were found to be mutated in BL patients, *ID3*, *BRAF* and *CREBBP* (Love *et al*., 2012). The *ID3* gene has been shown to increase cell cycle progression and expression of proliferation associated genes (Love *et al*., 2012), with *BRAF* having been shown to increase cellular growth (Davies *et al*., 2002) and *CREBBP* playing a critical role in growth control (Huang *et al*., 2010). It would be of interest to check the *c-Myc* translocation using fluorescent *in situ* hybridisation (FISH) in the AID knockdown cells as well as to check the expression and mutational status of *ID3*, *BRAF* and *CREBBP*.

As previously stated, only 60 – 70 % of adult BL patients achieve complete remission with chemotherapeutic treatment (Richter-Larrea *et al*., 2010) and it has also been shown that BL patients respond less effectively to chemotherapeutic drugs (Barta *et al*., 2015). Even HIV-positive patients undergoing combined therapy (HAART and chemotherapy) respond poorly (Barta *et al*., 2015). Thus to determine whether knockdown of AID caused the Ramos cells to become more sensitive to chemotherapeutic agents, doxorubicin, which is currently part of the regimen used to treat BL patients (Dunleavy *et al*., 2013), was added to the Ramos cells and proliferation and viability was determined using the WST-1 assay. Initially an IC50 of doxorubicin was determined as no consensus from the literature could be found. An IC50 looks at how much of a drug is required to reduce the cells by half over a given time point, which for this experiment was 48 hours (Figure 5.6). A concentration of 0.5 µg/ml was selected as the most effective concentration, as doxorubicin causes cell cycle arrest at G1 and G2, thus if the concentration is too low, cells remain in these phases producing cellular enzymes detected by WST-1, however, when the concentration increases enough apoptosis is induced (Tacar *et al*., 2013). The results of the WST-1 assay showed a proliferation decrease in the untreated cells of 8.6 % and 20.5 % for the AID-siRNA3 cells compared to the siRNA Neg and Ramos cells respectively (Figure 5.5). With the doxorubicin treated cells having a 27.7 % and 26.5 % decrease in proliferation observed for the AID-siRNA3 knockdown cells compared

to the siRNA Neg and Ramos control cells respectively. Thus it can be said that a reduction in AID expression does seem to make the Ramos cells more sensitive to the chemotherapeutic drug doxorubicin and AID overexpression may confer a greater growth advantage to these cancerous cells. Doxorubicin functions by intercalating with DNA, thereby ceasing DNA replication, and has been shown to activate the intrinsic apoptotic pathway which indirectly permeabilises the mitochondrial membrane by upregulating members of the intrinsic apoptotic pathway as described in Chapter 4 (Fulda and Debatin, 2006; Elmore, 2007). This cellular sensitivity could be a possible avenue of further research in the development of new treatments against cancers, by using AID as a therapeutic target strategy where AID is overexpressed, in cancers such as BL. If a treatment involved the addition of an AID repressor in conjunction with the chemotherapeutic regime already administered, there could be an improvement in the efficacy of treatment, such Wang *et al*. (2011) showed with the improved response of doxorubicin with the addition of ellipticine. Ellipticine is an anti-cancer compound that intercalates with DNA, inhibits the topoisomerase II enzyme and has been shown to reactivate mutant p53 (Wang *et al*., 2011; Stiborova *et al*., 2014).

To confirm the WST-1 assay results, the knocked down Ramos cells were exposed to the thymidine analog BrdU, which is incorporated into the DNA of actively dividing cells which can then be detected under fluorescence microscopy with the addition of florescent antibodies specific to BrdU. The BrdU results correlated with the WST-1 assay results showing that knockdown of AID in Ramos cells caused a decrease in proliferation as only 11% of cells were positive for BrdU (Figure 5.7). The results of this assay would ideally be repeated with an alternative stain as the Hoechst 33342 is quenched by BrdU, however, due to limited reagents we were unable to repeat this experiment (Latt, 1977).

Another hallmark of cancer is the cells ability to evade apoptosis (Hanahan and Weinberg, 2011). To determine whether a reduction in AID protein expression would render these cells more susceptible to apoptosis, the Ramos cells were subjected to the Annexin V detection assay. No differences were discernible, using the Annexin V assay, between the untreated AID knockdown and the control siRNA Ramos cells (Figure 5.8). This result differs from what was observed in the flow cytometric analysis which was used to measure the expression of specific cell surface markers (Appendix B, Figure B5). In that assay, a significant proportion of

apoptotic cells were observed among the AID-siRNA3 cell population, compared to the siRNA Neg cells. Compared to the untreated cells, there was approximately an 8 % increase in necrotic cells in the doxorubicin treated cells, with less cells in the pre-apoptotic stage of cell death (Figure 5.8; A and E). In the cells treated with doxorubicin, there was an increase in apoptosis observed in the AID-siRNA3 Annexin V cells compared to the siRNA Neg cells (Figure 5.8; F and H). This result reflects what was observed in the WST-1 assay earlier where proliferation and cell viability decreased in the AID-siRNA3 cells in the presence of doxorubicin (Figure 5.5). A possible reason for this could be due to the sensitivity of the Annexin V kit which may not pick up these changes due to the assay limitations, such as unbound labelled protein adding to the background emissions and false positive results due binding to aldehyde adducts (Demchenko, 2013). Future work may look at using the probe F2N12S, which is a small fluorescent molecule which is non-fluorescent when unbound and has a high affinity for only the outer leaflet of the cell membrane and can be quantified on an absolute scale (Demchenko, 2013).

The ability of cells to migrate is yet another key feature of cancer cells, especially in advanced stage types of cancers (Hanahan and Weinberg, 2011). The mobility of Ramos cells after AID was knocked down was investigated. The results showed that with a reduction in AID, migratory ability of these cells was decreased by approximately 6 % with a high level of variation (Figure 5.9). This was a very low percent migration which could be due to the fact that these are suspension cell lines and the majority of cells used with the Transwell assay system are adherent cell lines which do not have the risk of being removed with the washing steps. This assay was repeated, however, the knockdown confirmation was not acceptable thus these results were not included and due to time limitations it could not be repeated a third time. The results indicate that AID may be involved in migration, indirectly, and that more replicates will need to be done to validate this result. Love *et al*. (2012) showed that *LAMA3*, a regulator of cell migration, was mutated in BL patient samples, thus this may be the indirect link implicating AID in changes in migratory ability. As previously described in Section 5.2.2.5, cancerous cells, even of B-cell origin, have increased mobility. It has been shown that members of the miRNA-34 family, which inhibit the epithelial-to-mesenchymal transition, are induced by p53 (Rokovac *et al*., 2014). With Ramos cells having a mutated/deficient form of

p53 as discussed in Chapter 4, the miRNA-34 family will not be induced, thereby leading to increased migration of these cells.

With the cells seeming to be moving to a more non-cancerous identity, the cells stage of differentiation was determined. Three CD markers (CD10, CD19 and CD20) of interest were selected, which were all expressed between 98 – 100 % in the untreated Ramos cells (Appendix B, Figure B6). During the early development of cells, proliferation is rapid and as the cells become more differentiated and mature, proliferation decreases (Cooper, 2000). Thus cancerous cells take on a more "immature" cell type with increased proliferation, therefore we selected CD10 which is expressed in early immature B-cell development to determine whether knockdown of AID would cause the cells to move out of an immature cancerous phenotype to a more mature, normal B-cell type (Dogan *et al*., 2000). The marker CD20 was selected as this was the target for rituximab, the first monoclonal antibody approved for therapeutic use in cancer patients (Smith *et al*., 2003). Thus if a reduction in AID expression could decrease the CD20 marker expression, this would be indicative of AID knockdown as a possible treatment for cancer associated with AID overexpression. The marker CD19 is expressed on all B-cells and thus was used as a control B-cell selection (Ginaldi *et al*., 1998). With the reduction of AID expression, we were unable to detect a change in CD marker expression (Figure 5.10). This could be due to the transient nature of the siRNA knockdown, we detected after 48 hours and changes in the CD markers may take longer to alter to a detectable level by which time the AID knockdown may no longer be in effect or alternatively AID may not play a role in the alteration of CD marker expression.

We wanted to determine whether there would be a change in the cell cycle profile of Ramos cells with reduced AID expression. Typically cells replicate every 24 hours, however, cancerous cells have uncontrolled proliferation and thus are continuously dividing and may even have a faster proliferation rate. Cell cycle profiling was assessed to check whether the proliferation decrease caused by AID knockdown was due to checkpoints, such as those found in G1 and G2, being activated (Lapenna and Giordano, 2009). If these checkpoints were activated, cells would have halted or slowed down their proliferation rate. As is shown in Figure 5.11, there was no difference between the cell cycle profiles of Ramos cells in which AID was knocked down, compared to control cells. As it is known that Ramos is already able to bypass these DNA damage checkpoints (Allday *et al*., 1995), which are compromised in

these cells (despite the presence of DNA damage as demonstrated by the expression of phosphorylated γ-H2AX). With reduced AID expression, and therefore reduced insult to the genome, there was still no difference Future experiments should look at first treating the cells with an insult, such as UV light, which would induce further DNA damage and then determine the effect on cell cycle profiling.

Thus in this chapter we have shown that reducing AID has an impact on the phenotype of these BL cells, thus highlighting the need for cells to regulate its expression and further implicating it in cancer development.

Knockdown is a powerful technique which can be used to identify the mechanisms of certain genes, however, this technique poses limitations. One of the main limitations is the narrow time frame post-knockdown. Tests were performed to determine the optimal time of analysis after knockdown which was approximately 48 hours, with certain experiments requiring a greater time frame to perform, this reduced the scope of the possible downstream experiments. Another consideration is the half-life of AID, which has been shown to be approximately 20 hours in the cytoplasm, thus after 48 hours the reduction of AID expression may be limited by this high half-life (Aoufouchi *et al*., 2008). The knockdown experiment was optimised, however, due to unknown experimental errors, the knockdown expression was not always effective and some experiments required repeating. Due to the high cost of the siRNA and that suspension cell lines required over ten times more reagents than adherent cells, the cost limited the amount of experiments able to be performed.

This study opens up a wide scope of future work. The knockdown experiments should be repeated with a different BL cell line to, firstly, confirm the results, and secondly, to determine whether the effect could be altered with a change in p53 classification or EBV expression. Alternatively, the siRNA results should be confirmed in Ramos cells using another siRNA, possibly from a different company. An alternative to knockdown, which may be more effective, would be to use the Crispr-Cas9 system, which uses guide RNAs to disrupt the genes of interest (Ran *et al*., 2013). This is a relatively affordable and highly accurate technique. The resulting mutated AID cells would provide a longer time frame in which to perform more

experiments such as cell morphology studies, proliferation over a longer period of time, determining growth factor dependence, and signalling pathway investigations.

References

Adolph, K.W. 1996. *Microbial Genome Methods.* CRC Press. 1st Edition: 85-86

Alizadeh, A.A., Eisen, M.B., Davis, R.E., Ma, C., Lossos, I.S., Rosenwald, A., Boldrick, J.C., Sabet, H. *et al*. 2000. Distinct types of diffuse large B-cell lymphoma identified by gene expression profiling. *Nature.* 403(6769):503-511.

Allday, M.J., Inman, G.J., Crawford, D.H. & Farrell, P.J. 1995. DNA damage in human B cells can induce apoptosis, proceeding from G1/S when p53 is transactivation competent and G2/M when it is transactivation defective. *The EMBO Journal.* 14(20):4994-5005.

Aoufouchi, S., Faili, A., Zober, C., D'Orlando, O., Weller, S., Weill, J.C. & Reynaud, C.A. 2008. Proteasomal degradation restricts the nuclear lifespan of AID. *The Journal of Experimental Medicine.* 205(6):1357-1368.

Babbage, G., Ottensmeier, C.H., Blaydes, J., Stevenson, F.K. & Sahota, S.S. 2006. Immunoglobulin heavy chain locus events and expression of activation-induced cytidine deaminase in epithelial breast cancer cell lines. *Cancer Research.* 66(8):3996-4000.

Barta, S.K., Samuel, M.S., Xue, X., Wang, D., Lee, J.Y., Mounier, N., Ribera, J.M., Spina, M. *et al*. 2015. Changes in the influence of lymphoma- and HIV-specific factors on outcomes in AIDS-related non-Hodgkin lymphoma. *Annals of Oncology : Official Journal of the European Society for Medical Oncology / ESMO.* 26(5):958-966.

Bartel, D.P. 2004. MicroRNAs: genomics, biogenesis, mechanism, and function. *Cell.* 116(2):281-297.

Basso, K., Schneider, C., Shen, Q., Holmes, A.B., Setty, M., Leslie, C. & Dalla-Favera, R. 2012. BCL6 positively regulates AID and germinal center gene expression via repression of miR-155. *The Journal of Experimental Medicine.* 209(13):2455-2465.

Batsaikhan, B., Yoshikawa, K., Kurita, N., Iwata, T., Takasu, C., Kashihara, H. & Shimada, M. 2014. Expression of Stathmin1 in gastric adenocarcinoma. *Anticancer Research.* 34(8):4217-4221.

Beral, V., Peterman, T., Berkelman, R. & Jaffe, H. 1991. AIDS-associated non-Hodgkin lymphoma. *The Lancet.* 337(8745):805-809.

Blum, K.A., Lozanski, G. & Byrd, J.C. 2004. Adult Burkitt leukemia and lymphoma. *Blood.* 104(10):3009-3020.

Blumberg, D.D. 1987. Creating a ribonuclease-free environment. *Methods in Enzymology.* 152:20-24.

Borchert, G.M., Holton, N.W. & Larson, E.D. 2011. Repression of human activation induced cytidine deaminase by miR-93 and miR-155. *BMC Cancer.* 11:347-356.

Brady, G., Macarthur, G.J. & Farrell, P.J. 2008. Epstein-Barr virus and Burkitt lymphoma. *Postgraduate Medical Journal.* 84(993):372-377.

Breen, E.C., Rezai, A.R., Nakajima, K., Beall, G.N., Mitsuyasu, R.T., Hirano, T., Kishimoto, T. & Martinez-Maza, O. 1990. Infection with HIV is associated with elevated IL-6 levels and production. *Journal of Immunology.* 144(2):480-484.

Cancian, L., Bosshard, R., Lucchesi, W., Karstegl, C.E. & Farrell, P.J. 2011. C-terminal region of EBNA-2 determines the superior transforming ability of type 1 Epstein-Barr virus by enhanced gene regulation of LMP-1 and CXCR7. *PLoS Pathology.* 7(7):e1002164.

Chiba, T. & Marusawa, H. 2009. A novel mechanism for inflammation-associated carcinogenesis; an important role of activation-induced cytidine deaminase (AID) in mutation induction. *Journal of Molecular Medicine.* 87(10):1023-1027.

Choi, S.M., Liu, H., Chaudhari, P., Kim, Y., Cheng, L., Feng, J., Sharkis, S., Ye, Z. *et al*. 2011. Reprogramming of EBV-immortalized B-lymphocyte cell lines into induced pluripotent stem cells. *Blood.* 118(7):1801-1805.

Chow, A. 2010. Cell cycle control by oncogenes and tumor suppressors: driving the transformation of normal cells into cancerous cells. *Nature Education.* 3(9):1-7.

Cooper, G.M. 2000. Cell Proliferation in Development and Differentiation. 2nd Edition

Crouch, E.E., Li, Z., Takizawa, M., Fichtner-Feigl, S., Gourzi, P., Montano, C., Feigenbaum, L., Wilson, P. *et al*. 2007. Regulation of AID expression in the immune response. *The Journal of Experimental Medicine.* 204(5):1145-1156.

Dave, S.S., Fu, K., Wright, G.W., Lam, L.T., Kluin, P., Boerma, E., Greiner, T.C., Weisenburger, D.D. *et al*. 2006. Molecular diagnosis of Burkitt's lymphoma. *New England Journal of Medicine.* 354(23):2431-2442.

Davies, H., Bignell, G.R., Cox, C., Stephens, P., Edkins, S., Clegg, S., Teague, J., Woffendin, H. *et al*. 2002. Mutations of the BRAF gene in human cancer. *Nature.* 417(6892):949-954.

De Jonge, H., Fehrmann, R., De Bont, E., Hofstra, R., Gerbens, F., Kamps, W.A., De Vries, E., Van Der Zee, A. *et al*. 2007. Evidence based selection of housekeeping genes. *PloS One.* 2(9):e898.

Demchenko, A.P. 2013. Beyond annexin V: fluorescence response of cellular membranes to apoptosis. *Cytotechnology.* 65(2):157-172.

De Silva, Nilushi S., and Ulf Klein. (2015). Dynamics of B cells in germinal centres. *Nature Reviews Immunology* 15.3: 137-148.

Dogan, A., Bagdi, E., Munson, P. & Isaacson, P.G. 2000. CD10 and BCL-6 expression in paraffin sections of normal lymphoid tissue and B-cell lymphomas. *The American Journal of Surgical Pathology.* 24(6):846-852.

Donadoni, G., Bruno-Ventre, M. & Ferreri, A.J. 2013. Treatment of HIV-associated Burkitt lymphoma. *Hematology.* 1:38-52

Dorrington, R., Bourne, D., Bradshaw, D., Laubscher, R. & Timæus, I.M. 2001. *The impact of HIV/AIDS on adult mortality in South Africa.* Medical Research Council Cape Town. 1-54

Dorsett, Y., McBride, K.M., Jankovic, M., Gazumyan, A., Thai, T., Robbiani, D.F., Di Virgilio, M., San-Martin, B.R. *et al*. 2008. MicroRNA-155 suppresses activation-induced cytidine deaminase-mediated Myc-Igh translocation. *Immunity.* 28(5):630-638.

Drexler, H.G. & Uphoff, C.C. 2002. Mycoplasma contamination of cell cultures: Incidence, sources, effects, detection, elimination, prevention. *Cytotechnology.* 39(2):75-90.

Dunleavy, K., Pittaluga, S., Shovlin, M., Steinberg, S.M., Cole, D., Grant, C., Widemann, B., Staudt, L.M. *et al*. 2013. Low-intensity therapy in adults with Burkitt's lymphoma. *New England Journal of Medicine.* 369(20):1915-1925.

Duquette, M.L., Pham, P., Goodman, M.F. & Maizels, N. 2005. AID binds to transcription-induced structures in c-MYC that map to regions associated with translocation and hypermutation. *Oncogene.* 24(38):5791-5798.

Durandy, A. 2003. Activation-induced cytidine deaminase: a dual role in class-switch recombination and somatic hypermutation. *European Journal of Immunology.* 33(8):2069-2073.

Elmore, S. 2007. Apoptosis: a review of programmed cell death. *Toxicologic Pathology.* 35(4):495-516.

Endo, Y., Marusawa, H. & Chiba, T. 2011. Involvement of activation-induced cytidine deaminase in the development of colitis-associated colorectal cancers. *Journal of Gastroenterology.* 46(1):6-10.

Epeldegui, M., Thapa, D.R., De La Cruz, J., Kitchen, S., Zack, J.A. & Martínez-Maza, O. 2010. CD40 ligand (CD154) incorporated into HIV virions induces activation-induced cytidine deaminase (AID) expression in human B lymphocytes. *PLoS One.* 5(7):e11448.

Epeldegui, M., Breen, E.C., Hung, Y.P., Boscardin, W.J., Detels, R. & Martinez-Maza, O. 2007. Elevated expression of activation induced cytidine deaminase in peripheral blood mononuclear cells precedes AIDS-NHL diagnosis. *AIDS.* 21(17):2265-2270.

Faili, A., Aoufouchi, S., Guéranger, Q., Zober, C., Léon, A., Bertocci, B., Weill, J. & Reynaud, C. 2002. AID-dependent somatic hypermutation occurs as a DNA single-strand event in the BL2 cell line. *Nature Immunology.* 3(9):815-821.

Farrell, P.J., Allan, G.J., Shanahan, F., Vousden, K.H. & Crook, T. 1991. p53 is frequently mutated in Burkitt's lymphoma cell lines. *The EMBO Journal.* 10(10):2879-2887.

Ferlay, J., Soerjomataram, I., Dikshit, R., Eser, S., Mathers, C., Rebelo, M., Parkin, D.M., Forman, D. *et al*. 2015. Cancer incidence and mortality worldwide: sources, methods and major patterns in GLOBOCAN 2012. *International Journal of Cancer.* 136(5):E359-E386.

Fichtner-Feigl, S., Kesselring, R. & Strober, W. 2015. Chronic inflammation and the development of malignancy in the GI tract. *Trends in Immunology.* 36(8):451-459.

Freed-Pastor, W.A. & Prives, C. 2012. Mutant p53: one name, many proteins. *Genes & Development.* 26(12):1268-1286.

Freshney, R.I. 2010. Transformation and Immortalization. *Culture of Animal Cells.*

Fritz, E.L., Rosenberg, B.R., Lay, K., Mihailović, A., Tuschl, T. & Papavasiliou, F.N. 2013. A comprehensive analysis of the effects of the deaminase AID on the transcriptome and methylome of activated B cells. *Nature Immunology.* 14(7):749-755.

Fritz, E.L. & Papavasiliou, F.N. 2010. Cytidine deaminases: AIDing DNA demethylation? *Genes & Development.* 24(19):2107-2114.

Fulda, S. & Debatin, K. 2006. Extrinsic versus intrinsic apoptosis pathways in anticancer chemotherapy. *Oncogene.* 25(34):4798-4811.

Ginaldi, L., De Martinis, M., Matutes, E., Farahat, N., Morilla, R. & Catovsky, D. 1998. Levels of expression of CD19 and CD20 in chronic B cell leukaemias. *Journal of Clinical Pathology.* 51(5):364-369.

Gomez-Gonzalez, B. & Aguilera, A. 2007. Activation-induced cytidine deaminase action is strongly stimulated by mutations of the THO complex. *Proceedings of the National Academy of Sciences of the United States of America.* 104(20):8409-8414.

Gopal, S., Patel, M.R., Yanik, E.L., Cole, S.R., Achenbach, C.J., Napravnik, S., Burkholder, G.A., Reid, E.G. *et al*. 2013. Temporal trends in presentation and survival for HIV-associated lymphoma in the antiretroviral therapy era. *Journal of the National Cancer Institute.* 1:1-9.

Greisman, H.A., Lu, Z., Tsai, A.G., Greiner, T.C., Yi, H.S. & Lieber, M.R. 2012. IgH partner breakpoint sequences provide evidence that AID initiates t(11;14) and t(8;14) chromosomal breaks in mantle cell and Burkitt lymphomas. *Blood.* 120(14):2864-2867.

Gu, X., Shivarov, V. & Strout, M.P. 2012. The role of activation-induced cytidine deaminase in lymphomagenesis. *Current Opinion in Hematology.* 19(4):292-298.

Hanahan, D. & Weinberg, R.A. 2011. Hallmarks of cancer: the next generation. *Cell.* 144(5):646-674.

Hauptrock, B. & Hess, G. 2008. Rituximab in the treatment of non-Hodgkin's lymphoma. *Biologics : Targets & Therapy.* 2(4):619-633.

Hogenbirk, M.A., Heideman, M.R., Velds, A., van den Berk, P., Kerkhoven, R.M., van Steensel, B. & Jacobs, H. 2013. Differential programming of B cells in AID deficient mice. *PloS One.* 8(7):e69815.

Huang, X., Chen, S., Shen, Q., Yang, L., Li, B., Zhong, L., Geng, S., Du, X. *et al*. 2010. Analysis of the expression pattern of the BCL11B gene and its relatives in patients with T-cell acute lymphoblastic leukemia. *Journal of Hematology Oncology.* 3(1):44.

Iwakiri, D., Zhou, L., Samanta, M., Matsumoto, M., Ebihara, T., Seya, T., Imai, S., Fujieda, M. *et al*. 2009. Epstein-Barr virus (EBV)-encoded small RNA is released from EBV-infected cells and activates signaling from Toll-like receptor 3. *The Journal of Experimental Medicine.* 206(10):2091-2099.

Jemal, A., Bray, F., Center, M.M., Ferlay, J., Ward, E. & Forman, D. 2011. Global cancer statistics. *CA: A Cancer Journal for Clinicians.* 61(2):69-90.

Jemal, A., Bray, F., Forman, D., O'Brien, M., Ferlay, J., Center, M. & Parkin, D.M. 2012. Cancer burden in Africa and opportunities for prevention. *Cancer.* 118(18):4372-4384.

Jorissen, R.N., Lipton, L., Gibbs, P., Chapman, M., Desai, J., Jones, I.T., Yeatman, T.J., East, P. *et al*. 2008. DNA copy-number alterations underlie gene expression differences between microsatellite stable and unstable

colorectal cancers. *Clinical Cancer Research: An Official Journal of the American Association for Cancer Research.* 14(24):8061-8069.

Kawamura, K., Wada, A., Wang, J., Li, Q., Ishii, A., Tsujimura, H., Takagi, T., Itami, M. *et al*. 2015. Expression of activation-induced cytidine deaminase is associated with a poor prognosis of diffuse large B cell lymphoma patients treated with CHOP-based chemotherapy. *Journal of Cancer Research and Clinical Oncology.* 1-10.

Kim, S.K., Marusawa, H. & Chiba, T. 2014. Aberrant activation-induced cytidine deaminase (AID) expression is induced in the process of hepatitis C virus-associated hepatocarcinogenesis. *Cancer Research.* 74(19):5350-5350.

Kotani, A., Kakazu, N., Tsuruyama, T., Okazaki, I., Muramatsu, M., Kinoshita, K., Nagaoka, H., Yabe, D. *et al*. 2007. Activation-induced cytidine deaminase (AID) promotes B cell lymphomagenesis in Emu-cmyc transgenic mice. *Proceedings of the National Academy of Sciences.* 104(5):1616-1620.

Kou, T., Marusawa, H., Kinoshita, K., Endo, Y., Okazaki, I., Ueda, Y., Kodama, Y., Haga, H. *et al*. 2007. Expression of activation-induced cytidine deaminase in human hepatocytes during hepatocarcinogenesis. *International Journal of Cancer.* 120(3):469-476.

Kuo, L.J. & Yang, L.X. 2008. Gamma-H2AX - a novel biomarker for DNA double-strand breaks. *In Vivo.* 22(3):305-309.

Kusao, I.K., Troelstrup, D.L., Agsalda, M.A. & Shiramizu, B.T. 2012. Effective use of small-interfering RNA to characterize residual B-cell non-Hodgkin lymphoma cells following chemotherapy. *Journal of Hematological Malignancies.* 2(1):5-12.

Lapenna, S. & Giordano, A. 2009. Cell cycle kinases as therapeutic targets for cancer. *Nature Reviews Drug Discovery.* 8(7):547-566.

Latt, S.A. 1977. Fluorometric detection of deoxyribonucleic acid synthesis; possibilities for interfacing bromodeoxyuridine dye techniques with flow fluorometry. *The Journal of Histochemistry and Cytochemistry : Official Journal of the Histochemistry Society.* 25(7):913-926.

Lee, B.Y., Han, J.A., Im, J.S., Morrone, A., Johung, K., Goodwin, E.C., Kleijer, W.J., DiMaio, D. *et al*. 2006. Senescence-associated β-galactosidase is lysosomal β-galactosidase. *Aging Cell.* 5(2):187-195.

Lee, R.K., Cai, J.P., Deyev, V., Gill, P.S., Cabral, L., Wood, C., Agarwal, R.P., Xia, W. *et al*. 1999. Azidothymidine and interferon-alpha induce apoptosis in herpesvirus-associated lymphomas. *Cancer Research.* 59(21):5514-5520.

Lim, S.T., Karim, R., Nathwani, B.N., Tulpule, A., Espina, B. & Levine, A.M. 2005. AIDS-related Burkitt's lymphoma versus diffuse large-cell lymphoma in the pre-highly active antiretroviral therapy (HAART) and HAART eras: significant differences in survival with standard chemotherapy. *Journal of Clinical Oncology: Official Journal of the American Society of Clinical Oncology.* 23(19):4430-4438.

Lin, C., Yang, L., Tanasa, B., Hutt, K., Ju, B., Ohgi, K.A., Zhang, J., Rose, D.W. *et al*. 2009. Nuclear receptor-induced chromosomal proximity and DNA breaks underlie specific translocations in cancer. *Cell.* 139(6):1069-1083.

Liu, M., Duke, J.L., Richter, D.J., Vinuesa, C.G., Goodnow, C.C., Kleinstein, S.H. & Schatz, D.G. 2008. Two levels of protection for the B cell genome during somatic hypermutation. *Nature.* 451(7180):841-845.

Love, C., Sun, Z., Jima, D., Li, G., Zhang, J., Miles, R., Richards, K.L., Dunphy, C.H. *et al*. 2012. The genetic landscape of mutations in Burkitt lymphoma. *Nature Genetics.* 44(12):1321-1325.

Maeda, K., Singh, S.K., Eda, K., Kitabatake, M., Pham, P., Goodman, M.F. & Sakaguchi, N. 2010. GANP-mediated recruitment of activation-induced cytidine deaminase to cell nuclei and to immunoglobulin variable region DNA. *The Journal of Biological Chemistry.* 285(31):23945-23953.

Marusawa, H. 2008. Aberrant AID expression and human cancer development. *The International Journal of Biochemistry & Cell Biology.* 40(8):1399-1402.

Matsumoto, Y., Marusawa, H., Kinoshita, K., Endo, Y., Kou, T., Morisawa, T., Azuma, T., Okazaki, I. *et al*. 2007. Helicobacter pylori infection triggers aberrant expression of activation-induced cytidine deaminase in gastric epithelium. *Nature Medicine.* 13(4):470-476.

Matsumoto, Y., Marusawa, H., Kinoshita, K., Niwa, Y., Sakai, Y. & Chiba, T. 2010. Up-regulation of activation-induced cytidine deaminase causes genetic aberrations at the CDKN2b-CDKN2a in gastric cancer. *Gastroenterology.* 139(6):1984-1994.

Maul, R.W. & Gearhart, P.J. 2010. Chapter six-AID and Somatic Hypermutation. *Advances in Immunology.* 105:159-191.

Maurisse, R., De Semir, D., Emamekhoo, H., Bedayat, B., Abdolmohammadi, A., Parsi, H. & Gruenert, D.C. 2010. Comparative transfection of DNA into primary and transformed mammalian cells from different lineages. *BMC Biotechnology.* 10(9):1-9.

Mechtcheriakova, D., Svoboda, M., Meshcheryakova, A. & Jensen-Jarolim, E. 2012. Activation-induced cytidine deaminase (AID) linking immunity, chronic inflammation, and cancer. *Cancer Immunology, Immunotherapy.* 61(9):1591-1598.

Molyneux, E.M., Rochford, R., Griffin, B., Newton, R., Jackson, G., Menon, G., Harrison, C.J., Israels, T. *et al*. 2012. Burkitt's lymphoma. *The Lancet.* 379(9822):1234-1244.

Montoto, S., Wilson, J., Shaw, K., Heath, M., Wilson, A., McNamara, C., Orkin, C., Nelson, M. *et al*. 2010. Excellent immunological recovery following CODOX-M/IVAC, an effective intensive chemotherapy for HIV-associated Burkitt's lymphoma. *AIDS.* 24(6):851-856.

Muller, J.R., Janz, S., Goedert, J.J., Potter, M. & Rabkin, C.S. 1995. Persistence of immunoglobulin heavy chain/c-myc recombination-positive lymphocyte clones in the blood of human immunodeficiency virus-infected homosexual men. *Proceedings of the National Academy of Sciences of the United States of America.* 92(14):6577-6581.

Muñoz, D.P., Lee, E.L., Takayama, S., Coppe, J.P., Heo, S.J., Boffelli, D., Di Noia, J.M. & Martin, D.I. 2013. Activation-induced cytidine deaminase (AID) is necessary for the epithelial-mesenchymal transition in mammary epithelial cells. *Proceedings of the National Academy of Sciences of the United States of America.* 110(32):2977-2986.

Muramatsu, M., Sankaranand, V.S., Anant, S., Sugai, M., Kinoshita, K., Davidson, N.O. & Honjo, T. 1999. Specific expression of activation-induced cytidine deaminase (AID), a novel member of the RNA-editing deaminase family in germinal center B cells. *The Journal of Biological Chemistry.* 274(26):18470-18476.

Nagata, N., Akiyama, J., Marusawa, H., Shimbo, T., Liu, Y., Igari, T., Nakashima, R., Watanabe, H. *et al*. 2014. Enhanced expression of activation-induced cytidine deaminase in human gastric mucosa infected by Helicobacter pylori and its decrease following eradication. *Journal of Gastroenterology.* 49(3):427-435.

Nakanishi, Y., Kondo, S., Wakisaka, N., Tsuji, A., Endo, K., Murono, S., Ito, M., Kitamura, K. *et al*. 2013. Role of activation-induced cytidine deaminase in the development of oral squamous cell carcinoma. *PloS One.* 8(4).E62066

Nazari, M., Ghorbani, A., Hekmat-Doost, A., Jeddi-Tehrani, M. & Zand, H. 2011. Inactivation of nuclear factor-κB by citrus flavanone hesperidin contributes to apoptosis and chemo-sensitizing effect in Ramos cells. *European Journal of Pharmacology.* 650(2):526-533.

Neganova, I. & Lako, M. 2008. G1 to S phase cell cycle transition in somatic and embryonic stem cells. *Journal of Anatomy.* 213(1):30-44.

Nikfarjam, L. & Farzaneh, P. 2012. Prevention and detection of Mycoplasma contamination in cell culture. *Cell Journal.* 13(4):203-213.

Noy, A. 2010. Controversies in the treatment of Burkitt lymphoma in AIDS. *Current Opinion in Oncology.* 22(5):443-448.

O'Connor, P.M., Jackman, J., Jondle, D., Bhatia, K., Magrath, I. & Kohn, K.W. 1993. Role of the p53 tumor suppressor gene in cell cycle arrest and radiosensitivity of Burkitt's lymphoma cell lines. *Cancer Research.* 53(20):4776-4780.

Okazaki, I., Kotani, A. & Honjo, T. 2007. Role of AID in tumorigenesis. *Advances in Immunology.* 26(38):245-273.

Orthwein, A. & Di Noia, J.M. 2012. Activation induced deaminase: how much and where? *Seminars in Immunology.* 24(4):246-254.

Potter, H. & Heller, R. 2010. Transfection by electroporation. *Current Protocols in Molecular Biology.* Chapter 9:1-9.

Prelich, G. 2012. Gene overexpression: uses, mechanisms, and interpretation. *Genetics.* 190(3):841-854.

Ramiro, A.R. & Barreto, V.M. 2015. Activation-induced cytidine deaminase and active cytidine demethylation. *Trends in Biochemical Sciences.* 40(3):172-181.

Ramiro, A.R., Jankovic, M., Callen, E., Difilippantonio, S., Chen, H., McBride, K.M., Eisenreich, T.R., Chen, J. *et al*. 2006. Role of genomic instability and p53 in AID-induced c-myc–Igh translocations. *Nature.* 440(7080):105-109.

Ramiro, A.R., Jankovic, M., Eisenreich, T., Difilippantonio, S., Chen-Kiang, S., Muramatsu, M., Honjo, T., Nussenzweig, A. *et al*. 2004. AID is required for c-myc/IgH chromosome translocations in vivo. *Cell.* 118(4):431-438.

Ran, F.A., Hsu, P.D., Lin, C., Gootenberg, J.S., Konermann, S., Trevino, A.E., Scott, D.A., Inoue, A. *et al*. 2013. Double nicking by RNA-guided CRISPR Cas9 for enhanced genome editing specificity. *Cell.* 154(6):1380-1389.

Rebouças, E.D.L., Costa, J.J.D.N, Passos, M.J., Passos, J.R.D.S, Hurk, R.V.D. & Silva, J.R.V. 2013. Real time PCR and importance of housekeepings genes for normalization and quantification of mRNA expression in different tissues. *Brazilian Archives of Biology and Technology.* 56(1):143-154.

Revy, P., Muto, T., Levy, Y., Geissmann, F., Plebani, A., Sanal, O., Catalan, N., Forveille, M. *et al*. 2000. Activation-induced cytidine deaminase (AID) deficiency causes the autosomal recessive form of the Hyper-IgM syndrome (HIGM2). *Cell.* 102(5):565-575.

Richter-Larrea, J.A., Robles, E.F., Fresquet, V., Beltran, E., Rullan, A.J., Agirre, X., Calasanz, M.J., Panizo, C. *et al*. 2010. Reversion of epigenetically mediated BIM silencing overcomes chemoresistance in Burkitt lymphoma. *Blood.* 116(14):2531-2542. DOI:10.1182/blood-2010-02-268003 [doi].

Robbiani, D.F., Bothmer, A., Callen, E., Reina-San-Martin, B., Dorsett, Y., Difilippantonio, S., Bolland, D.J., Chen, H.T. *et al*. 2008. AID is required for the chromosomal breaks in c-myc that lead to c-myc/IgH translocations. *Cell.* 135(6):1028-1038.

Robbiani, D.F., Deroubaix, S., Feldhahn, N., Oliveira, T.Y., Callen, E., Wang, Q., Jankovic, M., Silva, I.T. *et al*. 2015. Plasmodium infection promotes genomic instability and AID-dependent B cell lymphoma. *Cell.* 162(4):727-737.

Robbiani, D.F. & Nussenzweig, M.C. 2013. Chromosome translocation, B cell lymphoma, and activation-induced cytidine deaminase. *Annual Review of Pathology: Mechanisms of Disease.* 8:79-103.

Rokavec, M., Oner, M.G., Li, H., Jackstadt, R., Jiang, L., Lodygin, D., Kaller, M., Horst, D. *et al*. 2014. IL-6R/STAT3/miR-34a feedback loop promotes EMT-mediated colorectal cancer invasion and metastasis. *The Journal of Clinical Investigation.* 124(4):1853-1867.

Schommers, P., Hentrich, M., Hoffmann, C., Gillor, D., Zoufaly, A., Jensen, B., Bogner, J.R., Thoden, J. *et al*. 2015. Survival of AIDS-related diffuse large B-cell lymphoma, Burkitt lymphoma, and plasmablastic lymphoma in the German HIV Lymphoma Cohort. *British Journal of Haematology.* 168(6):806-810.

Shimizu, T., Marusawa, H., Endo, Y. & Chiba, T. 2012. Inflammation-mediated genomic instability: roles of activation-induced cytidine deaminase in carcinogenesis. *Cancer Science.* 103(7):1201-1206.

Shinmura, K., Igarashi, H., Goto, M., Tao, H., Yamada, H., Matsuura, S., Tajima, M., Matsuda, T. *et al*. 2011. Aberrant expression and mutation-inducing activity of AID in human lung cancer. *Annals of Surgical Oncology.* 18(7):2084-2092.

Smith, M.R. 2003. Rituximab (monoclonal anti-CD20 antibody): mechanisms of action and resistance. *Oncogene.* 22(47):7359-7368.

Spender, L.C. & Inman, G.J. 2014. Developments in Burkitt's lymphoma: novel cooperations in oncogenic MYC signaling. *Cancer Management and Research.* 6(1):27.

Stavnezer, J. 2011. Complex regulation and function of activation-induced cytidine deaminase. *Trends in Immunology.* 32(5):194-201.

Stiborova, M., Poljakova, J., Mrizova, I., Borek-Dohalska, L., Eckschlager, T., Adam, V., Kizek, R. & Frei, E. 2014. Expression levels of enzymes metabolizing an anticancer drug ellipticine determined by electromigration assays influence its cytotoxicity to cancer cells—A comparative study. *International Journal of Electrochemistry and Science.* 9:5675-5689.

Tacar, O., Sriamornsak, P. & Dass, C.R. 2013. Doxorubicin: an update on anticancer molecular action, toxicity and novel drug delivery systems. *Journal of Pharmacy and Pharmacology.* 65(2):157-170.

Taub, R., Kirsch, I., Morton, C., Lenoir, G., Swan, D., Tronick, S., Aaronson, S. & Leder, P. 1982. Translocation of the c-myc gene into the immunoglobulin heavy chain locus in human Burkitt lymphoma and murine plasmacytoma cells. *Proceedings of the National Academy of Sciences of the United States of America.* 79(24):7837-7841.

Teng, G., Hakimpour, P., Landgraf, P., Rice, A., Tuschl, T., Casellas, R. & Papavasiliou, F.N. 2008. MicroRNA-155 is a negative regulator of activation-induced cytidine deaminase. *Immunity.* 28(5):621-629.

Thapa, D.R., Li, X., Jamieson, B.D. & Martínez-Maza, O. 2011. Overexpression of microRNAs from the miR-17-92 paralog clusters in AIDS-related non-Hodgkin's lymphomas. *PLoS ONE*. 6(6):E20781

Tomlins, S.A., Rhodes, D.R., Perner, S., Dhanasekaran, S.M., Mehra, R., Sun, X.W., Varambally, S., Cao, X. *et al*. 2005. Recurrent fusion of TMPRSS2 and ETS transcription factor genes in prostate cancer. *Science.* 310(5748):644-648.

Tosato, G. & Cohen, J.I. 2007. Generation of Epstein-Barr Virus (EBV)–Immortalized B Cell Lines. *Current Protocols in Immunology.* Unit 7.22:1-3

Tran, T.H., Nakata, M., Suzuki, K., Begum, N.A., Shinkura, R., Fagarasan, S., Honjo, T. & Nagaoka, H. 2010. B cell-specific and stimulation-responsive enhancers derepress Aicda by overcoming the effects of silencers. *Nature Immunology.* 11(2):148-154.

Vandesompele, J., De Preter, K., Pattyn, F., Poppe, B., Van Roy, N., De Paepe, A. & Speleman, F. 2002. Accurate normalization of real-time quantitative RT-PCR data by geometric averaging of multiple internal control genes. *Genome Biology.* 3(7):1-12.

Vaughan, A.T., Iriyama, C., Beers, S.A., Chan, C.H., Lim, S.H., Williams, E.L., Shah, V., Roghanian, A. *et al*. 2014. Inhibitory FcγRIIb (CD32b) becomes activated by therapeutic mAb in both cis and trans and drives internalization according to antibody specificity. *Blood.* 123(5):669-677.

Vermeulen, K., Van Bockstaele, D.R. & Berneman, Z.N. 2003. The cell cycle: a review of regulation, deregulation and therapeutic targets in cancer. *Cell Proliferation.* 36(3):131-149.

Wang, F., Liu, J., Robbins, D., Morris, K., Sit, A., Liu, Y. & Zhao, Y. 2011. Mutant p53 exhibits trivial effects on mitochondrial functions which can be reactivated by ellipticine in lymphoma cells. *Apoptosis.* 16(3):301-310.

Wang, J.H., Gostissa, M., Yan, C.T., Goff, P., Hickernell, T., Hansen, E., Difilippantonio, S., Wesemann, D.R. *et al*. 2009. Mechanisms promoting translocations in editing and switching peripheral B cells. *Nature.* 460(7252):231-236.

Wright, N.J., Hesseling, P.B., McCormick, P. & Tchintseme, F. 2009. The incidence, clustering and characteristics of Burkitt lymphoma in the Northwest province of Cameroon. *Tropical Doctor.* 39(4):228-230.

Wu, Y., Maruo, S., Yajima, M., Kanda, T. & Takada, K. 2007. Epstein-Barr virus (EBV)-encoded RNA 2 (EBER2) but not EBER1 plays a critical role in EBV-induced B-cell growth transformation. *Journal of Virology.* 81(20):11236-11245.

Yadav, A., Olaru, A., Saltis, M., Setren, A., Cerny, J. & Livák, F. 2006. Identification of a ubiquitously active promoter of the murine activation-induced cytidine deaminase (AICDA) gene. *Molecular Immunology.* 43(6):529-541.

Young, L.S. & Rickinson, A.B. 2004. Epstein–Barr virus: 40 years on. *Nature Reviews Cancer.* 4(10):757-768.

Zan, H. & Casali, P. 2013. Regulation of Aicda expression and AID activity. *Autoimmunity.* 46(2):83-101.

Appendix A: Recipes and reagents

30 % Acryl-bisacrylamide

	100 ml
Acrylamide	29 g
N, N'-methylenebisacrylamide	1 g
Make up to 100ml with dH_2O	

Heat to 37°C to dissolve and filter with a 0.44 µm filter

1 % Agarose gel

	40 ml
Agarose	0.4 g
1X TBE	40 ml

Pulse heat in a microwave with gentle agitation, before pouring add 2 µl Ethidium Bromide (10 mg/ml stock, Sigma- Aldrich)

10 % APS

	100 µl
Ammonium Persulfate	100 mg
dH_2O	100 µl

0.1 % crystal violet stain

	10 ml
Crystal Violet	100 mg
2 % Ethanol	100 µl

70 % Ethanol

	100 ml
100 % ethanol	70 ml
dH_2O	30 ml

0.1 M PIPES

	20 ml
PIPES	20 ml
Milk powder	0.6048 g

pH to 6.8

1.5 M Tris pH 6.8

	500 ml
Tris	60.5 g
dH_2O	300 ml

pH to 6.8 and adjust volume to 500 ml with dH_2O

1.5 M Tris pH 8.8

	500 ml
Tris	60.5 g
dH_2O	300 ml

pH to 8.8 and adjust volume to 500 ml with dH_2O

2 N Hydrocholoric acid

	50 ml
32 % HCl	19.2 ml
dH_2O	40.4 ml

10X PBS

	1000 ml
NaCl	80 g
KCl	2 g
Na_2HPO_4-$7H_2O$	26.8 g
KH_2PO_4	2.4 g

Make up in 1000 ml at pH 7.4

2X RNA loading buffer

	1000 µl
Formamide	900 µl
Sucrose	99 µl
Bromophenol Blue	0.5 µl
Xylene Cyanol	0.5 µl

10X Running buffer

	1000 ml
SDS	10 g
Tris	30.3 g
Glycin	144.1 g

Make up to 1000 ml with dH_2O

1X Running buffer

	1000 ml
10X Running Buffer	100 ml
dH_2O	900 ml

10 % SDS

	100 ml
SDS	10 g
dH_2O	90 ml

Adjust volume to 100 ml with dH_2O

5X SDS loading dye

	Volume	Final Concentration
2 M Tris-HCl ph 6.8	12.5 ml	250 mM
10 % SDS	10 g	10 %
100 % Glycerol	30 ml	30 %
β-mercaptoethanol	5 ml	5 %
0.04 % Bromophenol Blue	52 ml	0.04 %

12% SDS resolving gel

	Volume
H_2O	3.3 ml
30 % Acryl-bisacrylamide	4 ml
1.5 M Tris pH 8.8	2.5 ml
10 % SDS	100 µl
10 % APS	100 µl
TEMED	4 µl

5% SDS stacking gel

	Volume
H_2O	2.1 ml
30 % Acryl-bisacrylamide	500 µl
1.5 M Tris pH 6.8	380 µl
10 % SDS	30 µl
10 % APS	30 µl
TEMED	3 µl

10X TBE buffer

	1000 ml
Tris	108 g
Boric Acid	55 g
dH_2O	900 ml

Add 40 µl 0.5 M Na_2EDTA (pH 8.0) and adjust volume to 1000 ml

1X TBE buffer

	1000 ml
10X TBE	100 ml
dH_2O	900 ml

1X TBS

	200 ml
Tris	1.21 g
NaCl	1.75 g
dH_2O	200 ml

10X Transfer buffer

	1000 ml
Glycine	144 g
Tris	38 g

Make up to 1000 ml with dH_2O

1X Transfer buffer

	1000 ml
10X Transfer Buffer	100 ml
dH_2O	700 ml
Isopropanol	200 ml

Stored at 4 °C

β-galactosidase fixative (4 % paraformaldehyde)

	100 ml
Paraformaldehyde	0.2 g
1X PBS	5 ml

Heat to 60 °C to dissolve and store at -20 °C

2X Boiling blue

	Stock	**10 ml**
Tris-HCl pH6.8	1 M	1.25 ml
SDS	10 %	4 ml
β-mercaptoethanol		1 ml
Glycerol		2 ml
dH_2O		1.75 ml
Bromophenol Blue		Pinch

Store at -20°C

Borate buffer (0.1 M)

	100 ml
Sodium Borate	38.14 g
dH_2O	100 ml

Citric acid buffer

	Stock	**200 ml**
Citric Acid	0.1 M	39.4 ml
Sodium Phosphate	0.2 M	60.6 ml
dH_2O		100 ml

DEPC-treated H_2O

	100 ml
DEPC	100 µl
dH_2O	99.9 ml

Fixative

A ratio of 1:3 Glacial acetic acid:Methanol stored at 4 °C

Mounting fluid

	Stock	100 ml
0.1 M Citric Acid	1.05 g/50ml	22.2 ml
0.2 M $Na_2HPO_4.2H_2O$	1.41 g/50 ml	27.8 ml
Glycerol		50 ml

pH at 5.5

Hoechst 33342 stain (#H1399, Invitrogen, USA)

A stock of 10 mg/ml was diluted in dH_2O in a 1:15000 ratio

5 M NaCl

	20 ml
NaCl	5.84 g
dH_2O	20 ml

PBS/Tween

1X PBS	100 ml
Tween	1 ml

Make up to 1000ml with dH_2O

PBS/Tween + 5 % milk powder

	100 ml
PBS/Tween	100 ml
Milk powder	5 g

Propidium iodide stain

	Stock	8 ml
Triton X-100	100 %	8 µl
$MgCl_2$	1 M	16 µl
NaCl	5 M	160 µl
PIPES	0.1 M	800 µl
Propidium Iodide	1 mg/ml	80 µl
dH_2O		6.936 ml

RIPA buffer

	Stock	50 ml
150 nM NaCl	5 M	1.5 ml
1% Triton X-100	100 %	500 µl
0.1% SDS	10 %	500 µl
10 mM Tris pH 7.5	1 M	500 µl
1% Deoxycholate powder		0.5 g

Make up to 50 ml with dH_2O

RIPA solution

	1 ml
RIPA Buffer	858 µl
7X Protease Inhibitor	142 µl

Striping buffer

	Stock	Final Concentration	100 ml
β-mercaptoethanol	14.3 M	100 mM	0.69 ml
SDS	20 %	2 %	10 ml
Tris-HCl (pH 6.7)	1 M	62.5 mM	6.25 ml
dH_2O			83.06 ml

TBS/Tween

1X TBS	100 ml
Tween	1 ml

TBS/Tween + 5 % BSA

	5 ml
TBS/Tween	5 ml
BSA	0.25 g

Trypsin-EDTA

	1000 ml
NaCl	8 g
Na_2HPO_4	1.26 g
KCl	0.2 g
KH_2PO_4	0.2 g
Trypsin	0.5 g
EDTA	0.2 g

Make up to 1000 ml with dH_2O at pH 7.4 and filter sterilise (0.2 µm)

X-gal staining solution

	Stock	**1155 µl**
Citric Acid/Sodium Phosphate Buffer	40 mM	1000 µl
Potassium Ferricyanide	100 mM	50 µl
Potassium Ferrocyanide	100 mM	50 µl
$MgCl_2$	200 mM	10 µl
NaCl	6M	25 µl
X-gal	50 mg/ml	20 µl

pH at 6.0

Appendix B: Additional figures

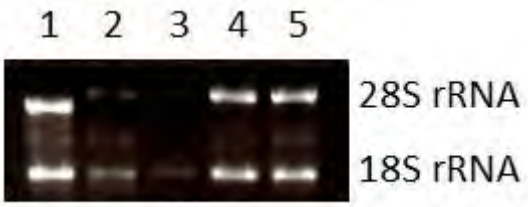

Figure B1: Gel electrophoresis of total RNA extracted from the prostate cell lines. The two sharp bands representing the 28S and 18S ribosomal subunits were observed in a 1 % agarose gel. (Lanes 1 – 5; Du145, LnCaP, PC-3, PNT1A and PNT2).

Figure B2: Gel electrophoresis of total RNA extracted from the oesophageal and head and neck cancer cell lines. The two sharp bands representing the 28S and 18S ribosomal subunits were observed in a 1 % agarose gel. (Lanes 1 – 5; KYSE-30, KYSE-520, OE19, OE33 and UMSCC22b).

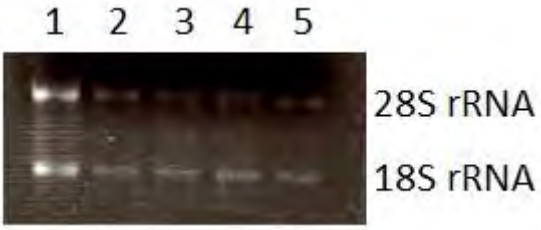

Figure B3: Gel electrophoresis of total RNA extracted from L1439A and the Burkitt's lymphoma cell lines. The two sharp bands representing the 28S and 18S ribosomal subunits were observed in a 1 % agarose gel. (Lanes 1 – 5; L1439A, BL2, P3HR1, Ramos and Seraphina).

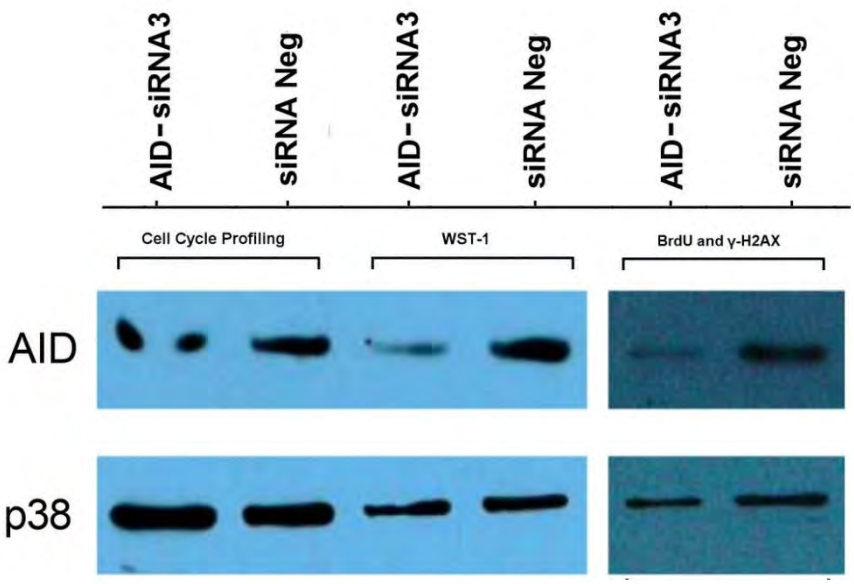

Figure B4: Representative knockdown confirmation of AID reduction in the selected downstream experiments. Western blot analysis displaying the protein expression levels of AID after these cells had been knocked down for the cell cycle profiling, WST-1, γ-H2AX and BrdU experiments using 1000 ng of each siRNA. 12 µl of protein in 2X boiling blue buffer was boiled at 95 °C for 10 minutes before being loaded and separated on a 12 % SDS-PAGE gel at 100 V for 200 minutes in 1X running buffer. The protein was then transferred onto a nitrocellulose membrane (Bio-Rad) for 75 minutes at 100 V in 1X transfer buffer. This was then detected using the Clarity™ Western ECL Substrate (Bio-Rad). To detect AID, mouse anti-AID (Invitrogen) was used, with a HRP bound goat anti-mouse secondary antibody (Bio-Rad). The p38 protein was detected using the rabbit anti-p38 antibody (Sigma-Aldrich) and the HRP bound goat anti-rabbit secondary antibody.

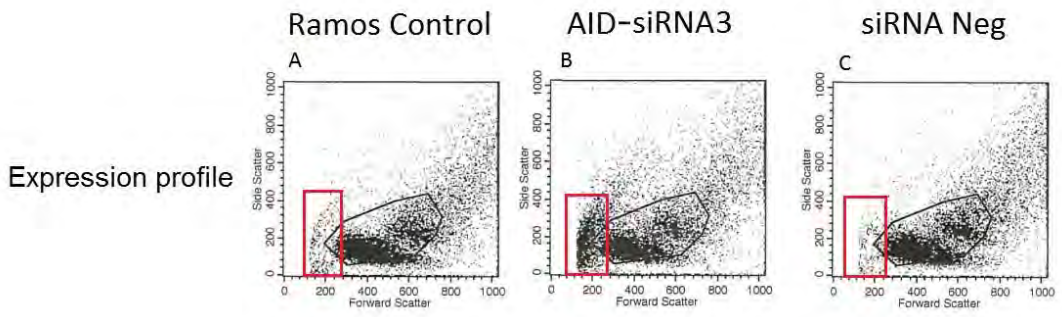

Figure B5: Expression profiles in control Ramos cells, AID-siRNA3 and siRNA Neg cells. Panel A is the expression profiles for the control cells, panel B is the AID-siRNA3 cells and panel C is the siRNA Neg cells. The red rectangles represent the apoptotic cells in each expression profile.

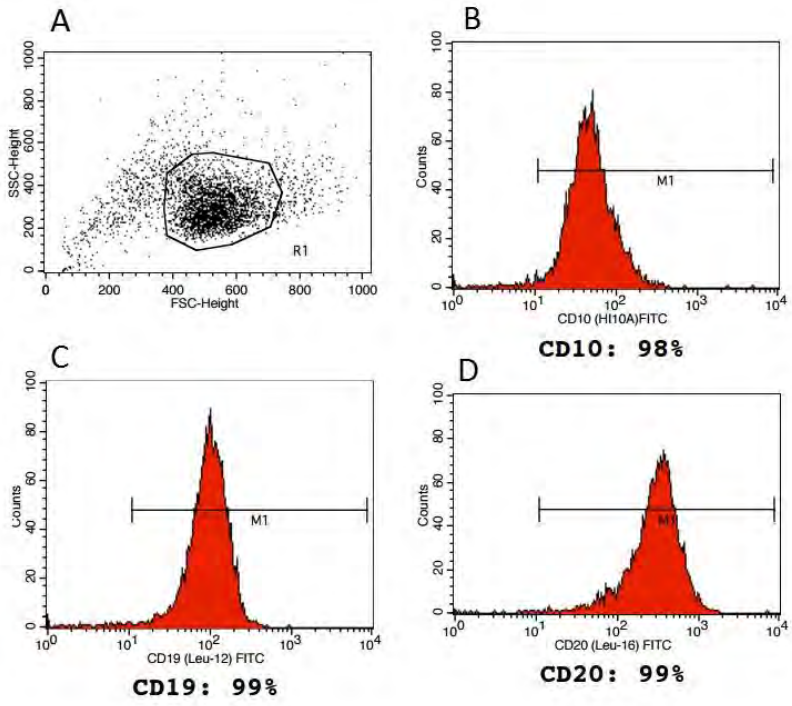

Figure B6: Flow cytometric analysis of the CD19, CD10 and CD20 cell surface expression in Ramos cells from the DSMZ database. Panel A is the expression profiles for the Ramos cells, B is expression profile for CD10, C is the expression profile for CD19 and D is the expression profile for CD20. Images were taken from https://www.dsmz.de/fileadmin/downloads/ACC/immunology/ACC%20603.pdf)

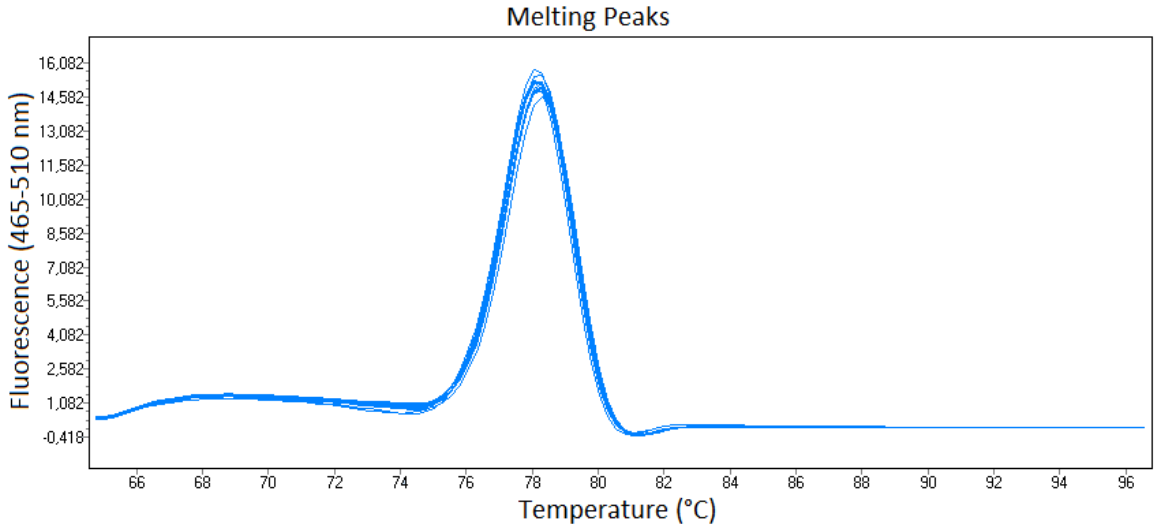

Figure B7: qPCR melting profile of AID. Melting profile of AID utilising a 1:10 serial dilution from 1 x 10^6 copies to 1 x 10^2 copies of the amplified PCR products.

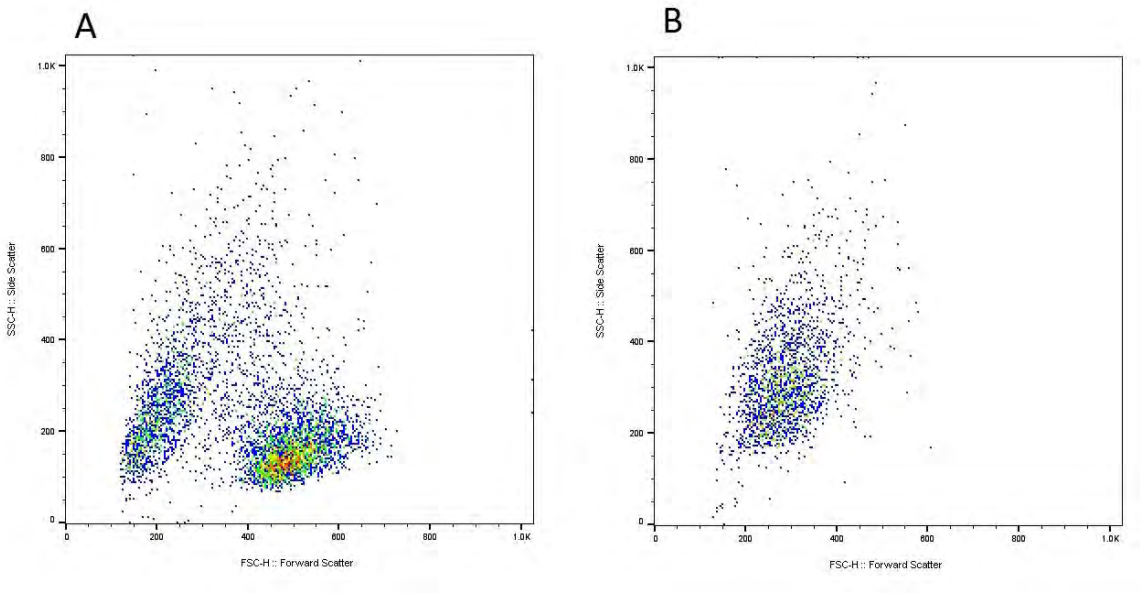

Figure B8: Expression profiles in Ramos cells nucleofected with pEGFP-N3-Empty and pEGFP-N3-AID. Panel A is the expression profiles for the pEGFP-N3-AID cells and panel B is the pEGFP-N3-AID cells.

Appendix C: Additional images

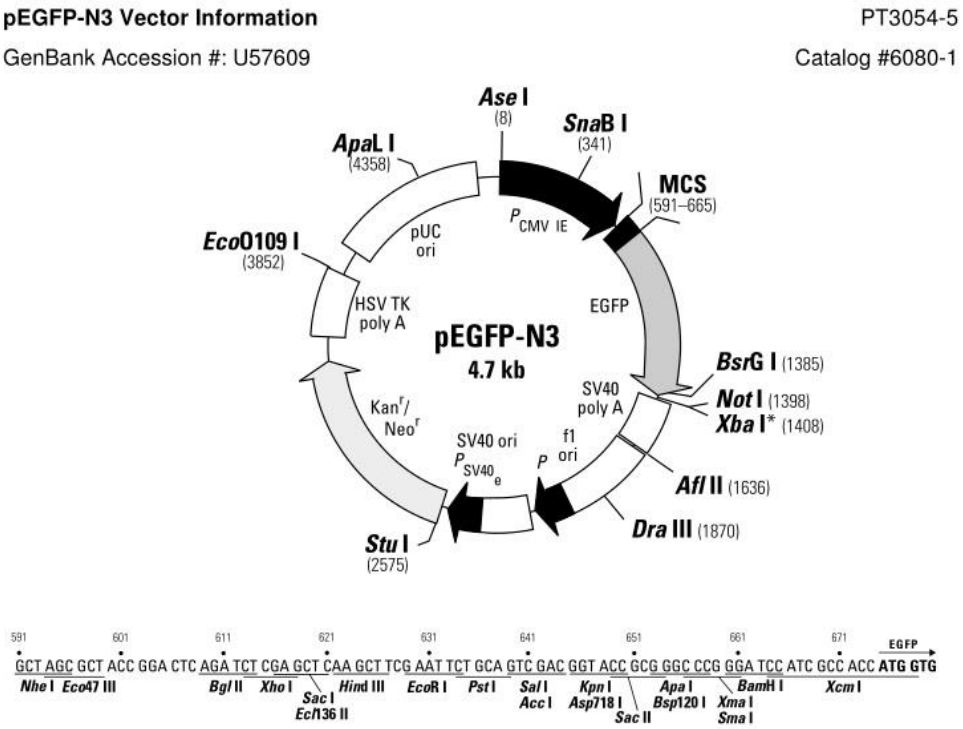

Figure C1: Diagram of the pEGFP-N3 vector. AID was cloned into the *Bam*HI and *Eco*RI site.

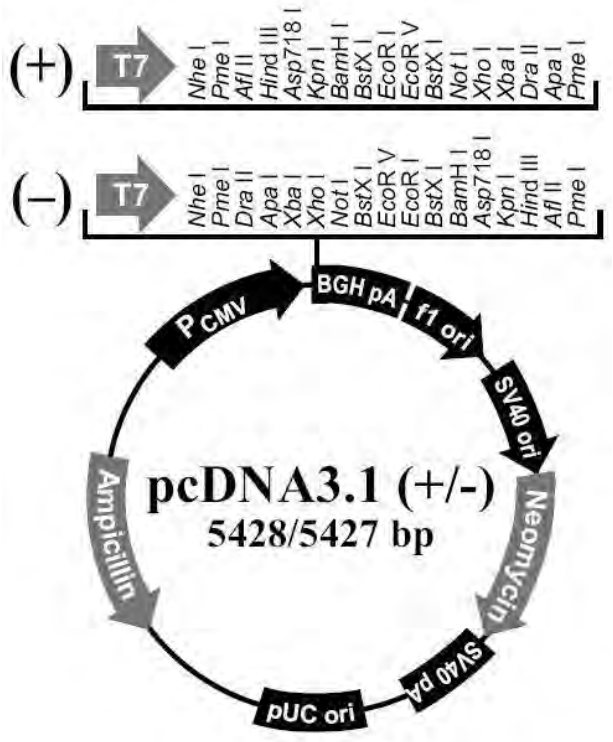

Figure C2: Diagram of the pcDNA-3.1 vector. AID was cloned into this plasmid.

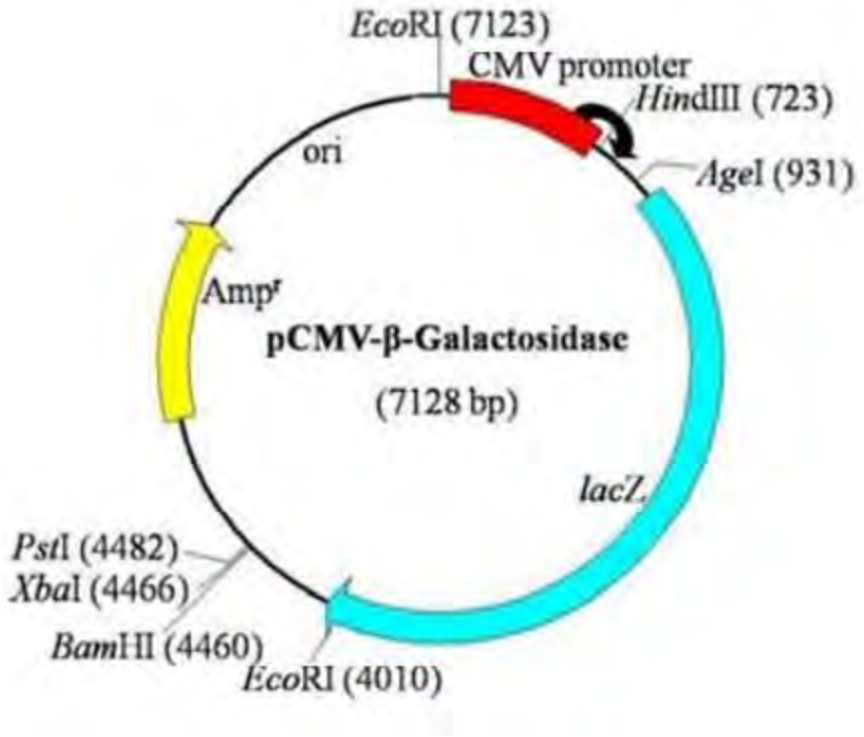

Figure C3: Diagram of the pCMV-β-Gal vector.

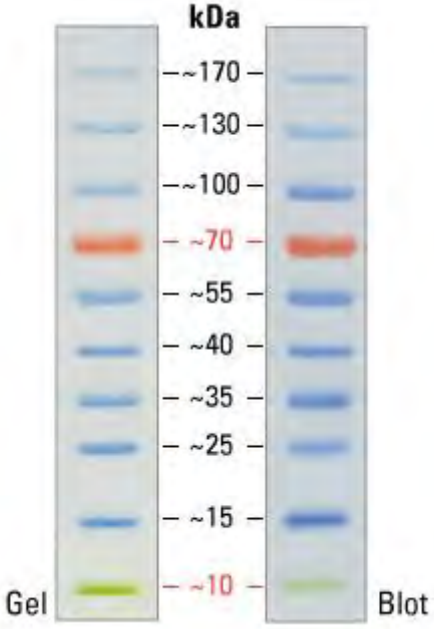

Figure C4: PageRuler™ Prestained Protein Ladder (Thermo Scientific™, USA).

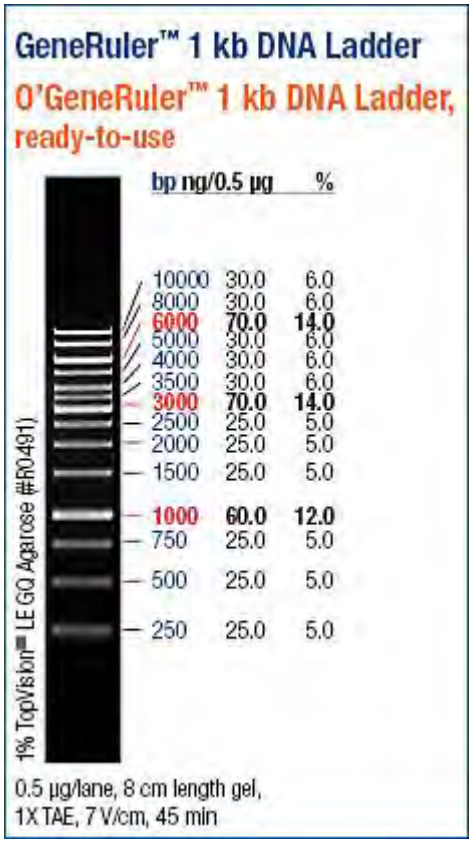

Figure C5: GeneRuler™ 1 kb DNA Ladder (Thermo Scientific™, USA).